NASA CR-102639

FINAL REPORT

on

A STUDY OF THE THERMAL CONDUCTANCE OF
BOLTED JOINTS

Funded as Part IV of the

NATIONAL AERONAUTICS AND SPACE ADMINISTRATION
MARSHALL SPACE FLIGHT CENTER
MULTIDISCIPLINARY RESEARCH GRANT
NGR-19-001-068

Report Prepared By

Dr. C. A. Whitehurst
Mr. W. T. Durbin
Division of Engineering Research
College of Engineering
Louisiana State University
Baton Rouge, Louisiana

NASA CR-102639

FINAL REPORT

on

A STUDY OF THE THERMAL CONDUCTANCE OF BOLTED JOINTS

Funded as Part IV of the

NATIONAL AERONAUTICS AND SPACE ADMINISTRATION
MARSHALL SPACE FLIGHT CENTER
MULTIDISCIPLINARY RESEARCH GRANT
NGR-19-001-068

Report Prepared By

Dr. C. A. Whitehurst
Mr. W. T. Durbin
Division of Engineering Research
College of Engineering
Louisiana State University
Baton Rouge, Louisiana

This Report Prepared By:

C. A. Whitehurst, Associate Professor
Division of Engineering Research

This Report Approved By:

E. J. Dantin, Director
Division of Engineering Research

ABSTRACT

The phenomena of heat transfer across the interface of discontinuous materials has received considerable attention during the last two decades. With the advances in space technology and related electronic systems, a consistent, unique, and effective means for reliably predicting imposed thermal resistances to design heat loads has been a research topic. A review, evaluation, comparison, and utilization of current literature in this field clearly indicates a need for a simplified experimental, design-oriented approach for predicting the thermal resistance of a bolted lap joint.

In this paper such a method is presented. Experimental work is given for comparison purposes with current literature, and a qualitative analysis is made on present theories to demonstrate the inherent difficulties in combining all of the relative variables related to a theoretically approximate solvable set of equations.

TABLE OF CONTENTS

LIST OF FIGURES

LIST OF TABLES

I. INTRODUCTION

In many mechanical design problems, it is very important to know the thermal conductivity of bolted or riveted joints used in the design. Heat may be generated on one side of a joint, whereas the other side may be acting as a heat sink. An example of this could be an electrical package bolted to the framework of a space vehicle. Heat generated by the electrical components must be dissipated by either conduction through the mounting joints or by a refrigeration system. If the maximum desired temperature of the electrical package and the temperature of the sink (vehicle framework) are known along with the thermal conductivities of the intermediate joints, then the amount of heat which will be dissipated to the sink can be calculated. The difference between the heat generated and the heat dissipated is the amount of refrigeration needed to properly cool the electrical package. However, if the joint thermal conductivities are not known, then a properly sized refrigeration system cannot be designed.

Much work has gone into developing an analytical method of predicting these conductivities, but there are many inherent difficulties in the various approaches. The stress and heat transfer patterns are three-dimensional, with discontinuities at the joint interface which make a theoretical prediction of thermal conductance extremely complicated. The accuracy of such a prediction is lessened by the numerous approximations which must be made so that the analytical equations can be applied to an actual situation. Another difficulty is encountered in trying to interpret the effect of the surface roughness at the joint interface on stress distributions, plate deflections, and thermal conductivities. The objective of this study is to develop a convenient and accurate method of predicting the thermal conductivity of fastened joints.

A method which shows considerable promise is the Equivalent Fin Method (EFM) and is the method of primary concern in this study. In the results of this study, the EFM is used in a comparison with previous studies. The EFM as derived in this study will determine a joint thermal conductivity which, when applied to the problem at hand, will represent the thermal conductivity of a piece of metal with a thickness and width equal to that of the parent metal from which the joint is formed, and with a length equal to the length of overlap of the joint. The joint conglomerate can then be considered to be a section of homogenous metal with a known thermal conductivity.

The first part of the experimental work was an investigation of the deflections in the joint caused by bolting or riveting the joint. For this and all of the experimental work on this project, a bolted lap joint was used as pictured in Figures I-1, I-2, and I-3. The bolts used are 3/8 inch, national coarse, standard button-head bolts constructed to close tolerances from 4140 carbon steel. All plates differ in surface finish and plate material, but all had the following dimensions:

Plate thickness = t = 0.1875 in.

Bolt hole diameter = 2t = 0.375 in.

Plate overlap = 10t = 1.875 in.

Plate width = 30t = 5.625 in.

Plate length = 25t = 4.69 in.

Included in the deflection studies was a photoelastic investigation of bolted plates where an attempt was made to determine the normal stresses

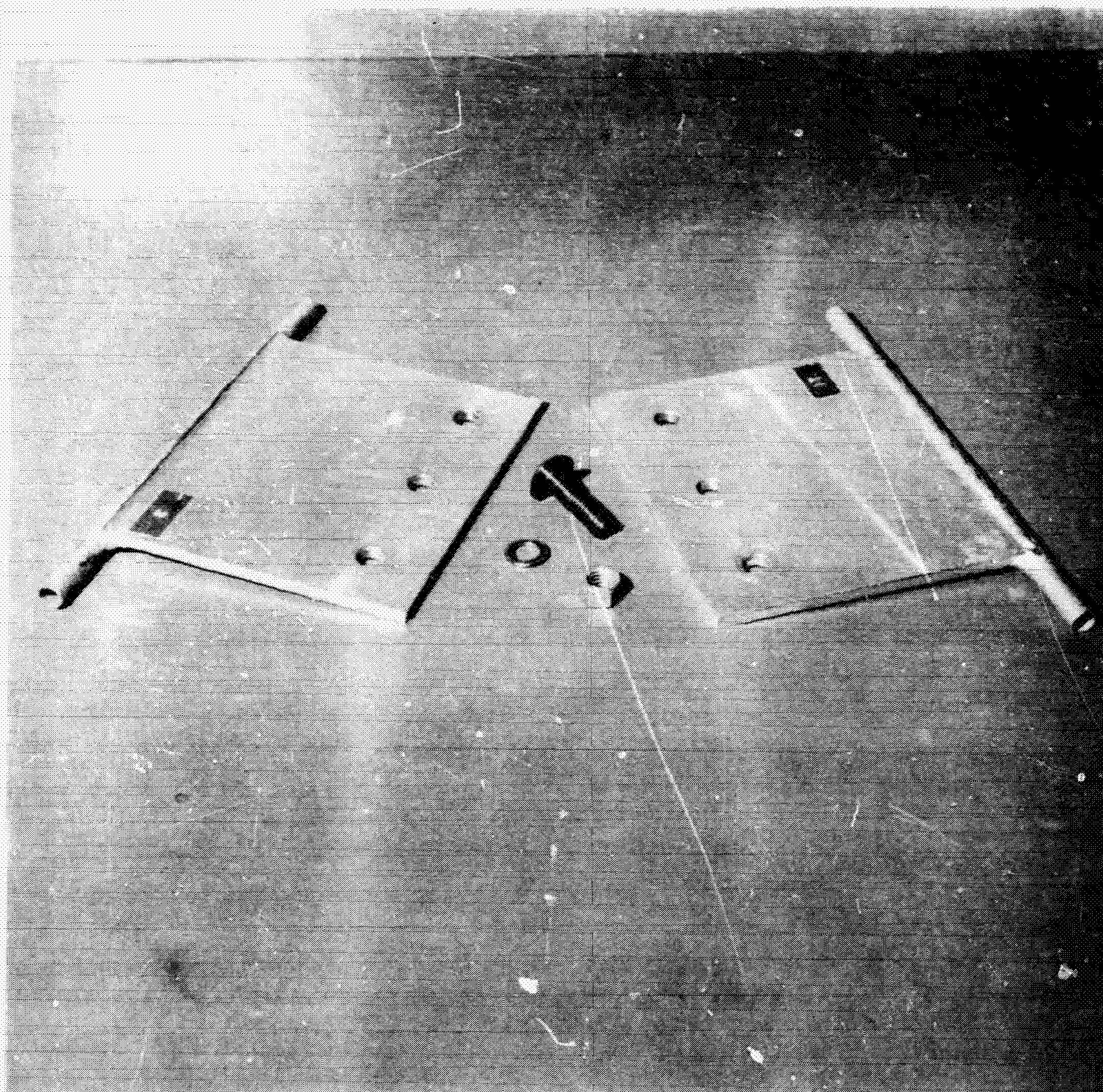

Figure I-1. Disassembled view of plates and button-head bolt.

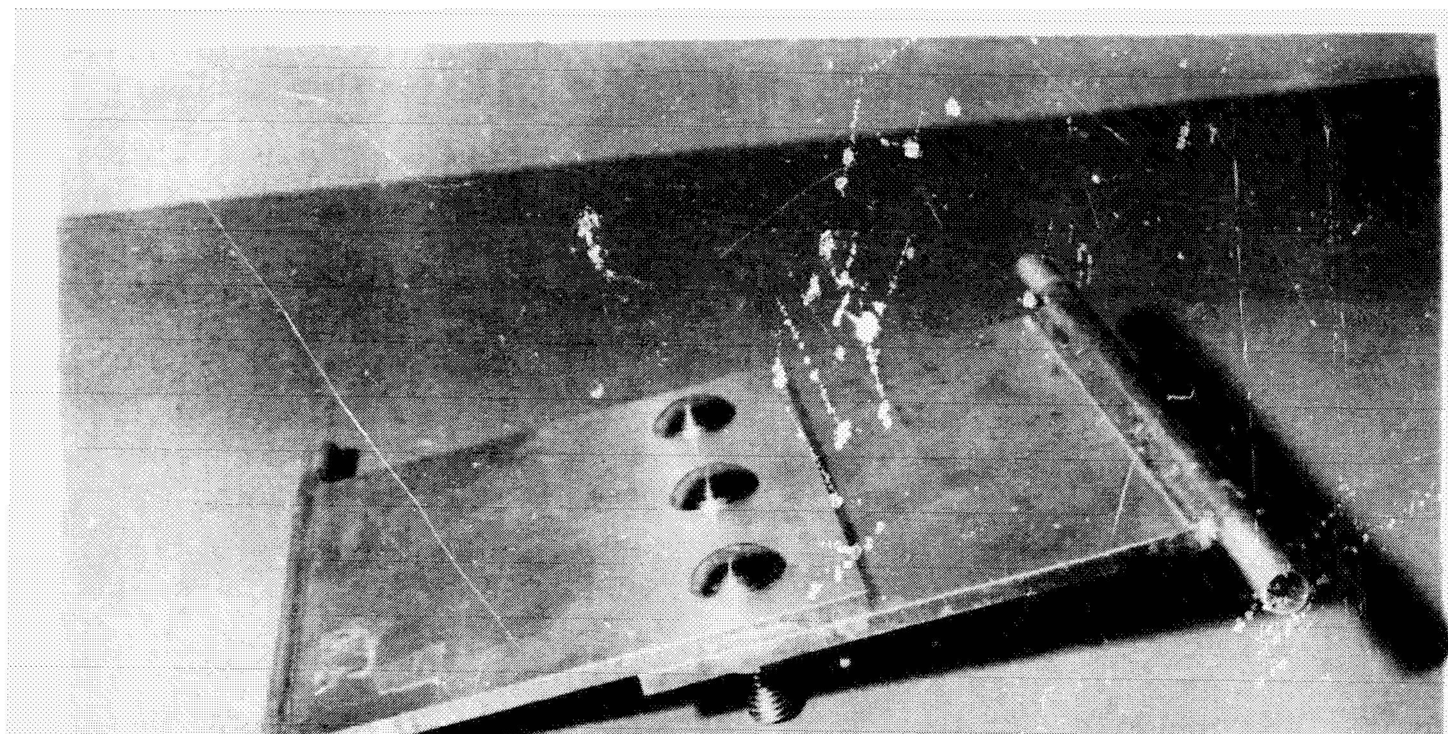

Figure I-2. Assembled view of test joint.

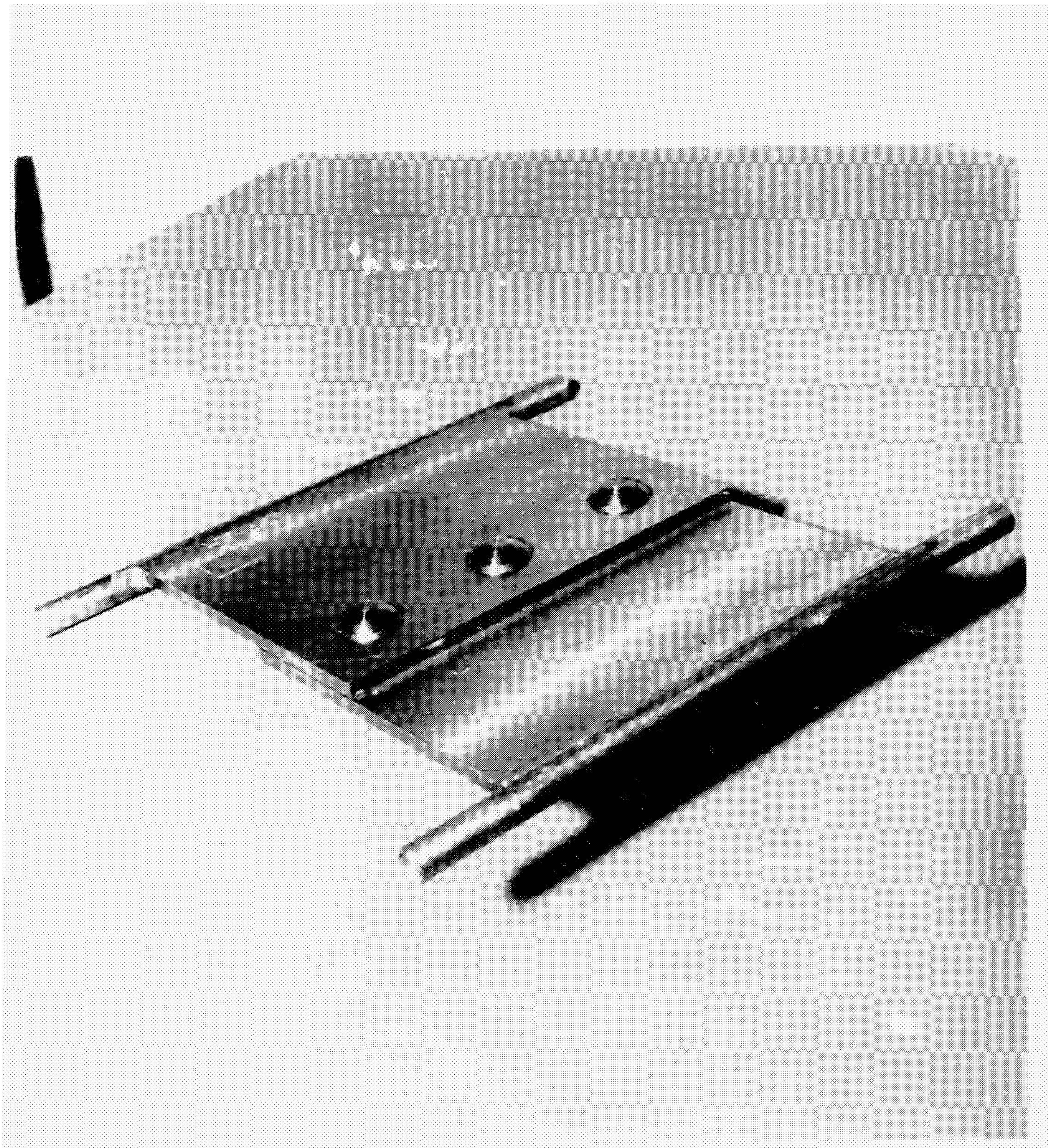

Figure I-3. Assembled view of test joint.

produced at the plate interface by the bolts. This helped define the point at which the normal stress decays to zero (r_σ) which is also the point where the plates are no longer in physical contact.

Joint thermal conductivity measurements comprised the final experimental efforts. Temperature profiles along the plates were measured with a torque on the bolts and a thermal load on the joint. Thermal conductivities were then calculated using the EFM. These measurements were made in a vacuum to give minimum heat losses and at standard atmospheric pressure for comparison purposes.

The desired results of this study was to develop an accurate method which a design engineer could use in determining the conductivity of fastened joints. This report will show that the EFM can be used as that tool.

II. TECHNICAL DISCUSSION

A. LITERATURE SURVEY AND REVIEW OF APPROACHES

A survey of literature concerned with the thermal conductivities of bolted joints and related subjects revealed many attempts at predicting the influence of various parameters on joint conductivity. Some investigators have tried to correlate these various influences into classical methods of predicting joint thermal conductivity. However, the number of variables which must enter into any correlation of this type is large. Among these are interface normal pressure, interface surface finish and waviness, material hardness, material thermal conductivity, joint temperature, interstitial fluid type and pressure, geometry of the joint, maximum amount of pre-load, amount of cycling, and elapsed time since joint construction. Although many of these variables have been investigated in various pieces of literature, no single study has correlated more than a few of these. Thus, there is no accurate way to predict the thermal conductivity of bolted joints. In this study the investigators will demonstrate a convenient and accurate method of determining joint thermal conductivities.

Even though a complete solution to the problem has not been developed, previous studies have produced valuable information in establishing trends of influence for many of the pertinent variables. This information and the information obtained in this study will be used to generalize the effect of each of these variables on joint thermal conductivity.

Much of the previous work has been concentrated on pairs of cylinders or blocks with their mating surfaces under uniform pressure (References 3, 4, 8, 9, 10, 11, 12, 13, 14, 16, and 18). The data obtained from these studies can not be used directly to predict the thermal conductivity of bolted joints because there has been no consideration given to the influence of the bolt or rivet, to the nonuniform pressure distribution produced by the bolts or rivets, or to the resulting plate deflections. This data must be coupled with correlations involving plate geometry and mechanical responses of the plates due to such things as temperature gradients, torquing, and creep. This viewpoint is also expressed in Reference 5, and states that "Data taken from machined blocks under various contact pressures and surface finishes is not applicable to riveted aircraft structural joints". Reference 1 presents a photoelastic photo which clearly indicates the nonuniform interface stresses and the actual plate deflections.

In Reference 7, a noteworthy attempt is made at a classical solution to the joint conductance problem considering as many variables as possible. The investigators on this project feel that the classical approach can only produce a very complicated set of equations that must be solved on a computer and will have built-in errors due to the assumptions and approximations which must be made.

The secondary objective of this study is to provide some quantitative data in the area of plate reactions to loading conditions. References 2, 5, and 7 have shown that such things as interface contact area, normal pressure distribution, and plate deflections are important in analyzing joint interfaces. No theoretical analysis will be done in this study. However, data will be taken to define the reaction trends of the test plates to the parameters of bolt torque, thermal gradients, and relaxation time.

B. THE EQUIVALENT FIN METHOD

The derivation of the EFM equations is extremely simple and can be done using the sample temperature distribution shown in Figure II-1.

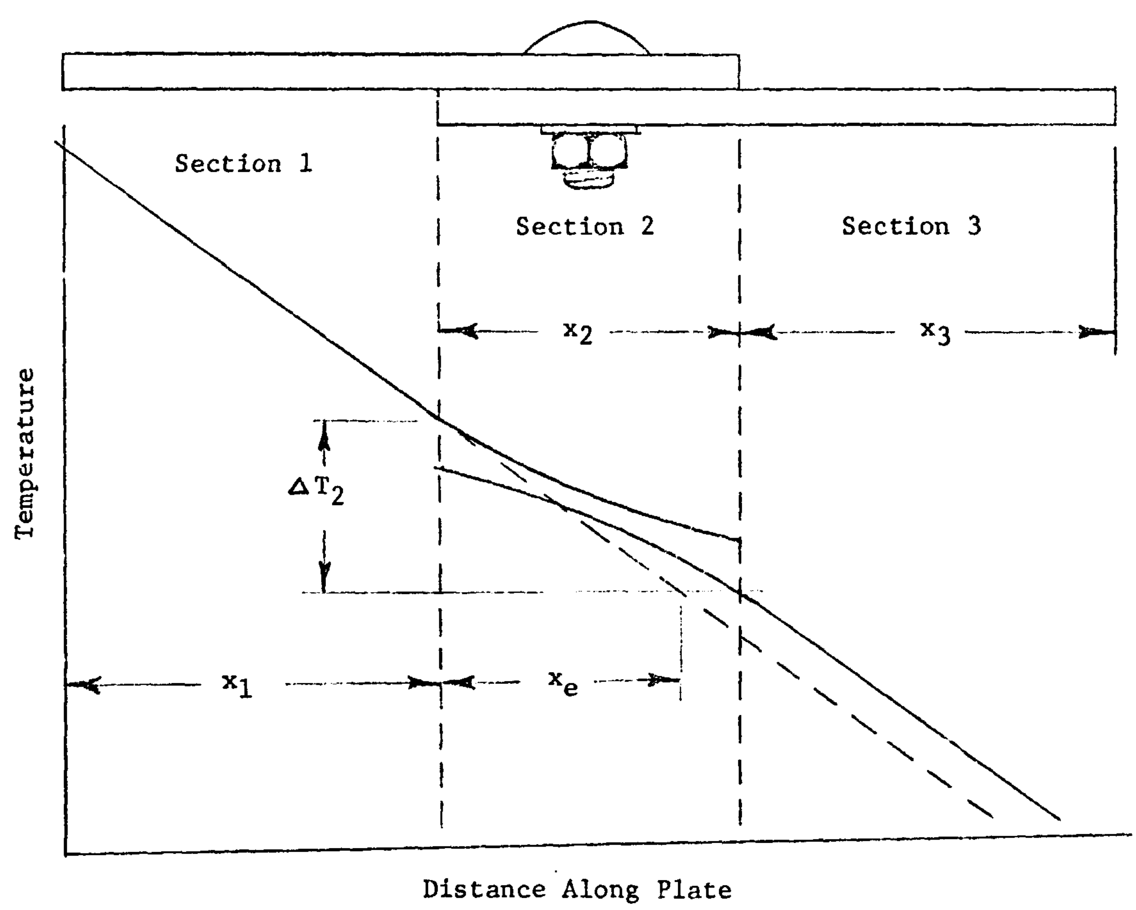

Figure II-1. Sample temperature distribution.

If the joint is properly insulated against heat loss, then the heat flow in sections 1 and 3 is one dimensional and the following equation can be written:

$$q_1 = q_2 = q_3 = - k_1A_1 \frac{dT}{dx}\Big)_1 = - k_3A_3 \frac{dT}{dx}\Big)_3$$

where q_1 = heat flowing through sec. 1,

q_2 = heat flowing through sec. 2,

q_3 = heat flowing through sec. 3,

$k_1 = k_3$ = thermal conductivity of the joint material = k, and

$A_1 = A_3$ = Cross-sectional area of the plates = A.

If section 2 is replaced with a single piece of metal having a cross-section equal to A, then

$$\frac{dT}{dx}\Big)_1 = \frac{\Delta T_2}{x_e} = \frac{dT}{dx}\Big)_3 \qquad \text{(eq. 1)}$$

where x_e = the equivalent length of section 2. Since $q_1 = q_2$ and $q_2 = -k_2A \frac{\Delta T_2}{x_2}$, then

$$kA \frac{dT}{dx}\Big)_1 = k_2A \frac{\Delta T_2}{x_2} = kA \frac{dT}{dx}\Big)_3$$

and

$$k \frac{dT}{dx}\Big)_1 = k_2 \frac{\Delta T_2}{x_2} = k \frac{dT}{dx}\Big)_3 \qquad \text{(eq. 2)}$$

Combining equations 1 and 2 and solving for k_2, the following equation is obtained:

$$k_2 = \frac{x_2}{x_e} k \qquad \text{(eq. 3).}$$

This is the basic EFM equation; and by graphically determining x_e, one can determine the thermal conductivity of the joint (k_2). Equation 3 can be applied to sections 1 and 2, to sections 2 and 3, or both, and the results averaged, which would minimize errors due to heat losses and would give more accurate results. Further, Equation 3 can be written as follows:

$$k_2 = \frac{(\Delta T_1)(x_2)}{(\Delta T_2)(x_1)} k \qquad \text{(equation 4 for sections 1 and 2)}$$

and

$$k_2 = \frac{(\Delta T_3)(x_2)}{(\Delta T_2)(x_3)} k \qquad \text{(equation 4 for sections 2 and 3).}$$

Again, calculations can be performed using either or both of these equations and the results averaged to give an accurate determination of k_2. This procedure was followed with the data obtained in this study and with data given in References 5 and 7 for a comparison.

The effectiveness of the EFM method can be determined by considering an "ideal" joint for which the temperature distribution and the thermal conductivity is known. Reference 5 measured the temperature distribution for the "ideal" joint shown in Figure II-2. Also shown on this plot is the ideal temperature distribution calculated as follows:

$$q_1 = q_2 = q_3 = q \text{ (for no heat losses)}$$

$$q = kA_1 \left.\frac{dT}{dx}\right)_1 = kA_2 \left.\frac{dT}{dx}\right)_2 = kA_3 \left.\frac{dT}{dx}\right)_3$$

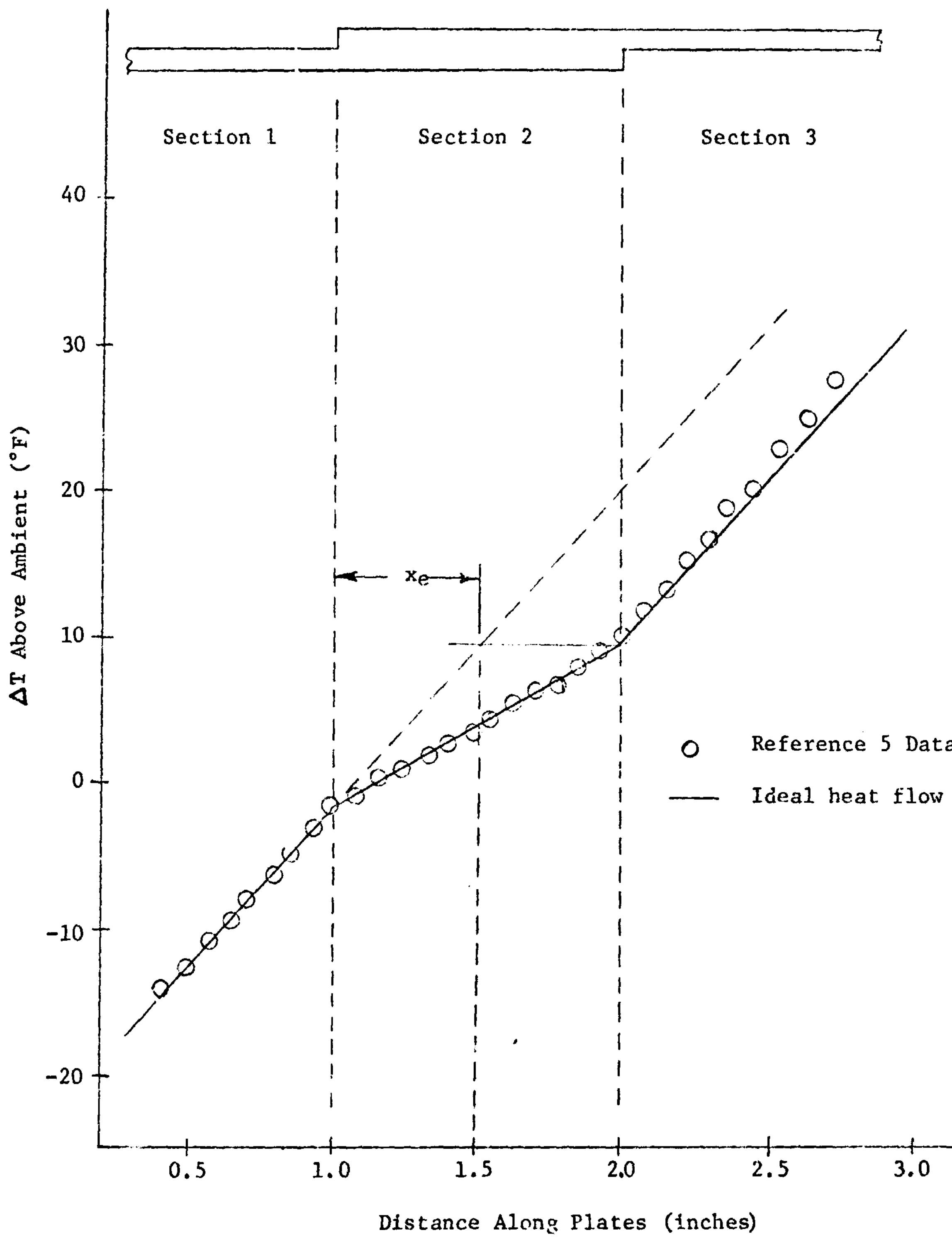

Figure II-2. Data replotted from Reference 5 for an Ideal Joint

$$A_1 = \frac{1}{2} A_2 = A_3 = A$$

$$A \left.\frac{dT}{dx}\right)_1 = 2A \left.\frac{dT}{dx}\right)_2 = A \left.\frac{dT}{dx}\right)_3$$

Therefore, $\left.\frac{dT}{dx}\right)_1 = \left.\frac{dT}{dx}\right)_3 = 2 \left.\frac{dT}{dx}\right)_2$. Using the ideal distribution and the EFM, k_2 for section 2 with an equivalent cross-sectional area, A, can be calculated as follows:

$$k_2 = \frac{x_2}{x_e} k = \frac{1.0}{0.5} k = 2k.$$

Therefore, the ideal conductivity for an ideal joint having perfect interface thermal contact is twice the conductivity of the plate material. This illustration does not take into consideration the additional cross-sectional area of the bolt head and nut which will contribute to the overall heat transfer area across a joint. The actual "ideal" conductivity may be in the neighborhood of 2.2k instead of 2.0k as is shown in Figure II-3.

All real joints will have conductivities less than the approximate ideal figure of 2.2k because real plate interfaces have irregularities which will resist the flow of heat across the interface. If the interface resistance is low and/or if the interface area of contact is large (two or three times as large as the joint cross-sectional area, A,) then the average temperature drop across the interface, ΔT_I, is small. The joint thermal conductivity will

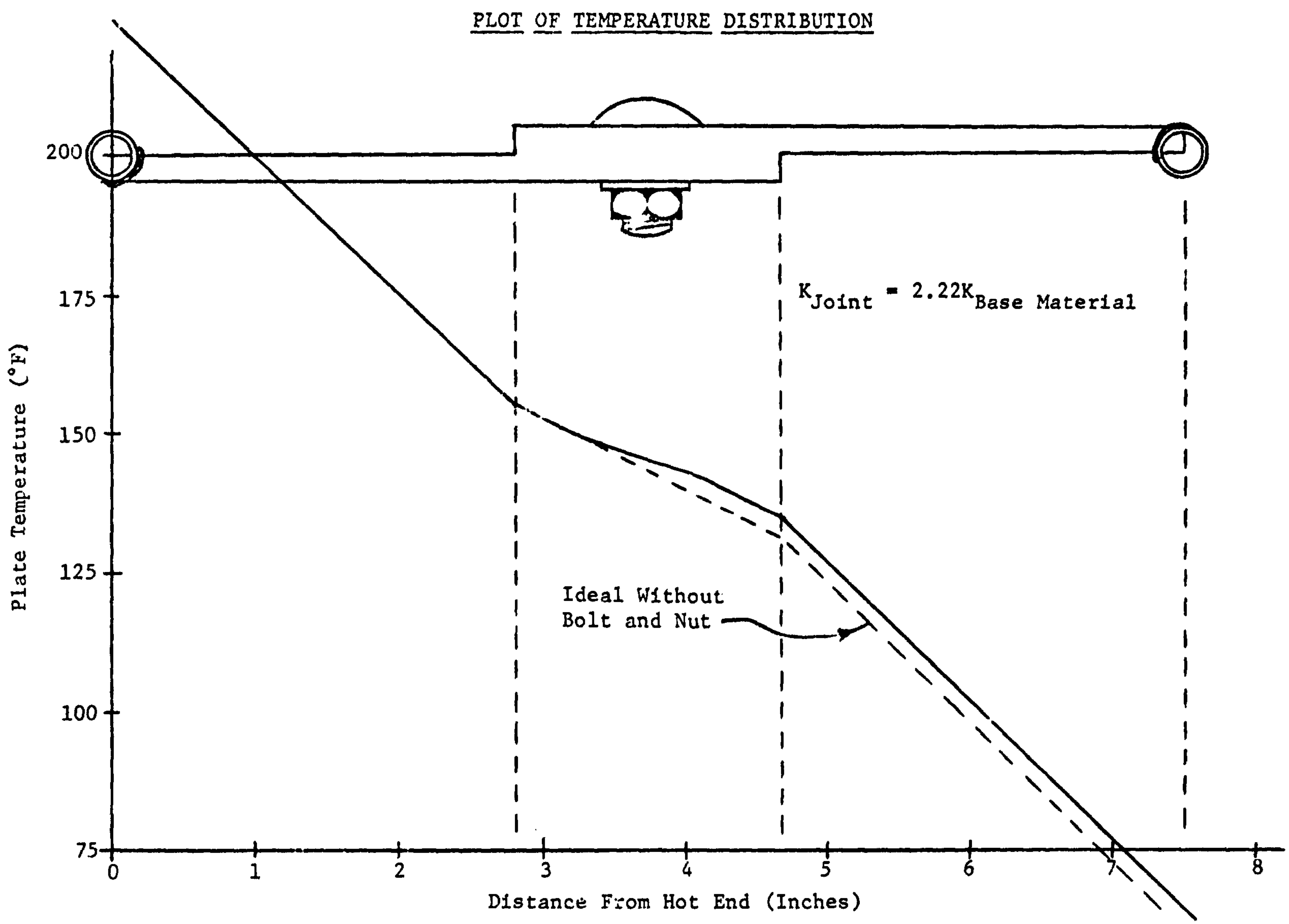

Figure II-3. Ideal joint with bolt and nut.

therefore be determined primarily by the conductivity of the plate material and the cross-sectional area of the joint and will approach the ideal conductivity of 2.2k. If ΔT_I is not small, then the joint thermal conductivity will be determined by both the plate thermal conductivity and the interface conductance. In this case the joint conductivity will be in the neighborhood of 1.5k, 1.0k, or 0.5k.

It must be pointed out that an interfacial material or fluid can greatly influence the interface conductance and, consequently, the joint conductivity. All data presented in this report will be from clean, bare metal interface surfaces in a vacuum environment. Reference 5 presents some data where interfacial materials are present. References 11 and 17 also worked with interfacial materials.

C. PHOTOELASTIC STUDY

One of the objectives of the deflection studies was to attempt to define the actual interface contact area for the test specimens. The outer radius of the contact zone, R_σ, would be the point at which the interface normal pressure became zero. Through the use of photoelasticity, a normal pressure distribution plot was made for a joint interface and R_σ was determined.

The model used for this study was composed of two plastic plates, 1/8" x 4" x 4", with a 1/4" button-head bolt at the center. A tensile load of 25 lbs. was used on the bolt, which corresponds to a 4800 lb. load on the metal plates used in this study. The stresses were frozen in the plastic plates at this load and the stress distribution, shown in Figure II-4, was obtained through photoelastic techniques. The values of normal stress on the ordinate scale have been scaled up to represent the stresses in metal plates.

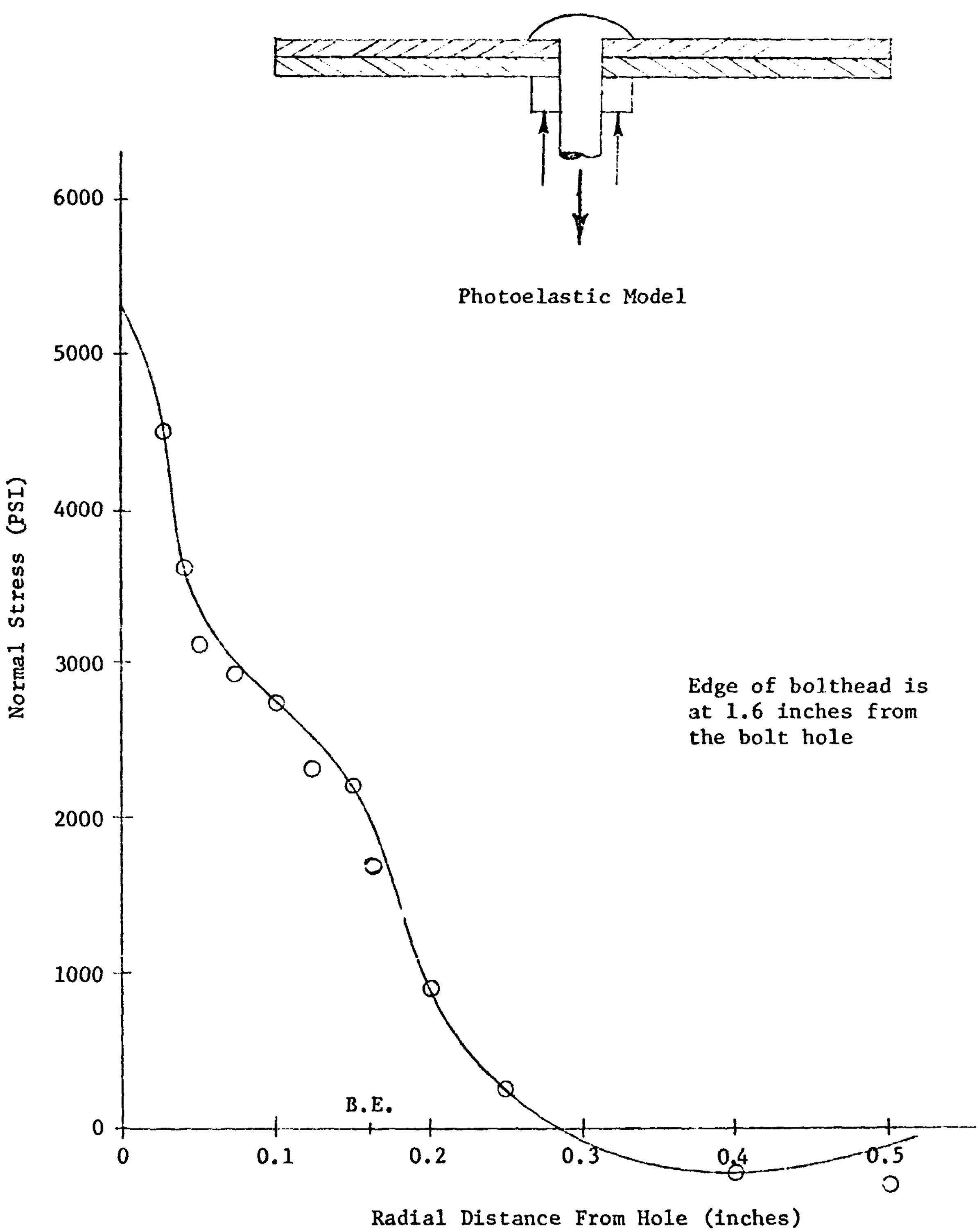

Figure II-4. Stress distribution for Photoelastic model

At a radial distance of approximately 0.28 inches from the bolt hole, the normal stress is zero. Outside this radius the compressive stress becomes a tensile stress. This was unexpected and thought to be strange. The same sort of tensile stress was found by E. Coker and L. Filon in a photoelastic study cited by Aron and Colombo in Reference 1. It was concluded in the photoelastic study conducted by Coker and Filon that the point of zero stress is independent of the load applied and was dependent only on the thickness of the beam. Aron and Colombo showed two photographs of identical photoelastic models where a small load was applied to the first model and a large load to the second. The area of contact is virtually constant for both loads.

Since only one load was used in this photoelastic study, no confirmation can be made as to the independence of the contact area to load. It is the opinion of this investigator that Aron and Colombo's conclusion is correct. Reference 7 also presented data which supports this conclusion.

The plate thickness and bolt diameters for the deflection test specimens were 3/16" and 3/8" respectively, which is in the same ratio as the photoelastic model. Therefore, to use the photoelastic results to determine the contact area for the deflection specimens, the radius of contact, R_σ, must be scaled up by 150%. R_σ from Figure II-4 is 0.28" plus the bolt hole radius R_s of 0.125". Therefore, the contact area, A_c, can be determined as follows:

$$
\begin{aligned}
A_c \text{ per bolt} &= \pi (R_\sigma^2 - R_s^2) \\
&= \pi (0.405^2 - 0.125^2) \text{ in}^2 \\
&= 0.466 \text{ in}^2.
\end{aligned}
$$

Since there are 3 bolts in the test joints, the total contact area is:

$$A_c = 3 \times 0.466 \text{ in}^2 = 1.40 \text{ in}^2.$$

This value of A_c can only be used as an approximate area because of the difference in joint configuration posed by the three bolts instead of one.

An important fact to be considered is the difference between the actual contact area, A_c, and the total interface area, A_I. A_I, which is 10.5 in^2 in this study, is considerably larger than A_c. Results obtained from machined blocks where plate deflections have not been included as a parameter and A_c is considered to be the same as A_I, cannot be used to predict the thermal conductivity of bolted joints.

III. EXPERIMENTAL PROCEDURES AND EQUIPMENT

A. TEST SPECIMENS

The test specimen decided upon for this study was a bolted lap joint as shown in Figure III-2. This joint configuration was chosen to simulate a large number of bolts or rivets in series along a lap joint (Figure III-1). This type of joint can be found on airplane or space vehicle side panels and in other structural applications. It

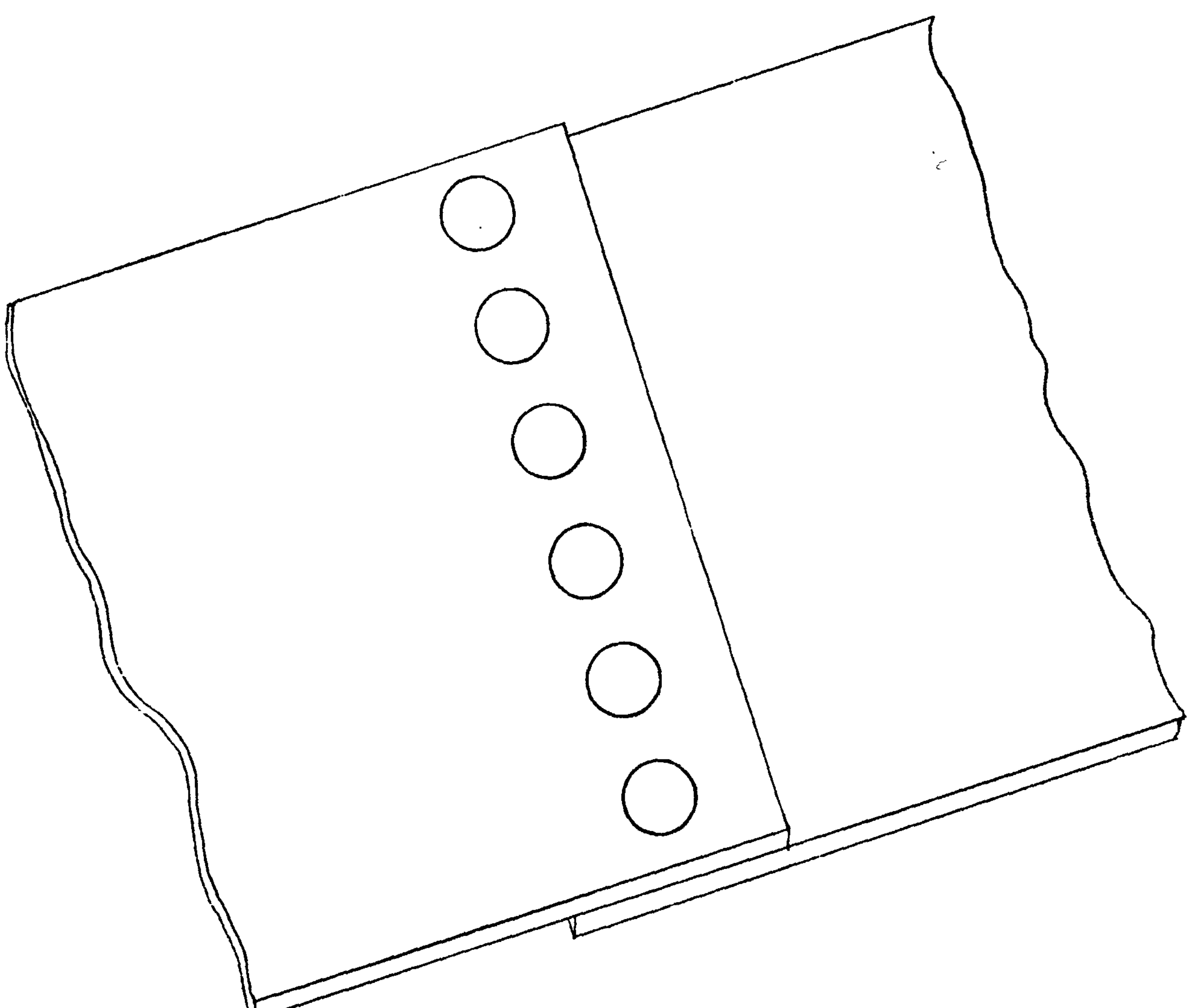

Figure III-1. Typical lap joint found on aircraft skins, etc.

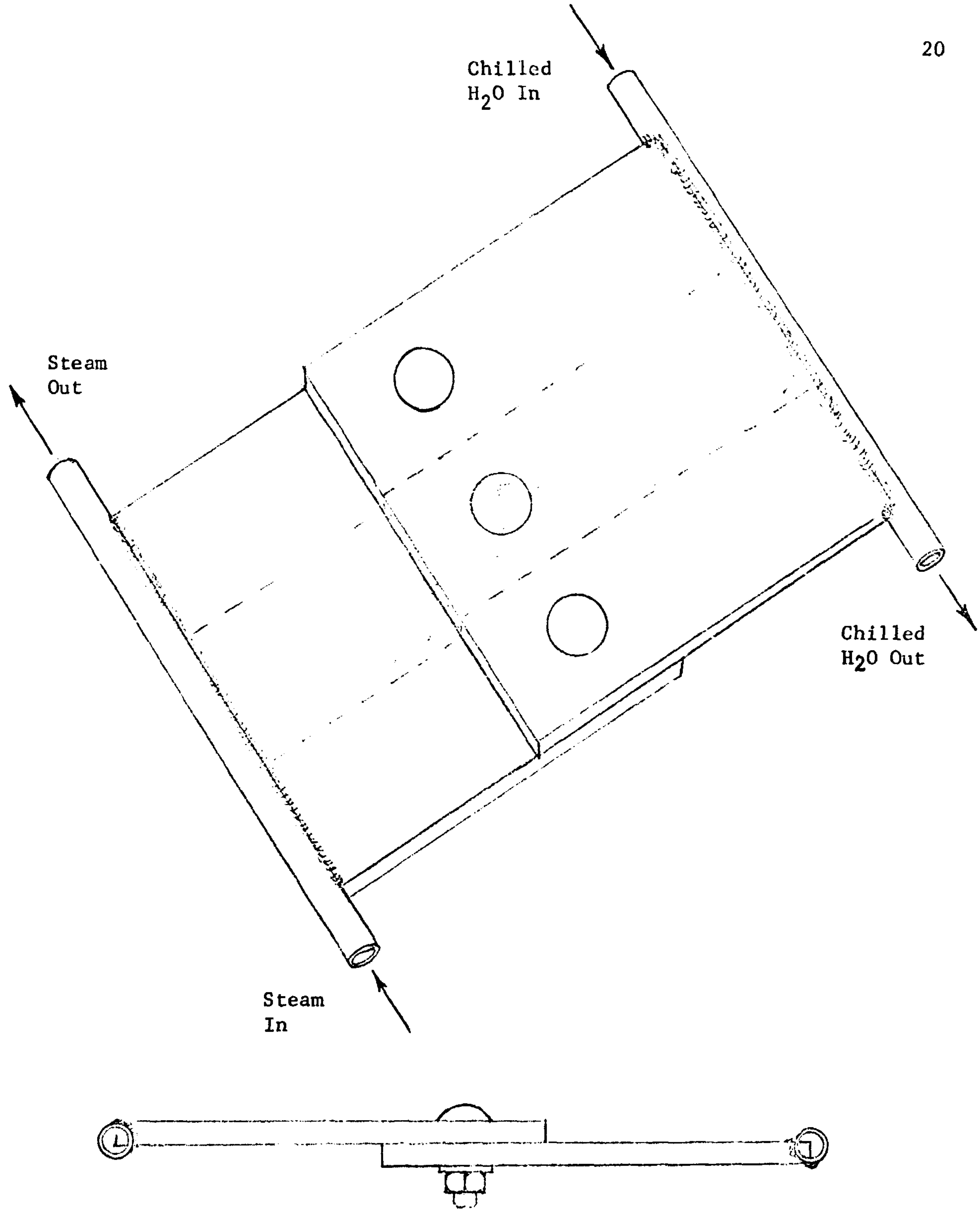

Figure III-2 Isometric veiw of test joint.

was decided that only three bolts in series were needed to produce an infinite joint affect on the center section (shaded area on Figure III-2). The center section of the joint was analyzed and the results obtained were assumed to be the same for all similar sections in an actual joint. The outer two sections were intended to provide the boundary conditions for the center section. The tubing on either end of the test plates was used to heat or cool the plate ends. Steam was passed through the hot end and chilled water at approximately 50°F through the cold end, giving an appropriate gradient of 162°F across the joint.

Six sets of test plates were constructed and studied. They are:

Test Plate No. 1 - Aluminum with 16 RMS

Test Plate No. 2 - Aluminum with 63 RMS

Test Plate No. 3 - Aluminum with 125 RMS

Test Plate No. 4 - Stainless Steel with 16 RMS

Test Plate No. 5 - Stainless Steel with 63 RMS

Test Plate No. 6 - Stainless Steel with 125 RMS.

The two types of materials were used to give an indication of the effect of plate material on plate deflections and joint conductivity. The three surface finishes were chosen to indicate the effect of surface finish on the same.

The bolts chosen were 3/8" National Coarse, Standard Button-head bolts constructed from 4140 carbon steel. The bolts and the plates were machined to close tolerances.

B. DEFLECTION STUDIES

The instrument used to measure plate deflections was an optical comparator (Figure III-3). Special jigs held the test specimen on the

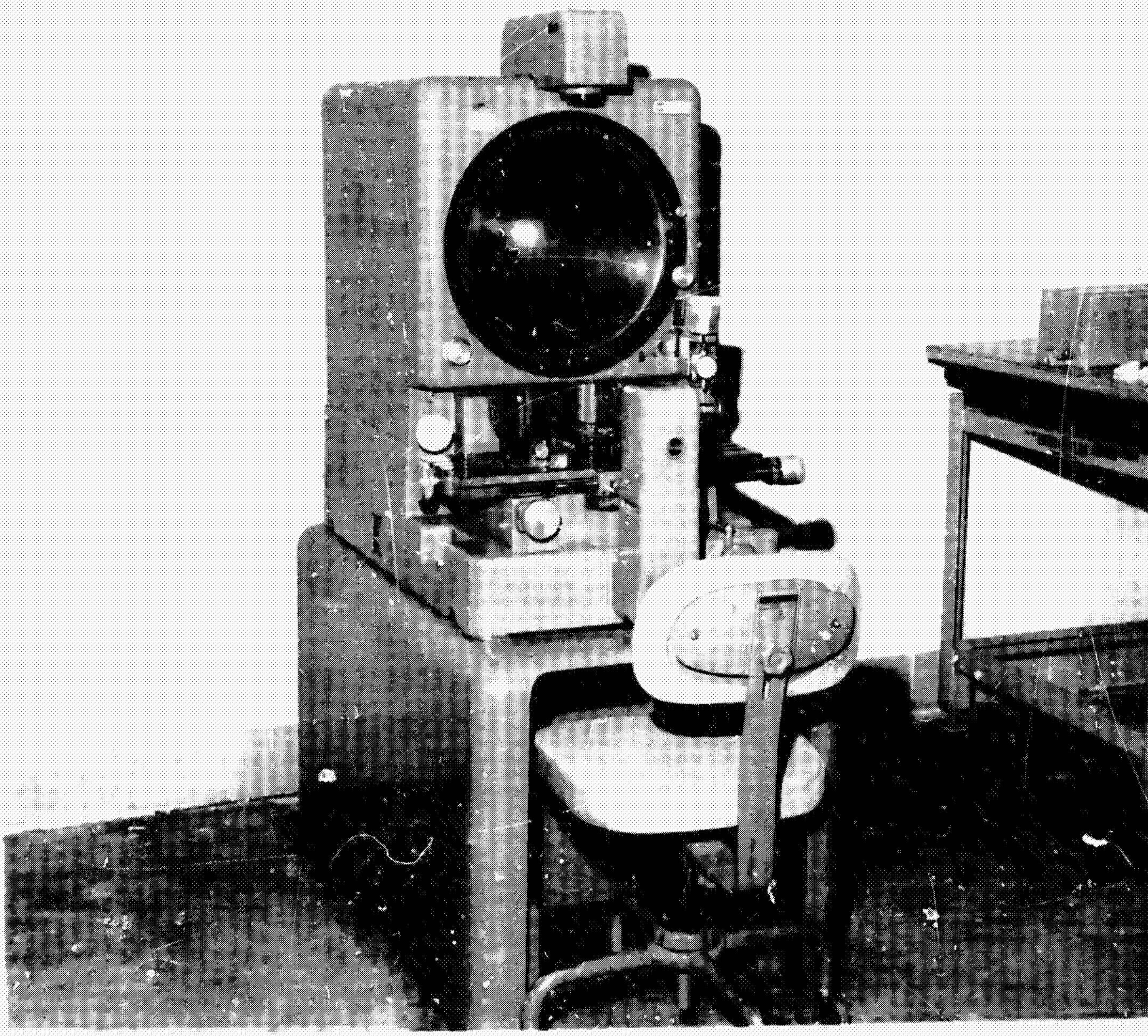

Figure III-3. Optical comparator.

comparator bed. In order to use this instrument, it was necessary to install point references on the surfaces of the test plates as shown in Figure III-4. For each pin on the top plate, there is a corresponding pin immediately below it on the bottom plate. The following procedure was used to obtain all deflection data.

The plates were bolted and torqued to 4 ft.lbs. The distance between the points of the pins was then measured for each pair of pins. The values obtained with 4 ft.lbs. of torque were used as references for determining the amount of deflection produced at a given pin location by a change in torque. This reference torque was chosen instead of a reference of 0 ft.lbs. because it was felt that initial and unpredictable reactions due to imperfections in the specimen must be overcome before meaningful data could be taken. Deflections for torques lower than 4 ft.lbs. can possibly be determined by extrapolation. The torque could then be increased to a new value and the values of pin distance again measured on the optical comparator.

There are three types of deflections that must be taken into consideration. Unlike previous studies, this project measured and considered all three. The first type of deflection will be called "creep", which is the change in deflection caused by passing time. It was speculated at the beginning of this study that there would be a transient response of the test specimen to the torquing operation. A study was undertaken to determine the existance of this creep, and if it did exist, to determine the magnitude and direction of the deflection change, the rate of creep, and the time required for the total creep to occur.

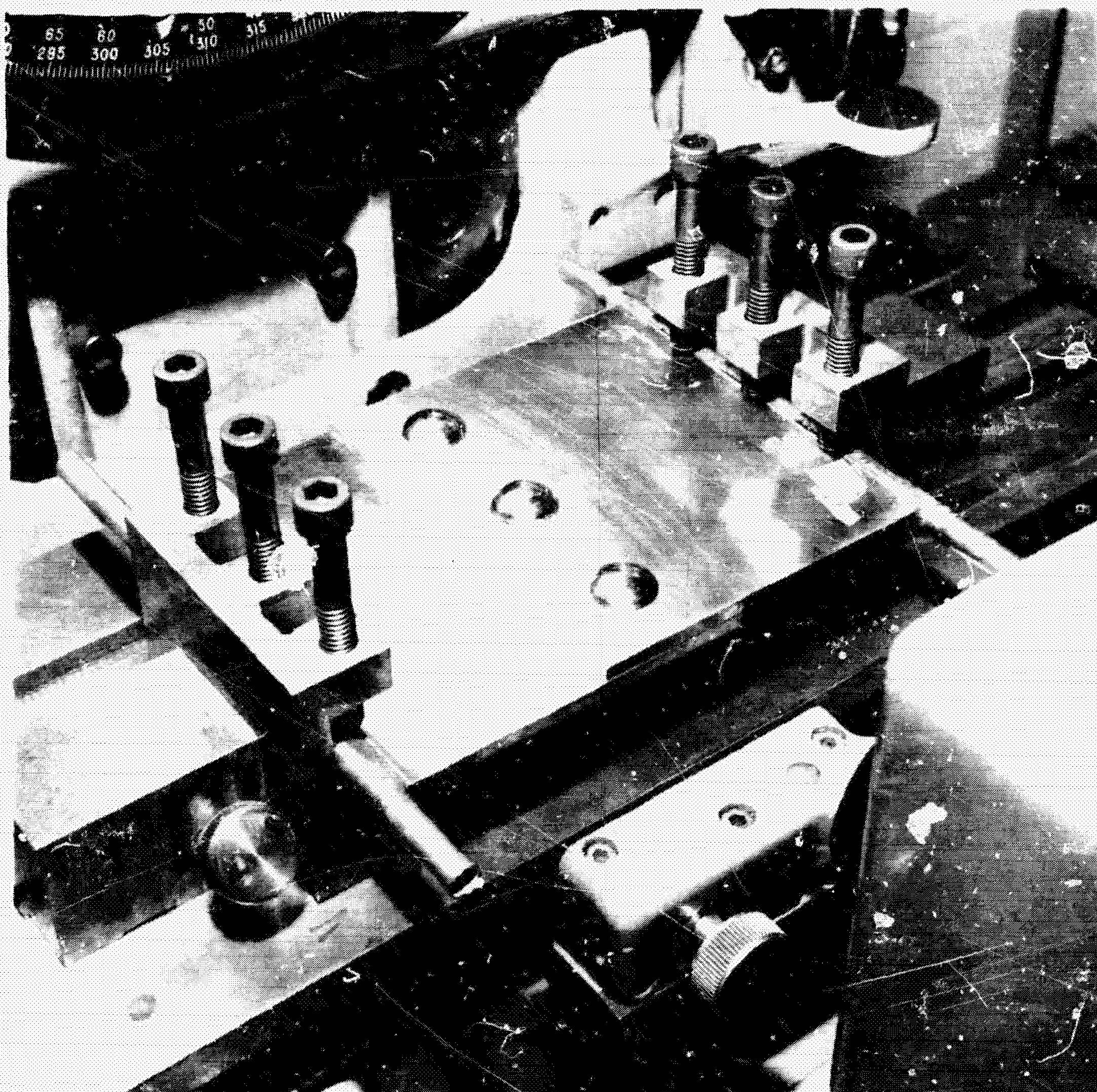

Figure III-4. Test specimen in optical comparator jig.

Since establishing a total time requirement for creep was the only necessity for this project, it was decided that only one of the six test specimens need be included in our study. The aluminum plate with the 125 RMS finish (Specimen number 3) was chosen since preliminary measurements indicated that it would have the greatest magnitude of creep and the longest total time requirement.

Specimen number 3 was torqued to 4 ft.lbs. at time = 0 and the values of pin distance read on the comparator. These values were used as a reference and at various time intervals the deviation from this reference was determined on the comparator. After the rate of creep had diminished to zero, the bolts were untorqued, retorqued to 25 ft.-lbs., and measurements taken as before. Once the total time required for creeping was determined, the test specimens could be torqued sufficiently in advance to allow them to creep before any testing was done.

The second type of deflections considered are "mechanical deflections", which are caused by the pressure applied by torquing the bolt. Most previous studies have limited their scope to this mode of deflection and have ignored the effect of creep and thermal deflections. Mechanical deflections do require the most extensive efforts.

The free body diagram shown in Figure III-5 indicates the moment produced by the bolt head and interface stresses. The resultants of these stresses are represented by F_1 and F_2. The moment produced by these two forces will cause the plate to deflect. The majority of the deflection work was directed towards determining these deflections as a function of torque, distance from bolt, and surface finish. Each of the six specimens were torqued to the reference torque of 4 ft.lbs. and

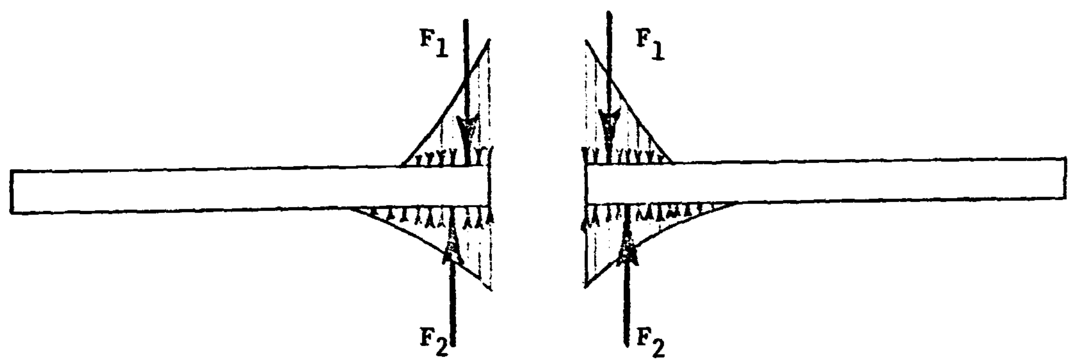

Figure III-5. Free body diagram of a plate with the distributed load.

after the required time for creeping, reference values for pin distances were read as before. The plates were then retorqued to 10 ft.lbs. and again allowed to creep. The deflections caused by the increase in torque were measured. The same procedure was followed for torques of 16, 22, and 28 ft.lbs. This data was analyzed to determine the plate deflection as a function of torque, plate material, and surface finish.

The third type of plate deflections considered were "thermal deflections", which are produced when a thermal gradient is applied to the joint. Initially, the specimens were torqued to 28 ft.lbs. and pin reference values read. A temperature gradient was then applied to the specimen by means of an apparatus which allowed steam at 212°F to flow across one end and chilled water at 50°F across the other. The deflection produced by this thermal load was measured for each pin position.

C. THERMAL CONDUCTIVITY MEASUREMENTS

Upon completion of the deflection studies, the pins were removed from each test specimen and all plate surfaces were cleaned thoroughly.

Foil thermocouples (RdF Corporation part number 20114-L10) were placed on the plates in the approximate positions shown in Figure III-6. The actual position of each thermocouple was measured after installation. The positions in the region of plate-overlap were not needed for the EFM calculations, but temperatures were recorded at these points for possible future interface conductance studies and to provide some insight into the heat paths and isotherms in the area of the bolt. In the joint region there is a thermocouple on the side of the joint opposite the ones shown. The inlet and outlet temperatures of the coolant and the heating streams were continually monitored.

The instrumented specimen was placed in a Tenny vacuum chamber (Figures III-7, III-8, and III-9) and situated on a plastic bucket such that the rim of the bucket contacted only the rubber supply lines to the heating and cooling tubes. The specimen was also encased in aluminum foil (not shown in Figure III-9) to guard against radiation losses. Heating was accomplished by using 212°F steam and cooling by using chilled water at 50°F, as was done in the thermal deflection studies.

Each specimen was torqued at 4, 16, and 28 ft.lbs., and temperature distributions were obtained for each torque. Specimen number 2 was not used in the thermal conductance studies because the regions under the nuts and bolts were plastically deformed when an attempt was made to obtain deflection data at a high torque value.

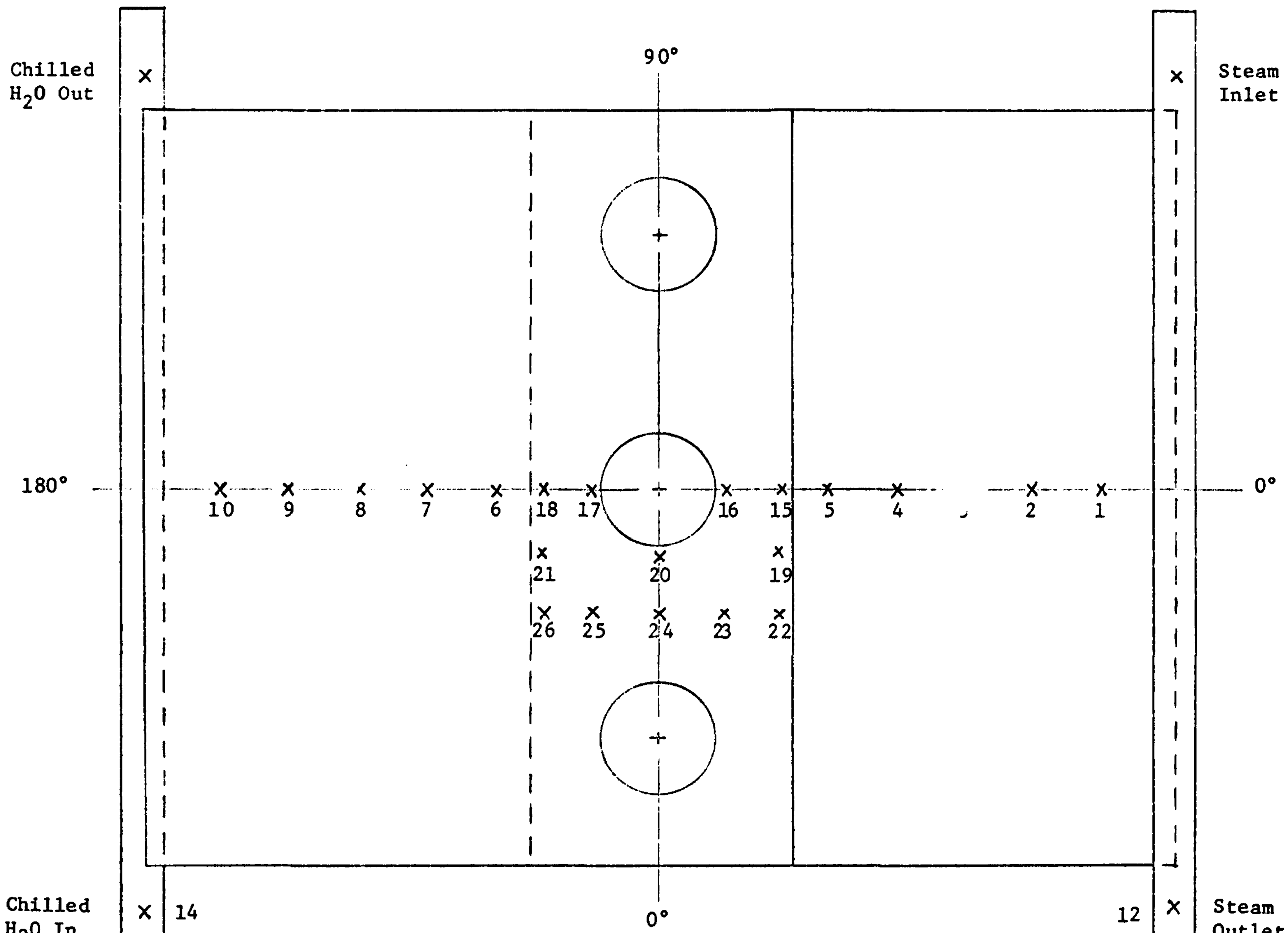

Figure III-6. Thermocouple Locations. (Figure drawn to scale)

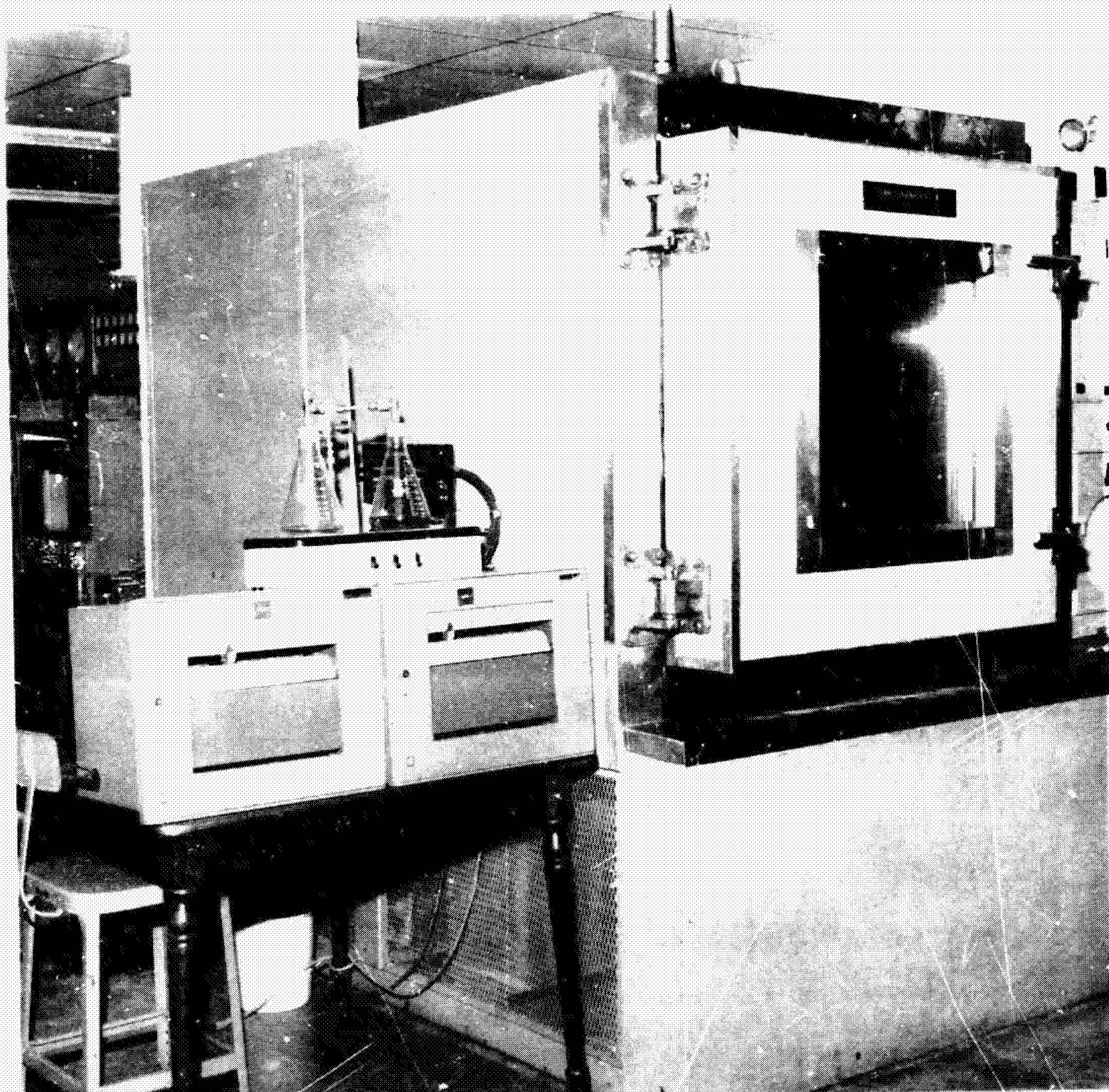

Figure III-7. Tenny vacuum chamber showing the heating and recording systems.

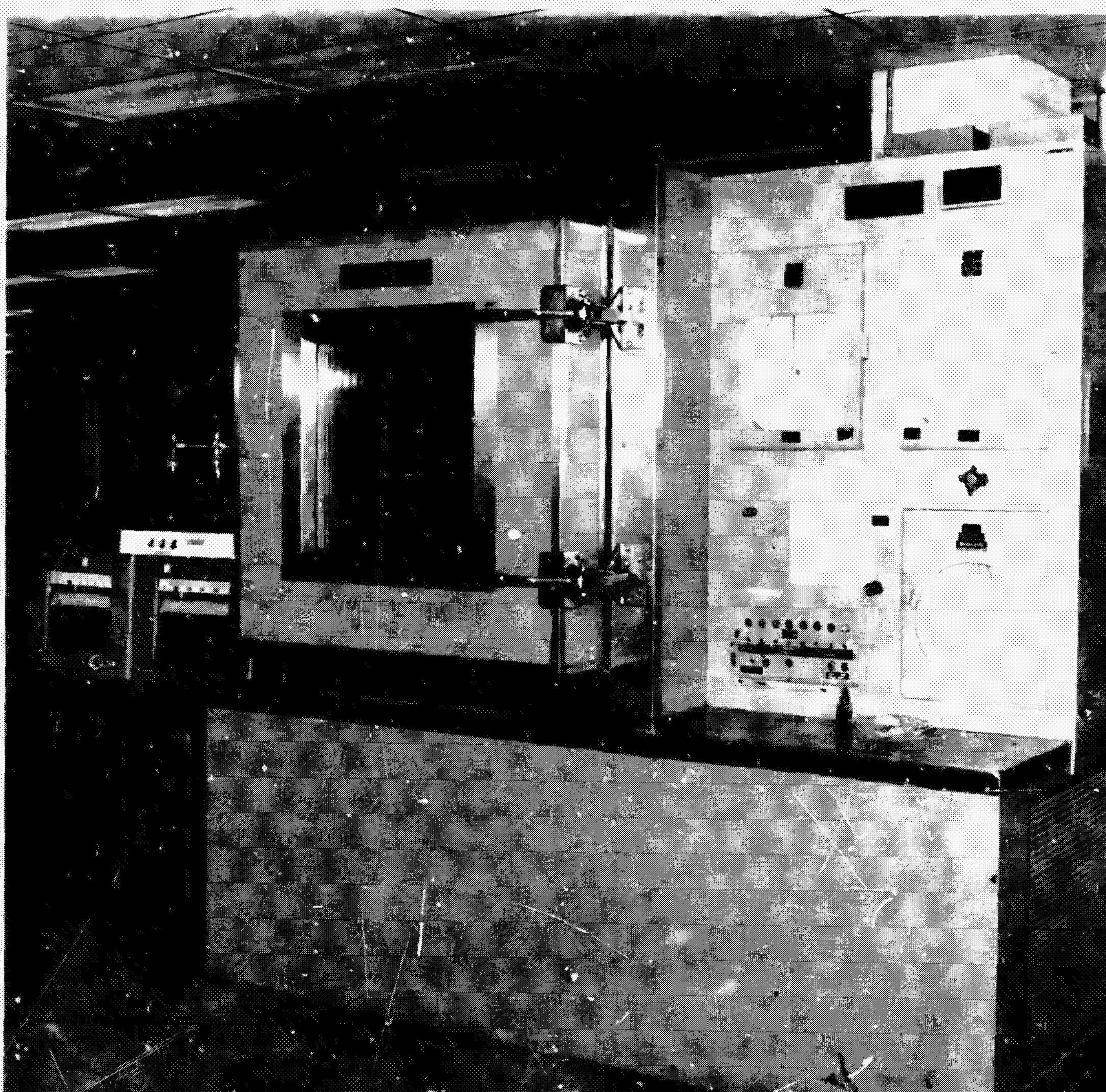

Figure III-8. Tenny vacuum chamber showing chamber and controls.

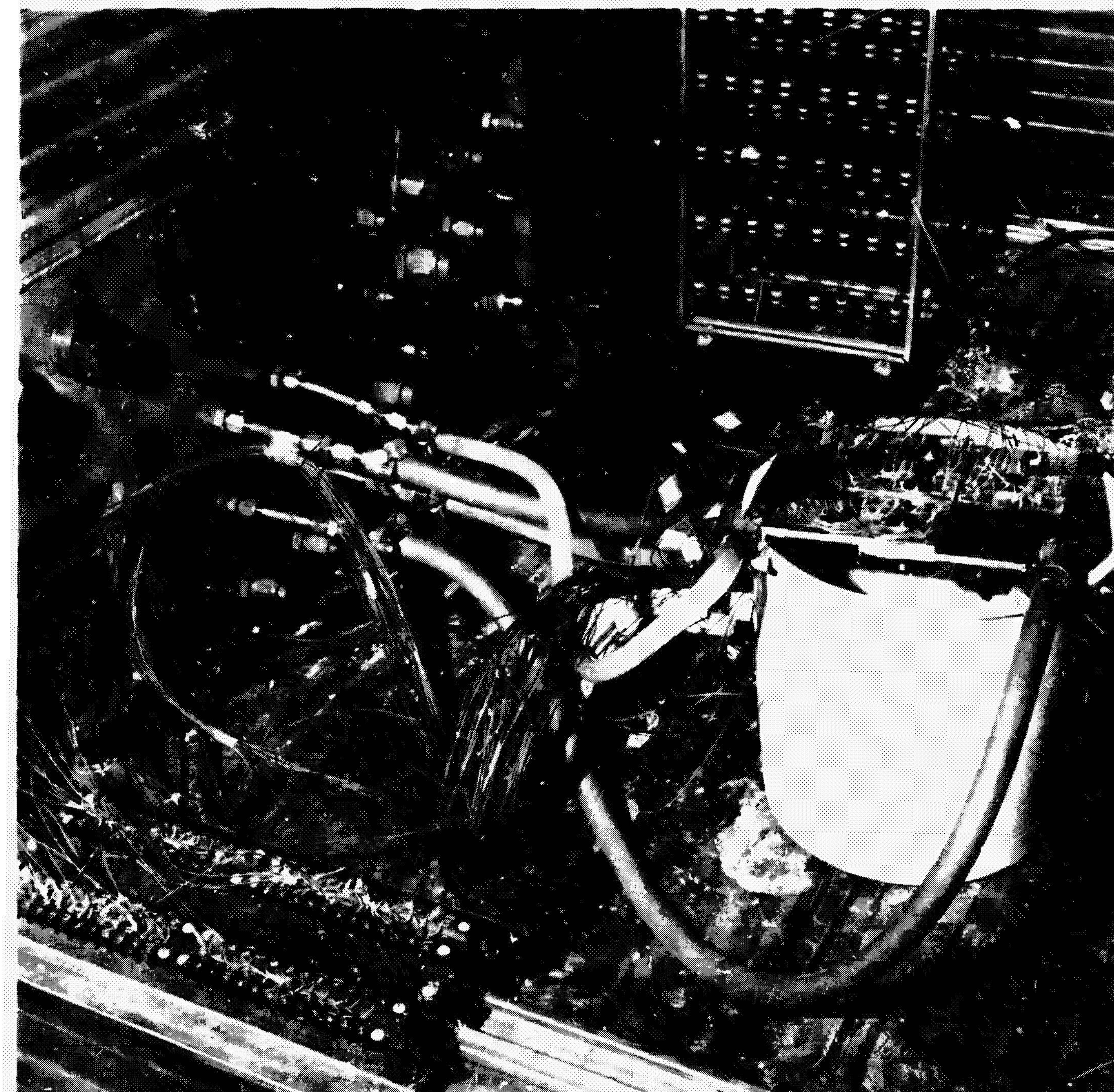

Figure III-9. Test specimen in vacuum chamber.

IV. DATA PRESENTATION AND DISCUSSION

A. DEFLECTION STUDY RESULTS

Initially, the intent of the investigation was to obtain qualitative rather than quantitative data in the deflection studies. It was felt that the optical comparator would provide the necessary accuracy. However, the deflections encountered were much smaller than had been anticipated and only through a quantitative look at the data could useful information be obtained. The average mechanical deflection for an aluminum specimen was only 3×10^{-4} inches and less than 1×10^{-4} inches for stainless steel. Since the accuracy that could be expected for a single deflection reading from the comparator was on the order of 1×10^{-4} inches, the basic data had a considerable amount of scatter. The same holds true for the creep and the thermal deflection data even though the absolute magnitude of the thermal deflections are on the order of 6×10^{-4} inches. To offset the scattering, symmetrical averaging and overall averaging techniques on particular parameters were used, and the deflection study data were generalized to give meaningful results.

Creep

The purpose of the creep study was to determine the time required for normalization of the creep reaction. This information was necessary to enable the researchers to allow the specimens to creep after torquing before any measurements were taken. This eliminated the effect of creep from the data being measured.

It was decided that Specimen 3 (125 RMS aluminum) would creep longer and to a greater extent than any other specimen; thus, tests were conducted using this plate. Torques of 4 and 25 ft.lbs. were used to show the effect at a low and high torque. The data obtained is presented in Tables IV-1 and IV-2 in basic form. There is considerable scatter in the data due to the small magnitudes involved; therefore, a quantitative approach was used to analyze the data. There was apparently no relation between creep and position on the plate, so all data taken at a particular elapsed time for a given torque was averaged and plotted on the time versus creep plot shown in Figure IV-1. This plot shows that after 36 hours the change in plate deflections due to creep is zero. The magnitude of creep is greater for 25 ft.lbs. of torque, but the time required for stabilization is virtually the same.

It was concluded from the creep study that a normalization time of 36 hours would be required after each torquing operation.

Mechanical Deflections

The mechanical deflection data is tabulated in basic form in Tables IV-3, IV-4, and IV-5. The only averaging done to this data was in combining repetitive readings for the same pin pair and in averaging symmetrical pin pairs between the bolt heads, i.e., pin positions 1 and 10, 2 and 9, etc. at 90°, were averaged to obtain data for positions 1, 2, etc. at 90° respectively and similarily at 270°. The negative numbers indicate a decrease in the distance between the tips of a pin pair and the positive numbers indicate a increase. The scatter is apparent, but it is easy to see the effect of torque and radial distance. The

CREEP DATA

Time Lapse (hrs.)	5	24	29	28
$\phi = 0°$				
Pin No. 1	-8	-26	-6	4
Pin No. 2	-2	-4	13	14
Pin No. 3	13	12	13	12
Pin No. 4	5	12	17	22
Pin No. 5	12	25	26	21
$\phi = 90°$				
Pin No. 1	-2	8	12	12
Pin No. 2	-8	7	15	7
Pin No. 3	8	1	2	-3
Pin No. 4	-2	21	15	13
Pin No. 5	9	19	24	15
$\phi = 180°$				
Pin No. 1	6	4	-2	17
Pin No. 2	14	10	3	17
Pin No. 3	7	8	2	18
Pin No. 4	-8	-13	-1	1
Pin No. 5	12	7	1	15
$\phi = 270°$				
Pin No. 1	11	0	9	7
Pin No. 2	15	5	9	18
Pin No. 3	7	-1	-7	-2
Pin No. 4	22	19	0	9
Pin No. 5	-3	2	-5	4

(Deflections are given in 10^{-5} inches)

Table IV-1. Creep Data at a Torque of 4 ft.lbs.

CREEP DATA

Time Lapse (hrs.)	5	24	29
$\phi = 0°$			
Pin No. 1	40	34	41
Pin No. 2	9	22	21
Pin No. 3	-12	-14	-22
Pin No. 4	-7	5	-2
Pin No. 5	14	34	24
$\phi = 90°$			
Pin No. 1	35	35	
Pin No. 2	15	25	
Pin No. 3	11	26	
Pin No. 4	12	32	
Pin No. 5	-5	16	
$\phi = 180°$			
Pin No. 1	30	22	34
Pin No. 2	-7	-8	-2
Pin No. 3	20	14	25
Pin No. 4	10	4	6
Pin No. 5	-1	11	25
$\phi = 270°$			
Pin No. 1	4	-10	
Pin No. 2	0	4	
Pin No. 3	15	14	
Pin No. 4	12	4	
Pin No. 5	-14	-8	

(Deflections are given in 10^{-5} Inches)

Table IV-2. Creep Data at a Torque of 25 ft.lbs.

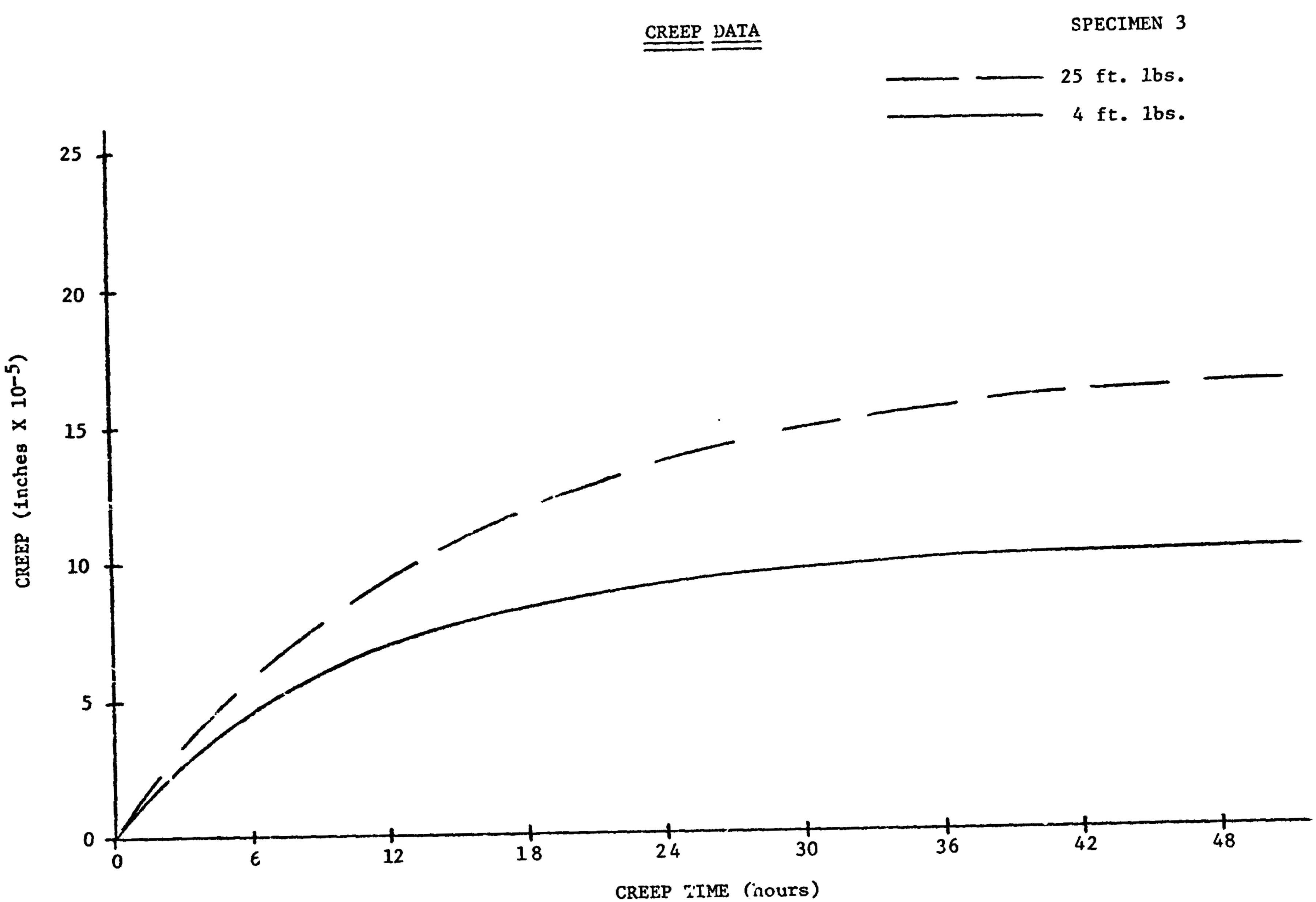

Figure IV-1. General representation of the response of the specimen as a function of time.

Plate # 1

Angle	Torque	Pin Number 1	2	3	4	5
0	10	-29	[illegible]	15	-6	-2
	16	2	20	35	32	37
	22	-1	10	30	21	54
	28	20	24	66	63	88
180	10	0	3	-9	1	14
	16	11	13	14	16	36
	22	13	30	28	26	50
	28	37	44	37	38	73
90	10	0	7	5	12	-4
	16	47	35	32	42	15
	22	40	38	39	40	22
	28	50	42	54	56	48
270	10	17	8	12	8	25
	16	35	25	39	40	45
	22	29	26	42	50	56
	28	52	31	60	51	60

Plate # 2

Angle	Torque	Pin Number 1	2	3	4	5
0	10	-31	-28	[illegible]	7	-7
	16	-5	8	[illegible]	34	41
	22	36	20	81	106	147
	28	--	--	--	-	--
180	10	26	14	13	-26	32
	16	43	27	56	-28	68
	22	39	41	44	10	75
	28	--	--	--	--	--
90	10	6	21	6	-2	17
	16	25	--	30	23	34
	22	25	--	22	15	20
	28	--	--	--	--	--
270	10	18	7	33	32	27
	16	24	23	39	42	40
	22	16	15	25	34	27
	28	--	--	--	--	--

Table IV-3 Tabulation of Mechanical Deflection data for plates 1 and 2. Angle is the angular position in degrees, torque is in ft. lbs., and the deflections in 10^{-3} inches.

Plate # 3

Angle	Torque	Pin Number 1	2	3	4	5
0	10	23	17	-4	32	21
	16	23	28	14	39	33
	22	12	34	36	71	84
	28	13	41	37	73	74
180	10	13	37	25	20	42
	16	9	31	38	11	43
	22	28	59	80	25	77
	28	36	73	84	28	99
90	10	29	27	27	33	31
	16	25	24	34	42	35
	22	34	50	47	56	59
	28	42	50	43	56	59
270	10	--	32	28	20	23
	16	--	30	28	27	35
	22	--	31	40	42	51
	28	--	47	55	52	56

Plate # 4

Angle	Torque	Pin Number 1	2	3	4	5
0	10	-17	8	-29	1	5
	16	-18	8	-12	5	12
	22	-14	28	21	23	55
	28	-10	27	37	29	67
180	10	24	19	40	14	-6
	16	42	11	47	10	11
	22	40	27	75	6	-8
	28	27	23	71	17	17
90	10	-5	-7	-3	-1	2
	16	-17	-10	-2	-5	-3
	22	-3	-10	-8	-5	-1
	28	-5	-4	2	-6	9
270	10	-4	1	-9	-11	-7
	16	-2	2	-7	-4	10
	22	5	6	-1	-7	--
	28	3	8	3	4	3

Table IV-4 Tabulation of Mechanical Deflection data for plates 3 and 4. Angle is the angular position in degrees, torque is in ft. lbs., and the deflections in 10^{-5} inches.

Plate # 5

Angle	Torque	Pin Number 1	2	3	4	5
0	10	-14	-13	-9	-18	-9
	16	-10	-3	-1	-7	-3
	22	1	-12	-9	-2	-5
	28	15	-18	-10	2	-4
180	10	-31	8	-30	-11	-29
	16	9	29	-22	-14	-34
	22	-11	25	-22	-17	-23
	28	-14	49	-21	-5	-18
90	10	--	7	5	2	7
	16	--	7	--	7	8
	22	--	9	9	10	17
	28	--	8	7	7	15
270	10	-18	-6	-8	13	-6
	16	-2	8	1	27	4
	22	-3	8	11	17	7
	28	-28	12	20	31	17

Plate # 6

Angle	Torque	Pin Number 1	2	3	4	5
0	10	-4	8	12	31	5
	16	4	28	12	28	19
	22	-4	5	-2	30	28
	28	-9	3	2	32	39
180	10	-30	-13	-6	-6	-7
	16	-23	-8	-12	9	5
	22	-38	-8	-14	-14	18
	28	-33	-12	-1	1	22
90	10	15	2	5	-9	-14
	16	6	-2	--	-2	-11
	22	--	8	5	1	1
	28	--	--	--	--	--
270	10	6	-9	1	4	5
	16	15	-5	9	12	10
	22	16	-10	2	17	11
	28	--	--	--	--	--

Table IV-5 Tabulation of Mechanical Deflection data for plates 5 and 6. Angle is the angular position in degrees, torque is in ft. lbs., and the deflections in 10^{-5} inches.

deflection increases as torque increases and as the radial distance from the bolt hole increases.

The first step in the quantitative analysis of the mechanical deflection data was to determine the general effect of torque on the deflections. To accomplish this, all deflections taken for all pin locations on all three aluminum specimens at a given torque were averaged and plotted as shown in Figure IV-2. This clearly shows the increase in deflection is a linear function of torque and that torque is a major variable which must be considered when investigating plate deflections. The same plot was made for the three stainless steel specimens and the results are shown in Figure IV-3. This plot is nonlinear at small torque values, suggesting that the plot for the aluminum specimens may be nonlinear in the same fashion at torques below 4 ft.lbs. Figures IV-2 and IV-3 indicate the difference in deflection magnitudes between the aluminum and the stainless steel specimens.

The next step in the analysis was to determine the influence of surface finish on deflections. This was done by plotting torque versus deflection curves for each of the six specimens. All deflections measured at a given torque for each specimen were averaged and plotted. The results for the aluminum specimens is presented in Figure IV-4 and for stainless steel in Figure IV-5. The conclusion drawn from these plots is that the influence of surface finish is small and may be neglected if an accuracy greater than 1×10^{-4} inches is not required. It also appears that the trend of this influence is that the greater the surface roughness, the greater the deflections.

DEFLECTION DATA

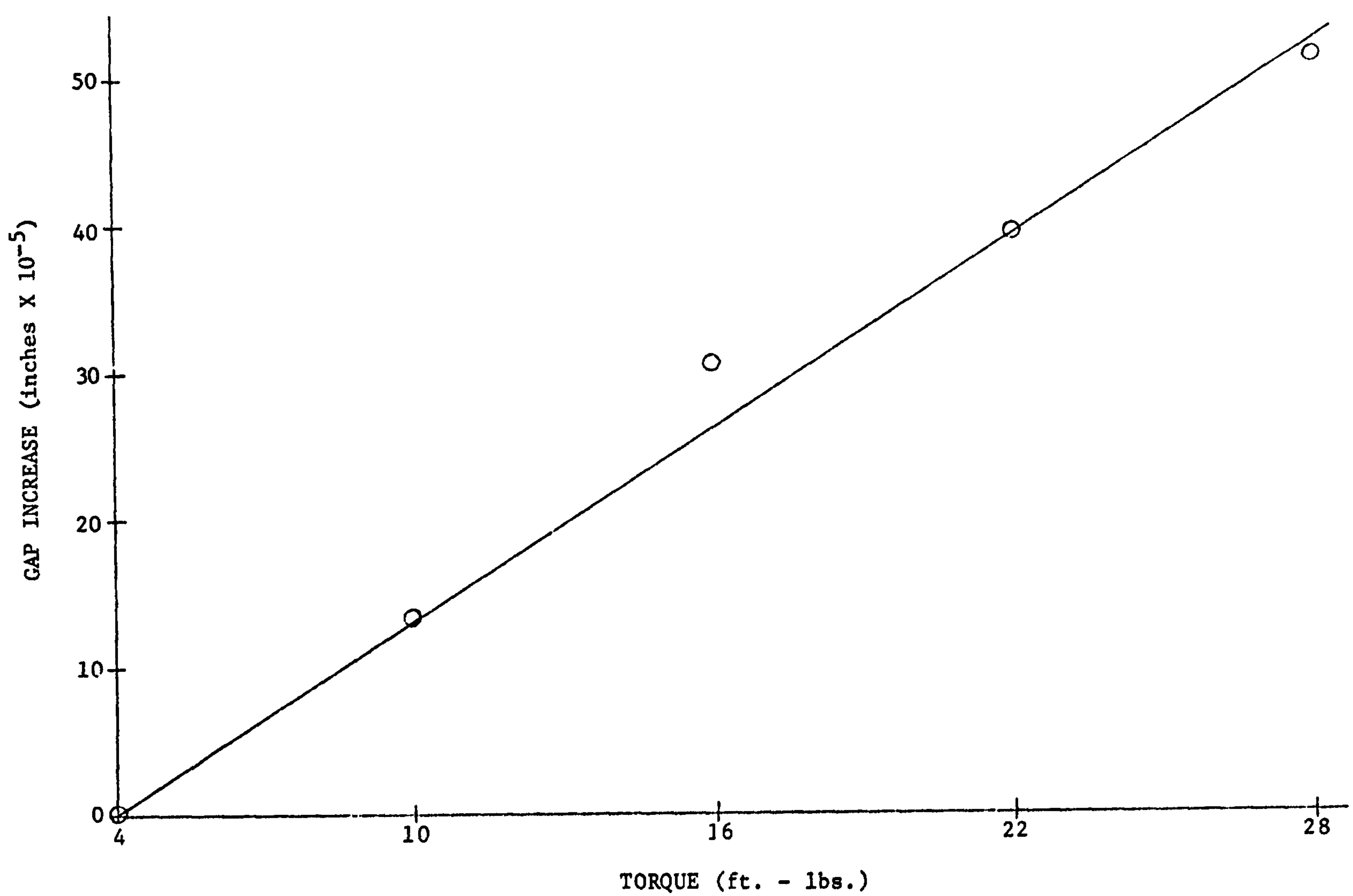

Figure IV-2. Plot of the average of all mechanical deflections at a given torque of all aluminum specimens.

DEFLECTION DATA

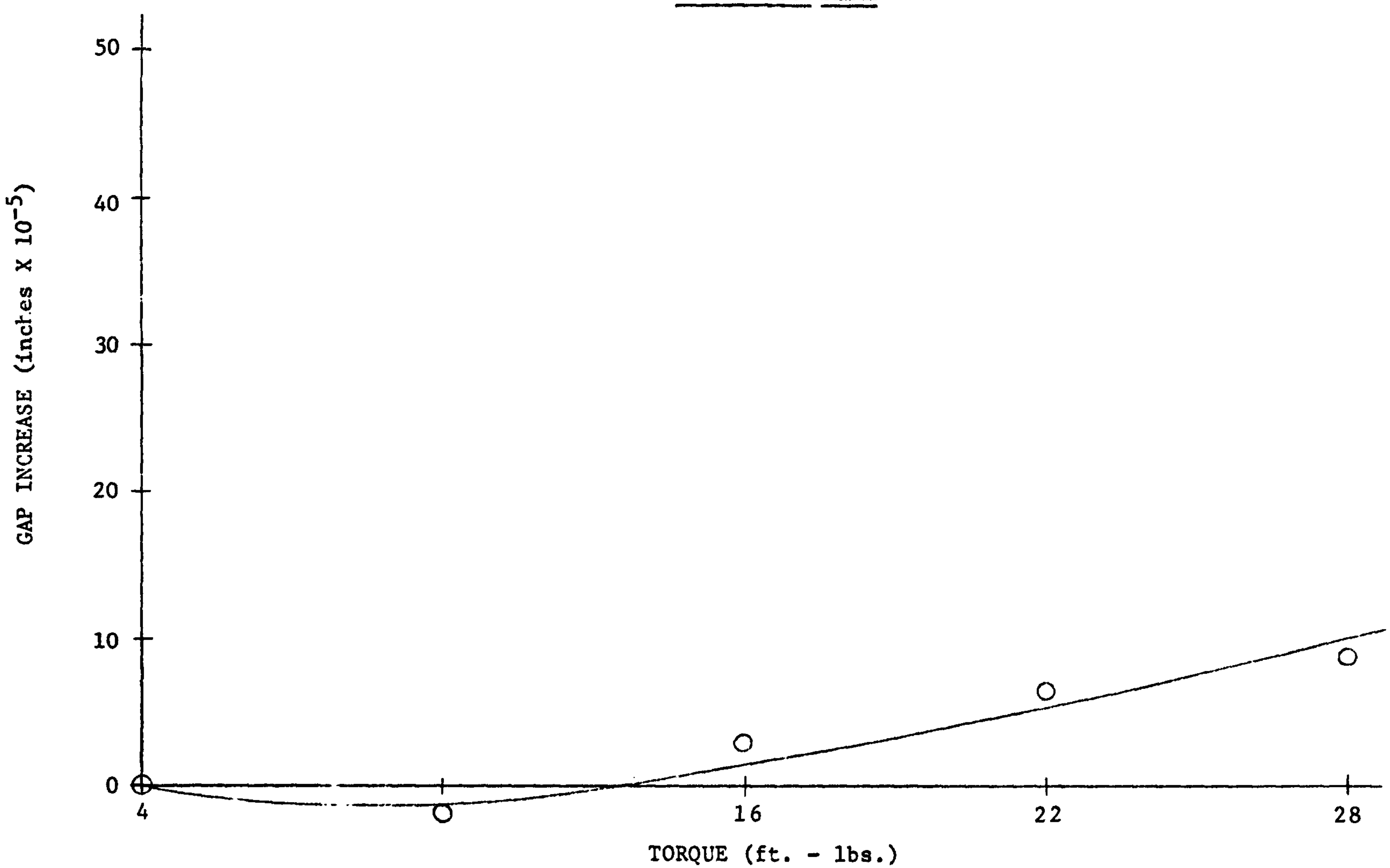

Figure IV-3. Plot of the average of all mechanical deflections at a given torque for all stainless steel specimens.

DEFLECTION DATA

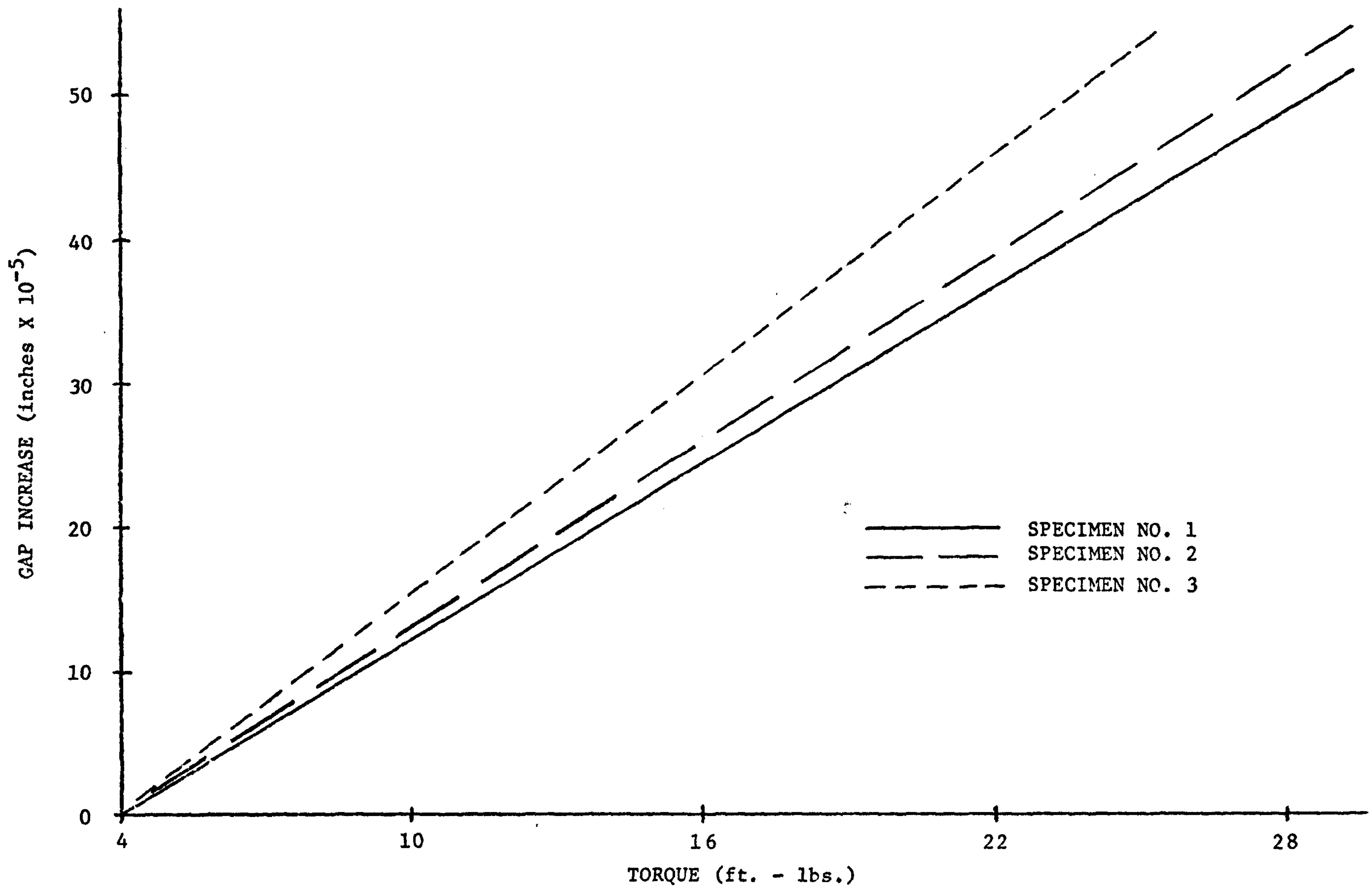

Figure IV-4. Generalized plot indicating deflection trends of the Aluminum Specimens as functions of Torque and Surface finish.

DEFLECTION DATA

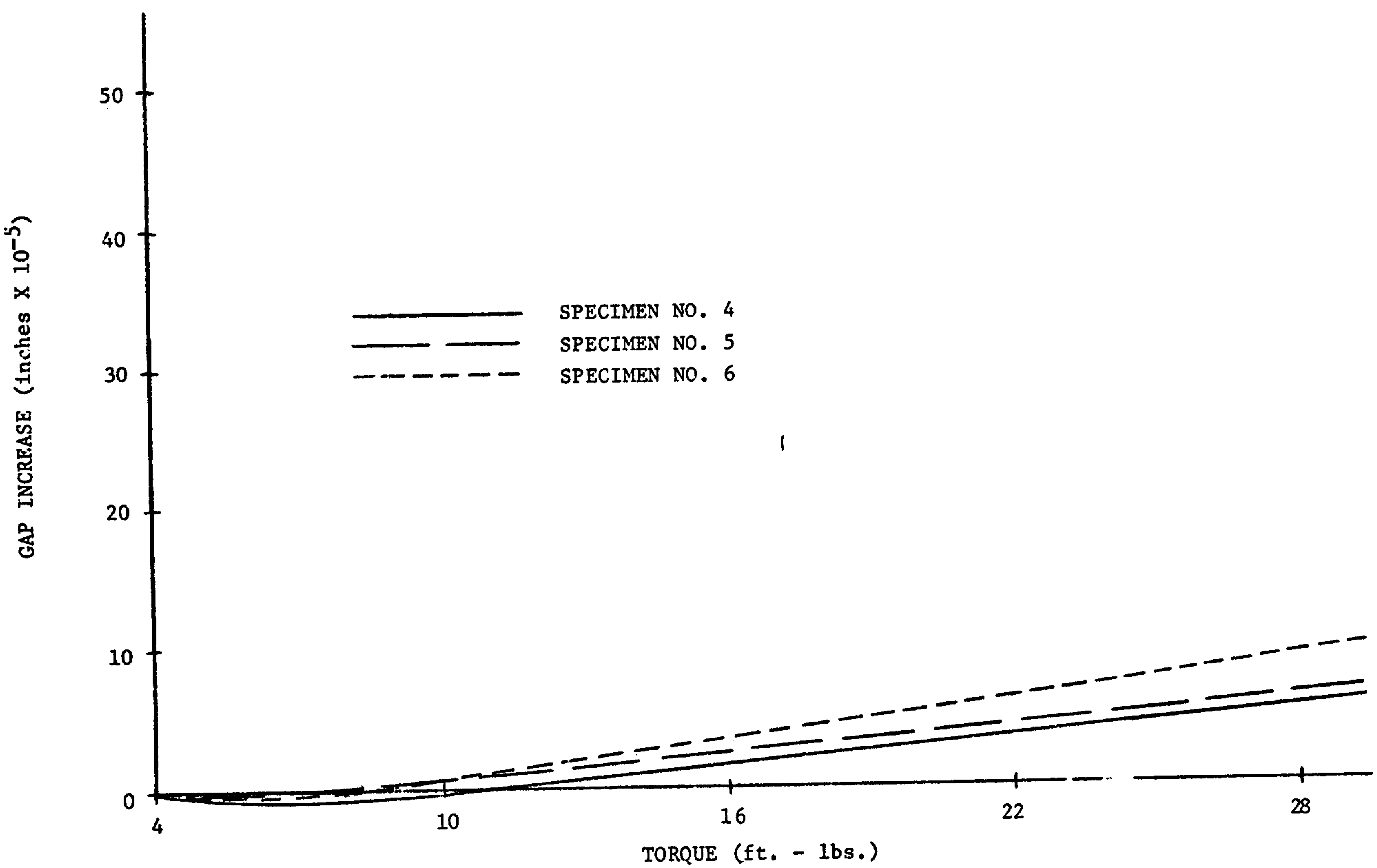

Figure IV-5. Generalized plot indicating deflection trends of the Stainless Steel Specimens as functions of Torque and Surface finish.

The final step in the analysis was to define the deflections as functions of pin position. Since the influence of surface finish was found to be small, the results of all three aluminum specimens were again averaged to reduce the scatter in the basic data. The deflections for radial positions 0° and 180° were expected to be different for those at 90° and 270°; therefore, the positions were analyzed separately. All deflections measured at pin location 1 for 0° and 180° radial positions on all aluminum specimens were averaged. These values, along with the averages obtained in a similar manner for pin locations 2 through 5, were plotted to obtain curve number 1 in Figure IV-6. Curve number 2 was obtained using radial positions at 90° and 270° for all aluminum specimens. Curves 3 and 4 were from the stainless steel specimens using 0° and 180° radial positions and 90° and 270° radial positions respectively. All of the curves indicate an increase in deflection as the radial distance from the bolt hole increases, but only curve 1 shows a large increase. It is reasonable to assume that the slopes of curves 1 and 3 would be greater than the slopes of curves 2 and 4 respectively, because curves 1 and 3 are plotted towards free edges where curves 2 and 4 have restrained edges. This slope difference for the stainless steel specimens is hard to ascertain since the deflections involved are so small.

Thermal Deflections

The objective of the thermal deflection study was to determine the effect, if any, of a thermal gradient across the joint on plate deflections. It was found that there was indeed an effect and that

DEFLECTION DATA

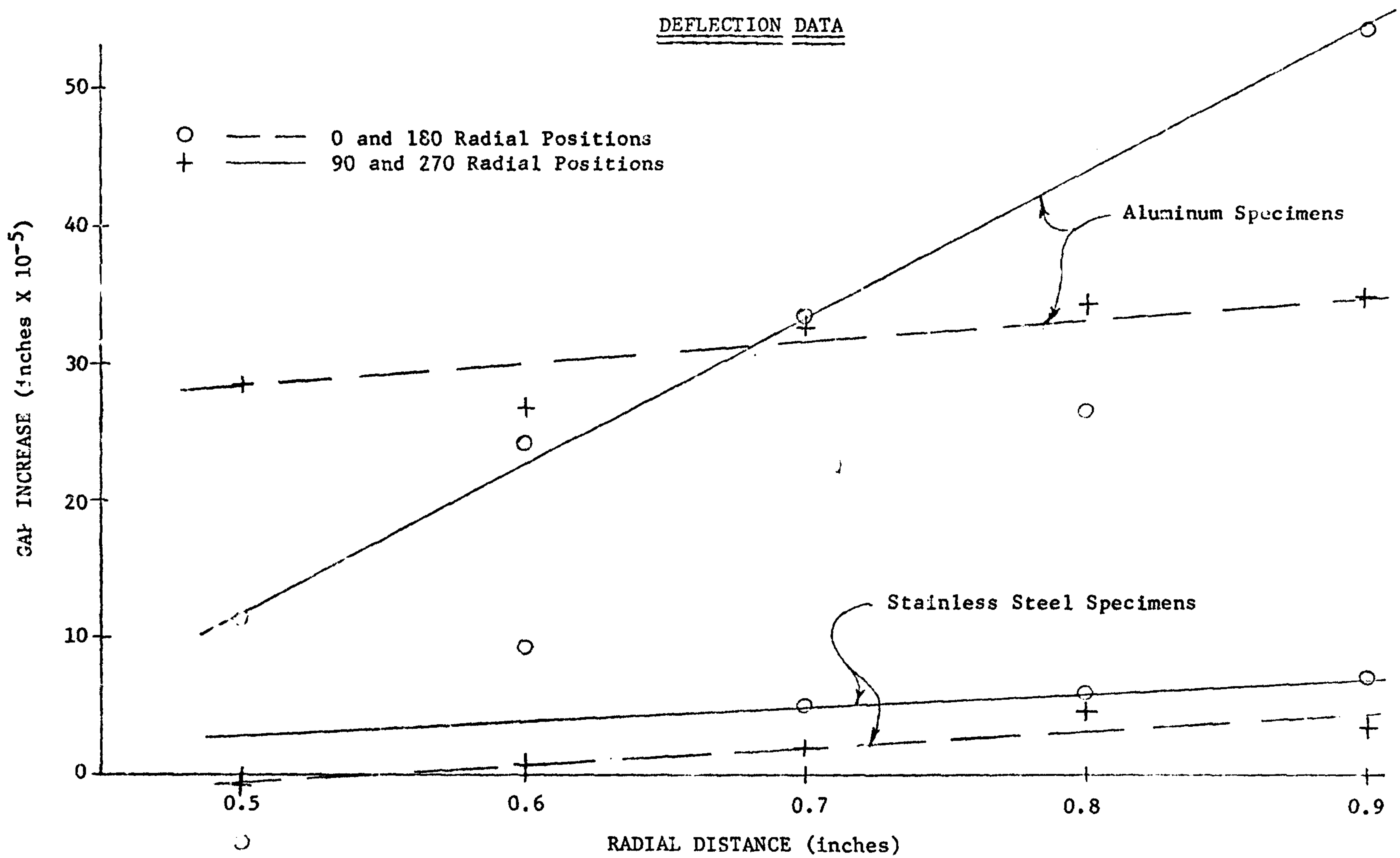

Figure IV-6. Generalized plot indicating relative deflection trends of Aluminum and Stainless Steel as a function of radial distance from Bolt.

this effect was large in comparison to the creep and mechanical deflections. It was also discovered that this effect was opposite in direction from the creep and mechanical reactions and in general was greatly different. The basic data obtained is presented in Table IV-6. These numbers represent the change in pin to pin distance obtained when a temperature drop of approximately 15 to 20°F was imposed on the joint at a torque of 28 ft.lbs.

As in the previous deflection measurements, the data is scattered; but, through averaging, an overall look reveals the trends of certain variables. There appears to be no difference between the data for the aluminum specimens and the stainless steel specimens. To verify this observation, an average of all thermal deflections for the aluminum specimens was compared to the average thermal deflection for the stainless steel ones. Deflections of -4.45×10^{-4} and -4.60×10^{-4} inches, respectively, were obtained; therefore, it was concluded that thermal deflections are independent of these two plate materials.

The next variable considered was position. It was apparent from the tabulated data that the deflections for positions between the bolt heads (angle = 90° and 270°) were larger in absolute magnitude than for positions at angles of 0° and 180°. However, deflections for pins 1 through 5 at a particular radial position seem to be almost constant. This is shown in Figure IV-7 where each point is the average of the data taken for all specimens at the indicated positions. There is a slight decrease in the absolute magnitude of the deflections as the radial distance increases.

Finally, an analysis of surface finish versus thermal deflections was made. This was done by taking the average deflection for each

THERMAL DEFLECTION DATA

		Pin Number				
Plate No.	Angle	1	2	3	4	5
1	0°	-45	-14	-21	-10	--
	180°	-30	-12	-11	-10	-15
	90°	-88	-93	-98	-90	-86
	270°	-102	-80	-105	--	-62
3	0°	18	17	27	20	12
	180°	-1	-78	-22	5	-23
	90°	-71	-84	-46	-87	-63
	270°	-94	-71	-47	-52	-70
4	0°	-48	-45	-56	-38	-65
	180°	-23	-19	-33	-11	-1
	90°	-89	-91	-102	-59	-90
	270°	-71	-75	-99	-78	-77
5	0°	-28	-23	-14	-4	-26
	180°	-15	-10	-10	-2	-4
	90°	-93	-89	-91	-91	-85
	270°	-106	-89	-93	-102	-91
6	0°	2	0	-1	1	-20
	180°	-12	-10	-16	7	0
	90°	-55	-28	-20	-6	-16
	270°	-65	-81	-84	-75	-81

Table IV-6. Tabulation of basic Thermal Deflection Data

THERMAL DEFLECTION DATA

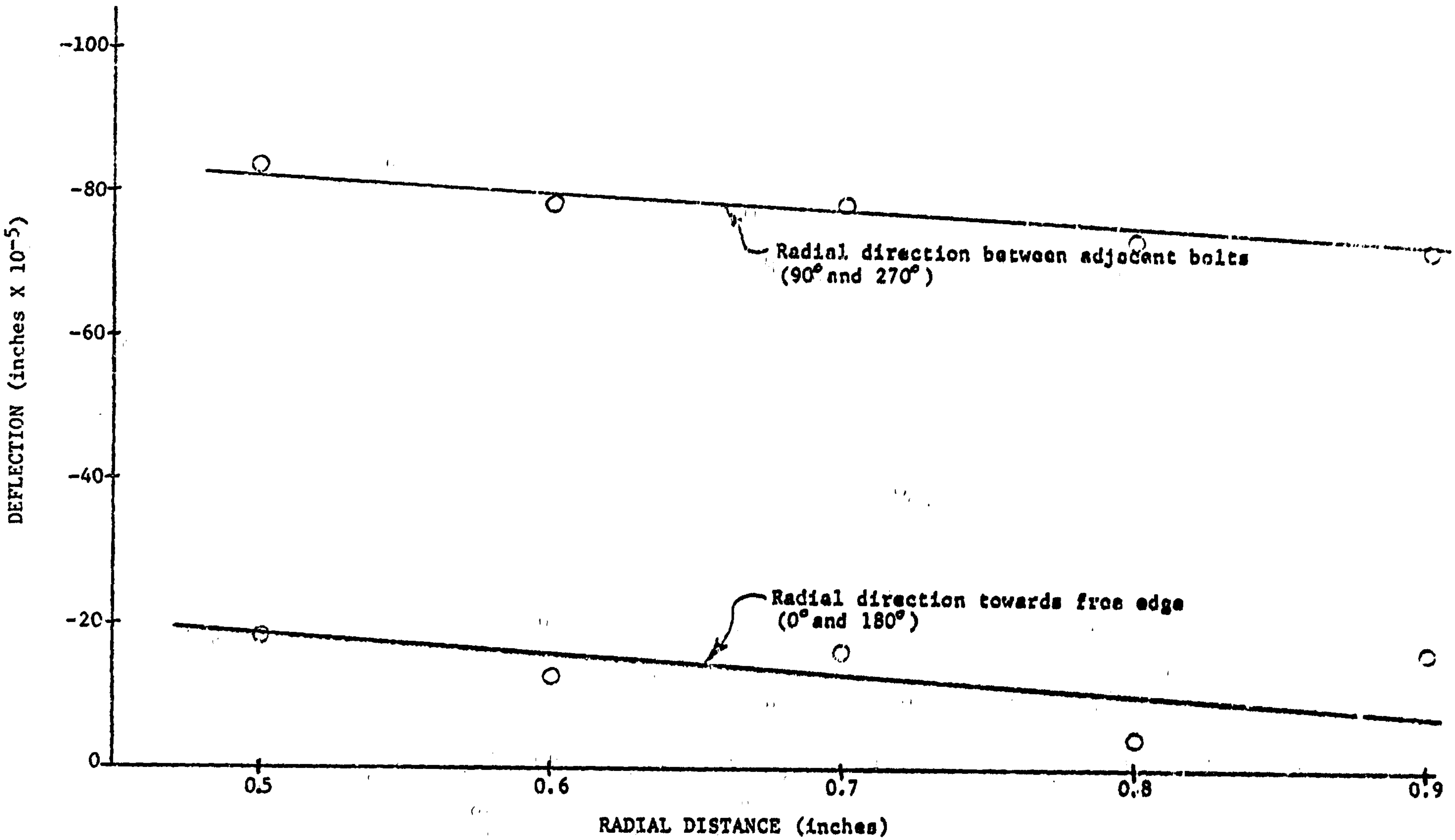

Figure IV-7 : Generalized plot showing reaction of the specimens at various positions on the plates to the thermal load.

specimen and making a plot of surface finish versus deflection as shown in Figure IV-8. The data is insufficient to confirm this plot as conclusive results; therefore, it will only be concluded here that the effect of surface finish is a decrease in deflections as surface roughness increases.

It was decided that data should be taken to determine whether or not the plates would return to their original position after the thermal gradient had been removed. Specimen number 5 was used for this. After the completion of the regular testing, the specimen was allowed to cool until it was in equilibrium with the surroundings. This required about 2 hours. The deflections of six selected pins were then measured and compared to the measurements taken prior to the thermal load application. The deflections had returned to within an average of 1.4×10^{-4} inches. The deflections were measured once again at approximately 18 hours after removal of the thermal load, and the deflections were within an average of 0.6×10^{-4} inches of the original deflection measured prior to the application of the thermal load. No further measurements were taken, but it was assumed that the specimen had returned to its original condition.

B. JOINT CONDUCTIVITY DATA

The data obtained in the joint conductance study is presented in Tables IV-7 through IV-11. The temperature numbers correspond to the locations indicated in Figure III-6. The "u" and "b" suffixes on the numbers refer to upper and bottom thermocouples, respectively. No use was made of temperatures 15 through 26 in this study except to gain some insight into paths of heat flow. Temperatures 11 through 14 were used

THERMAL DEFLECTION DATA

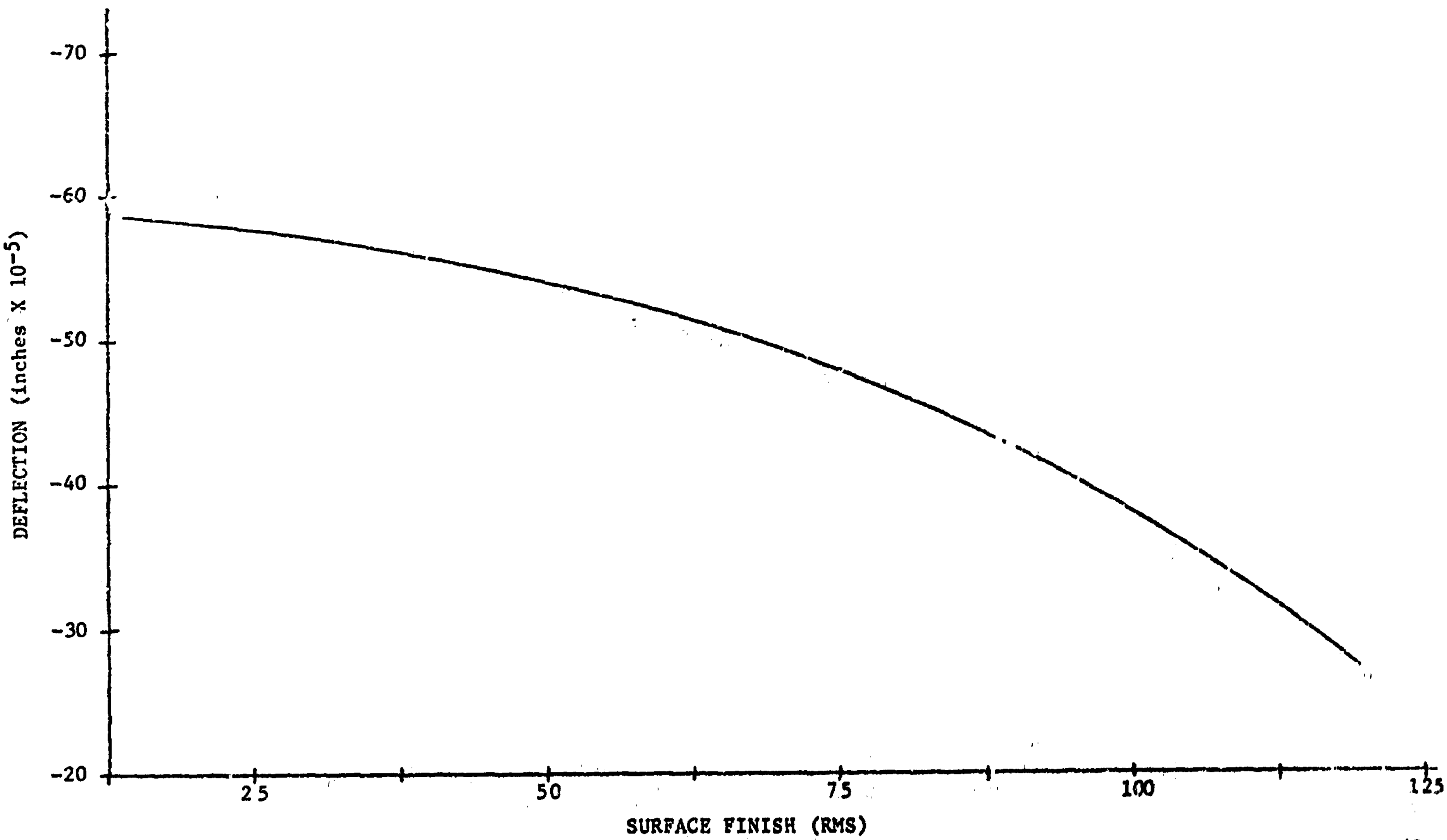

Figure IV-8 : Generalized plot indicating the effect of surface finish on Thermal Deflections.

PLATE NO. 1	Torque (ft.lbs.)		
Thermocouple Number	16	22	28
1	---	---	---
2	191	190	192
3	181	180	182
4	172	171	172
5	163	152	164
6	123	120	123
7	113	110	113
8	104	102	105
9	94	92	95
10	86	85	89
11	212	212	212
12	212	212	212
13	71	69	70
14	70	65	67
15u	143	143	---
15b	155	155	156
16u	144	143	144
16b	148	148	149
17u	133	133	134
17b	138	137	139
18u	126	125	127
18b	138	138	139
19u	143	142	144
19b	157	157	158
20u	139	138	140
20b	143	143	144
21u	126	125	126
21b	138	138	139
22u	143	142	144
22b	157	156	157
23u	141	141	142
23b	149	149	150
24u	138	137	139
24b	143	142	144
25u	132	131	132
25b	140	139	141
26u	125	124	126
26b	138	138	139
Ambient Temperature	58	61	60
Ambient Press. (mm Hg)	2	2	2

Table IV-7. Temperature distribution data for specimen 1. All temperatures are in degrees Fahrenheit.

PLATE NO. 3	Torque (ft.lbs.)		
Thermocouple Number	4	16	28
1	195	195	193
2	187	188	186
3	176	177	176
4	167	168	166
5	160	161	159
6	---	120	118
7	110	112	110
8	101	103	100
9	90	92	89
10	80	82	79
11	212	212	212
12	212	212	212
13	68	71	69
14	59	60	61
15u	142	142	141
15b	155	155	155
16u	142	142	141
16b	147	147	147
17u	131	131	130
17b	136	136	136
18u	124	124	123
18b	136	136	136
19u	141	141	140
19b	156	156	156
20u	137	137	136
20b	140	141	140
21u	123	123	122
21b	136	137	136
22u	141	141	140
22b	156	157	156
23u	140	140	139
23b	148	148	148
24u	137	136	135
24b	141	141	141
25u	131	130	130
25b	137	138	138
26u	123	122	122
26b	135	137	137
Ambient Temperature	68	68	66
Ambient Press. (mm Hg)	2	2	2

Table IV-8. Temperature distribution data for specimen 3. All temperatures are in degrees Fahrenheit.

PLATE NO. 4	Torque (ft.lbs.)		
Thermocouple Number	4	16	28
1	192	194	194
2	183	185	185
3	169	170	171
4	156	157	159
5	144	145	147
6	108	110	111
7	97	100	100
8	86	89	88
9	74	76	75
10	63	66	65
11	212	212	212
12	212	212	212
13	45	51	47
14	41	46	44
15u	130	131	134
15b	139	140	143
16u	129	130	132
16b	131	132	134
17u	119	121	123
17b	121	123	125
18u	114	115	117
18b	118	120	122
19u	130	131	133
19b	140	141	144
20u	124	126	127
20b	126	128	130
21u	111	113	114
21b	119	121	123
22u	---	132	134
22b	141	142	144
23u	129	130	132
23b	132	134	136
24u	124	126	127
24b	126	128	130
25u	118	120	122
25b	121	123	125
26u	111	113	115
26b	119	120	123
Ambient Temperature	66	66	66
Ambient Press. (mm Hg)	2	2	2

Table IV-9. Temperature distribution data for specimen 4. All temperatures are in degrees Fahrenheit.

PLATE NO. 5	Torque (ft.lbs.)		
Thermocouple Number	4	16	28
1	195	193	194
2	184	183	185
3	170	169	172
4	160	158	163
5	149	146	152
6	116	111	117
7	106	100	107
8	97	90	99
9	---	78	89
10	75	66	79
11	212	212	212
12	212	212	212
13	59	46	63
14	53	42	56
15u	137	134	137
15b	143	141	146
16u	135	132	136
16b	136	133	138
17u	126	123	127
17b	127	124	129
18u	120	116	121
18b	125	121	127
19u	137	134	137
19b	144	142	147
20u	---	---	---
20b	---	---	---
21u	119	115	121
21b	126	122	127
22u	138	135	138
22b	145	143	147
23u	135	132	136
23b	137	134	139
24u	130	127	132
24b	132	128	134
25u	126	122	127
25b	128	125	130
26u	119	115	120
26b	126	122	127
Ambient Temperature	66	66	66
Ambient Press. (mm Hg)	2	2	2

Table IV-10. Temperature distribution data for specimen 5. All temperatures are in degrees Fahrenheit.

PLATE NO. 6	Torque (ft.lbs.)		
Thermocouple Number	4	16	28
1	196	194	196
2	182	181	183
3	169	170	170
4	155	155	156
5	145	146	148
6	108	112	111
7	96	101	100
8	84	90	88
9	72	77	75
10	60	65	62
11	---	---	---
12	212	212	212
13	46	50	46
14	40	45	43
15u	132	133	134
15b	141	143	144
16u	130	132	133
16b	133	135	136
17u	121	124	124
17b	122	125	126
18u	113	117	116
18b	121	124	125
19u	131	133	134
19b	141	143	144
20u	---	---	---
20b	---	---	---
21u	110	115	114
21b	121	125	125
22u	131	134	134
22b	142	144	145
23u	129	132	132
23b	133	136	137
24u	125	128	128
24b	127	130	131
25u	117	122	122
25b	123	127	127
26u	110	115	115
26b	120	124	125
Ambient Temperature	71	75	73
Ambient Press. (mm Hg)	2	2	2

Table IV-11. Temperature distribution data for specimen 6. All temperatures are in degrees Fahrenheit.

to monitor heating and cooling H_2O lines. Thermocouples 13 and 14 were placed on the outside of the cooling tube and do not represent the actual temperature of the cooling water, but represent the ΔT across the cold end of the plate. Temperatures 1 through 10 were plotted in Figures IV-10 through IV-24 and represent the temperature distributions along the specimens. These plots were used with the EFM to determine the thermal conductivity of the joints for each test condition. A sample calculation showing the procedure used is given below (Figure IV-9 shows a sample temperature distribution plot which indicates how the values used in the calculations were obtained):

<u>Plate 1</u> = <u>16 ft.lbs. Torque</u>

Applying equation 3 from Chapter II to sections 1 and 2, we get the following:

$$k_2 = \frac{x_2}{x_e} k_1 = \frac{1.875 \text{ in.}}{4.40 \text{ in.} - 2.81 \text{ in.}} k_1 = 1.179k_1$$

$$k_2 = 135.6 \frac{\text{BTU}}{\text{hr.ft.}^\circ\text{F}}$$

Applying equation 3 to specimens 2 and 6 gives:

$$k_2 = 1.187k_1 = 136.2 \frac{\text{BTU}}{\text{hr.ft.}^\circ\text{F}}$$

Applying equation 4 to sections 1 and 2, yields:

$$\Delta T_1 = (211 - 158)^\circ\text{F} = 53^\circ\text{F}$$

$$\Delta T_2 = (158 - 128)^\circ\text{F} = 30^\circ\text{F}$$

$$x_1 = 2.81 \text{ in.}$$

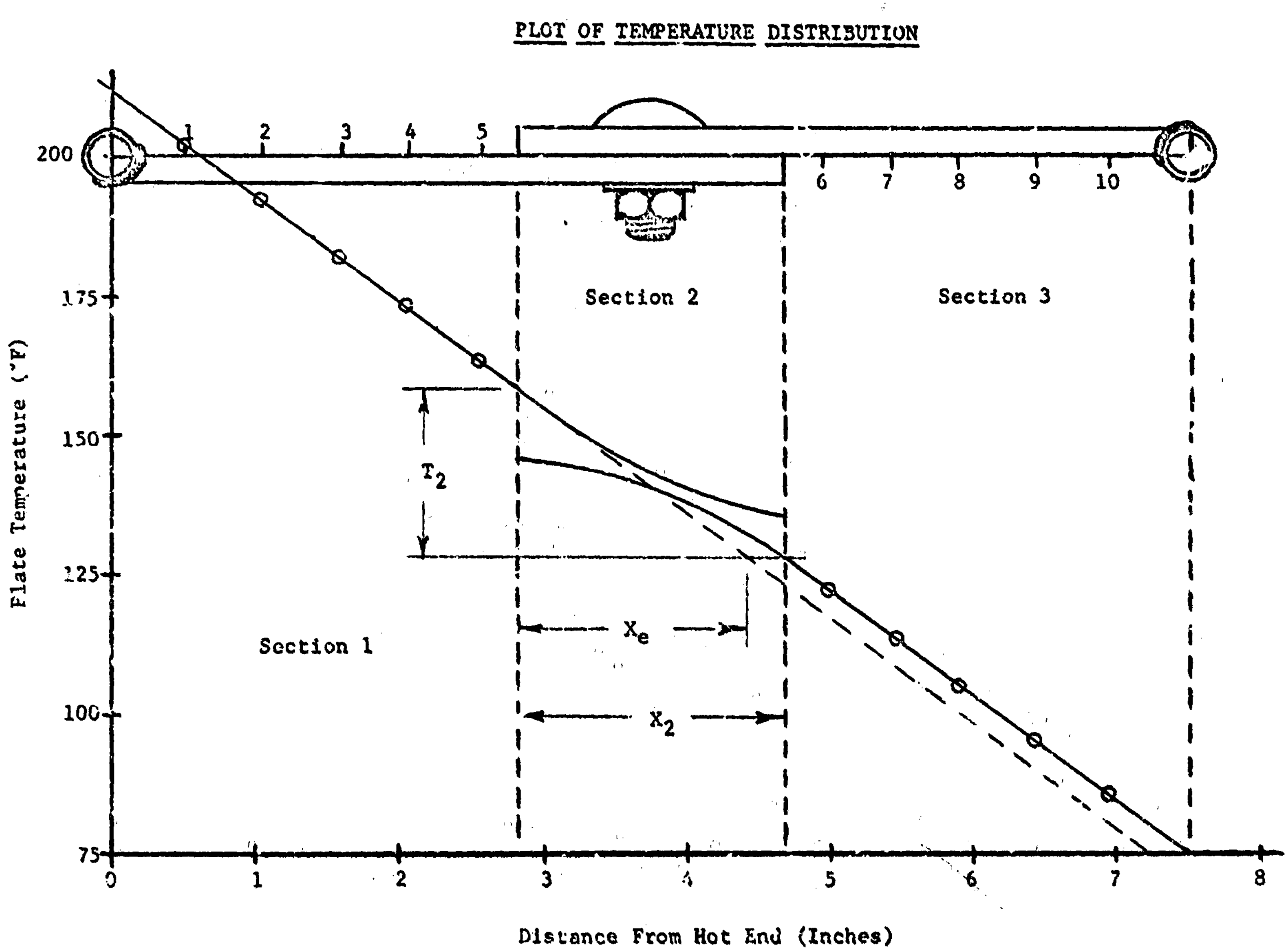

Figure IV-9. Sample temperature distribution plot for joint thermal conductivity determination.

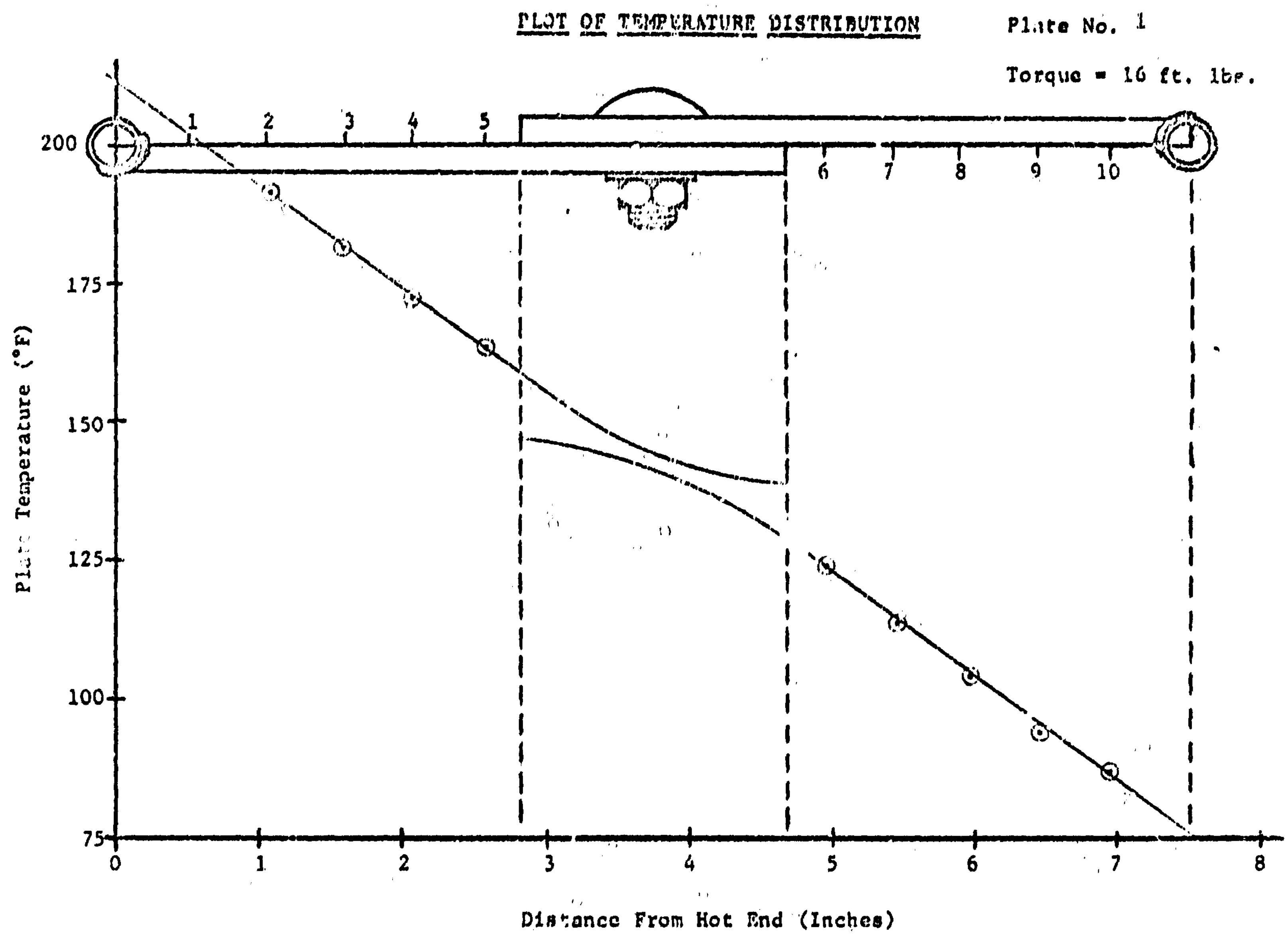

Figure IV-10. Temperature distribution plot for joint thermal conductivity determination.

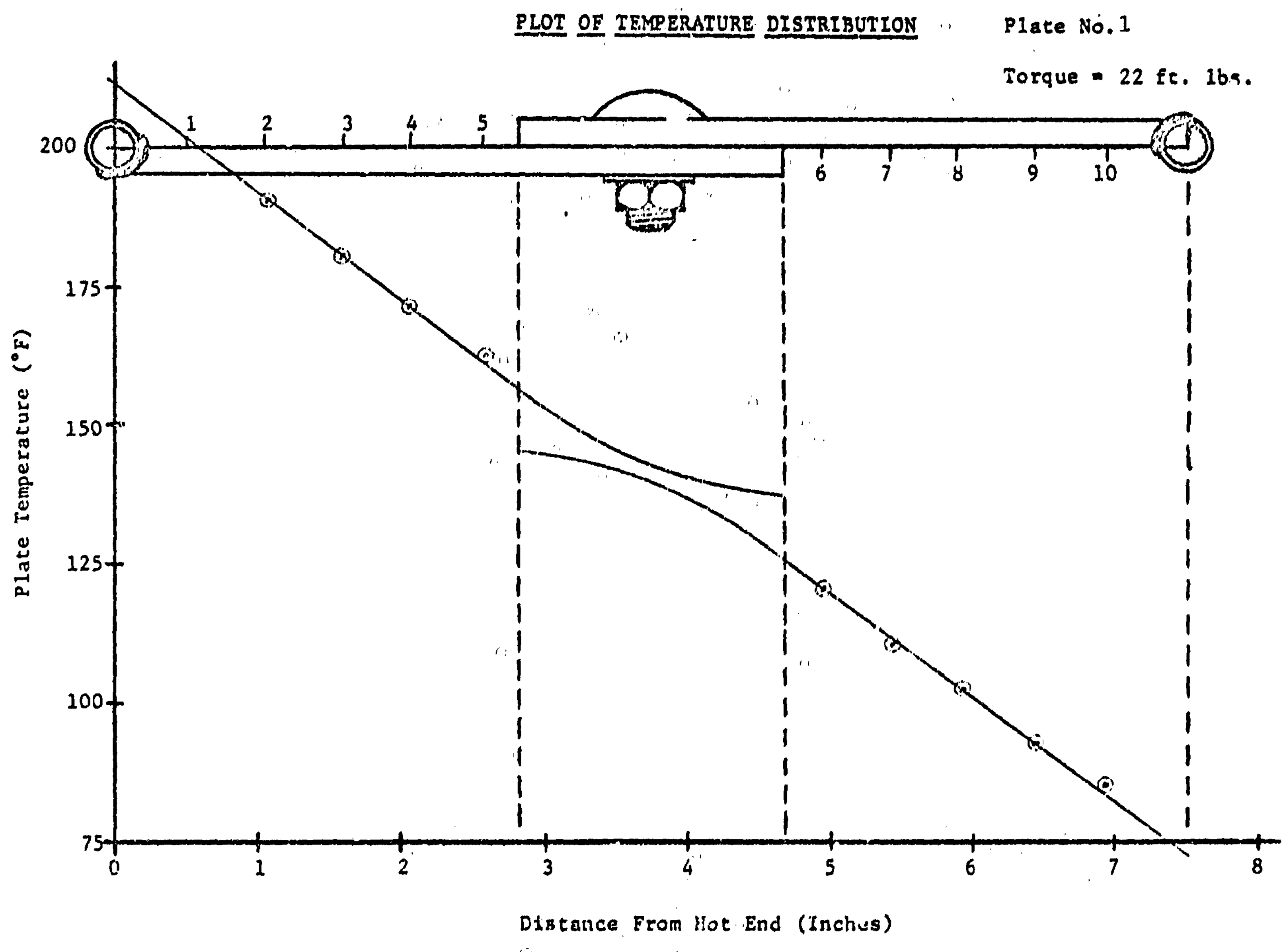

Figure IV-11 Temperature distribution plot for joint thermal conductivity determination.

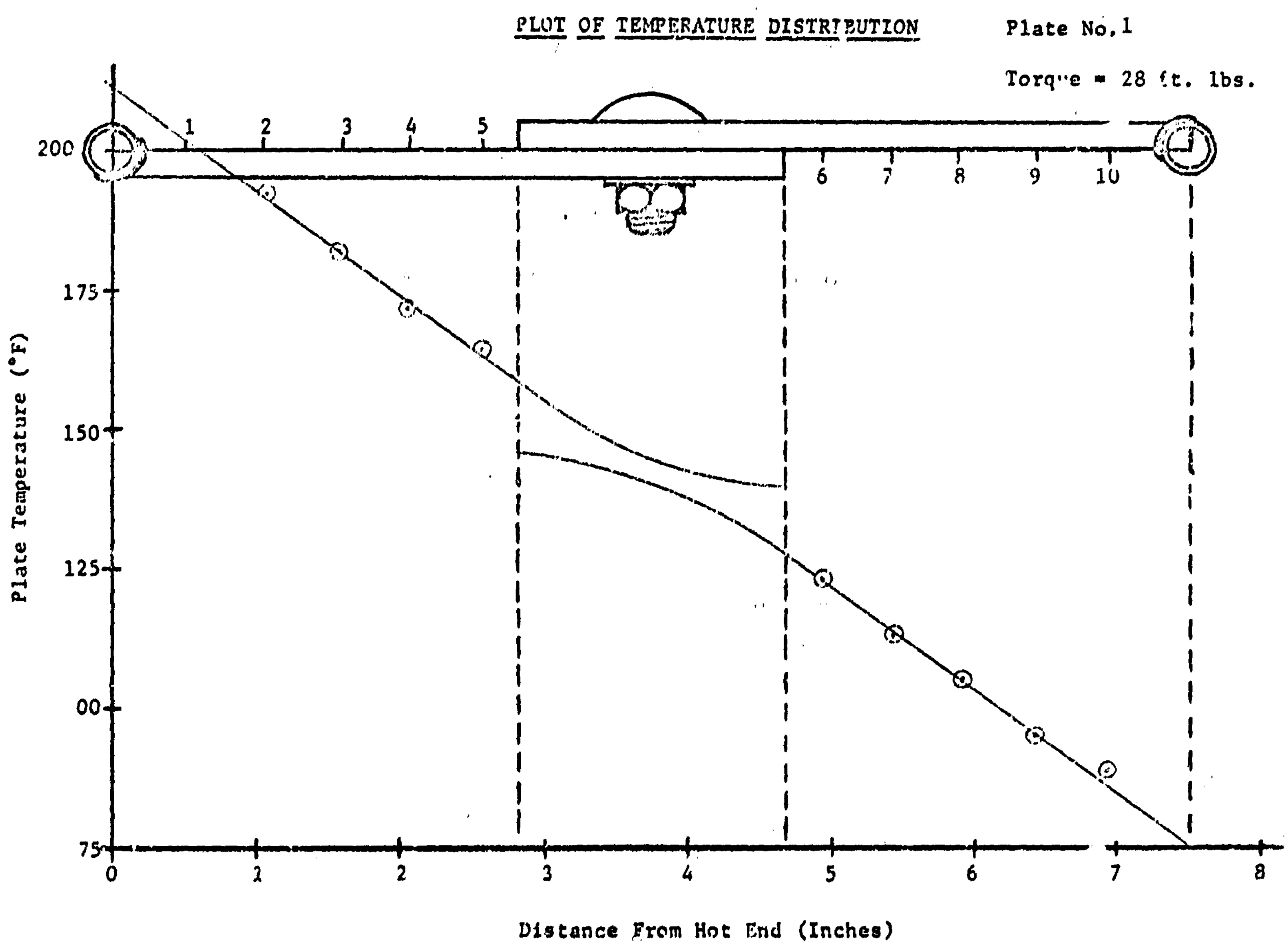

Figure IV-12. Temperature distribution plot for joint thermal conductivity determination.

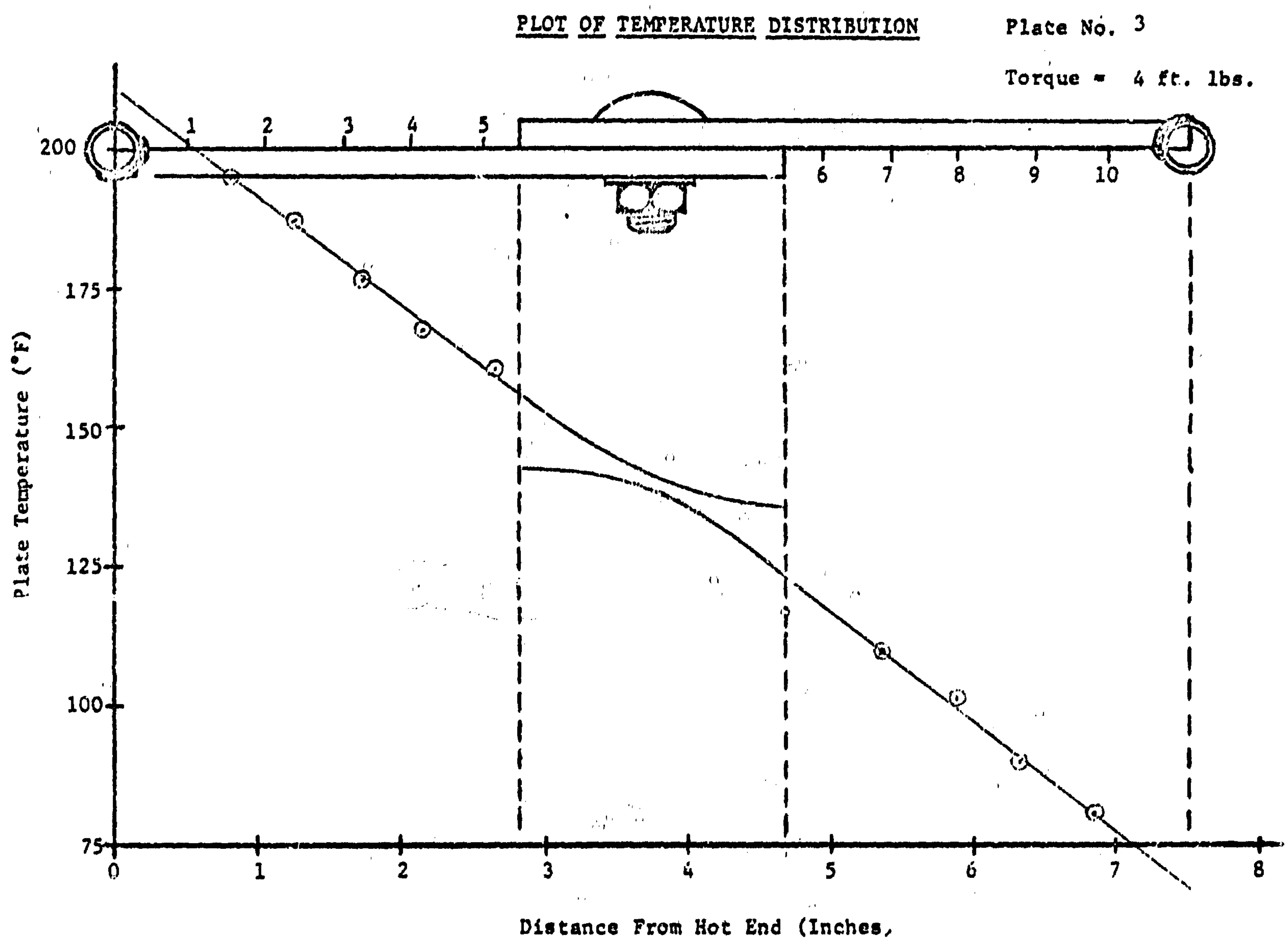

Figure IV-13 Temperature distribution plot for joint thermal conductivity determination.

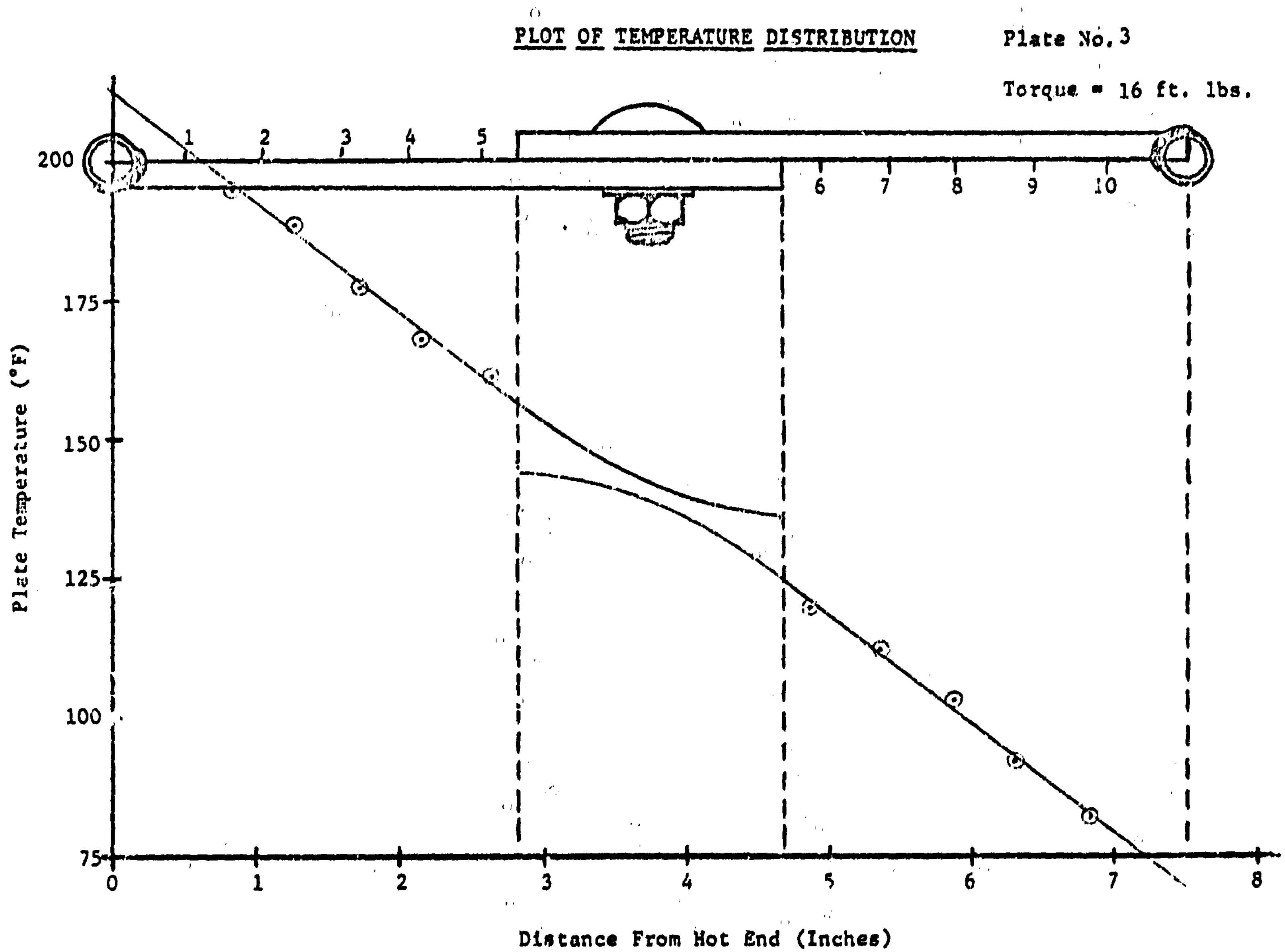

Figure IV-14. Temperature distribution plot for joint thermal conductivity determination.

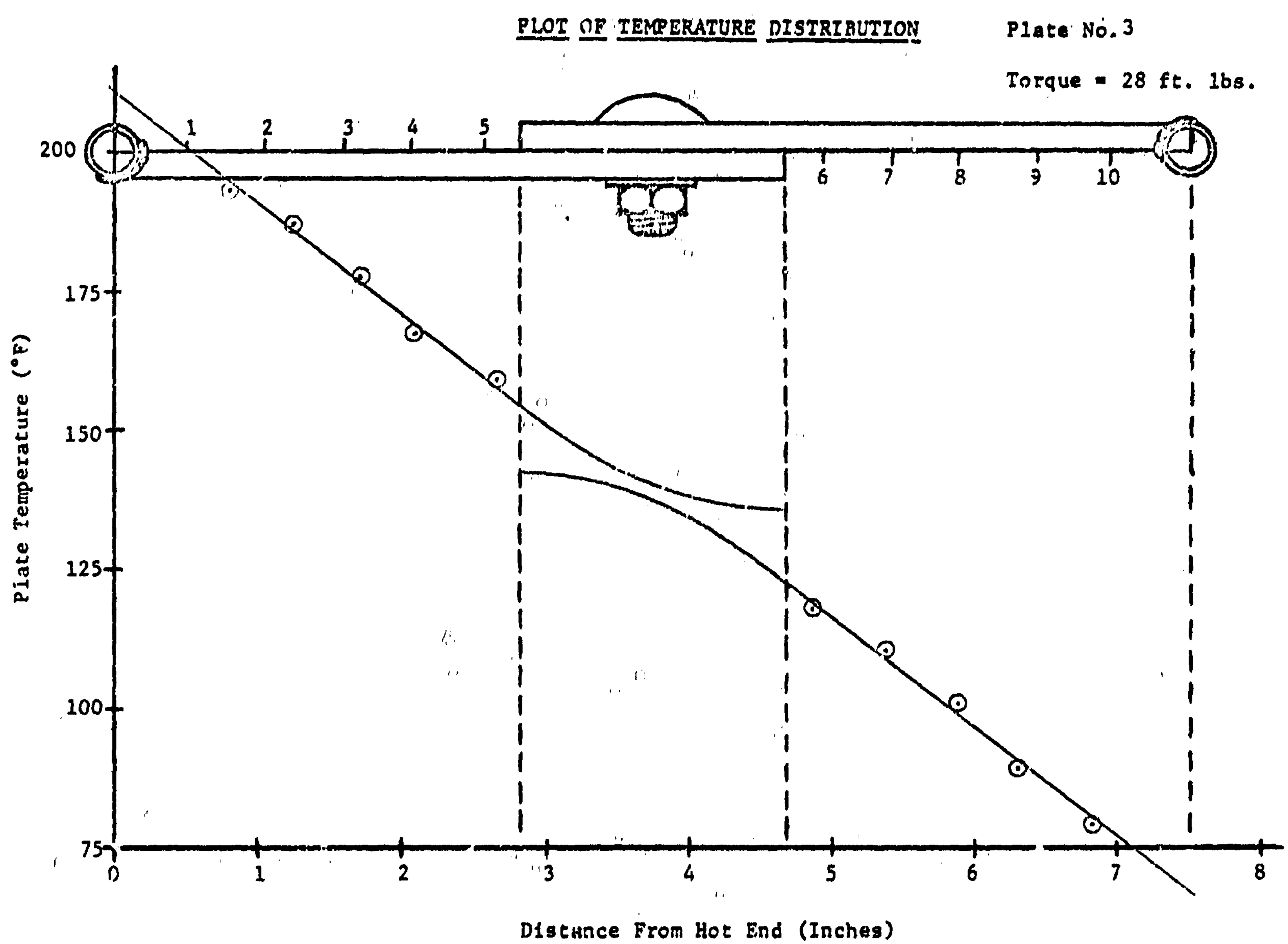

Figure IV-15. Temperature distribution plot for joint thermal conductivity determination.

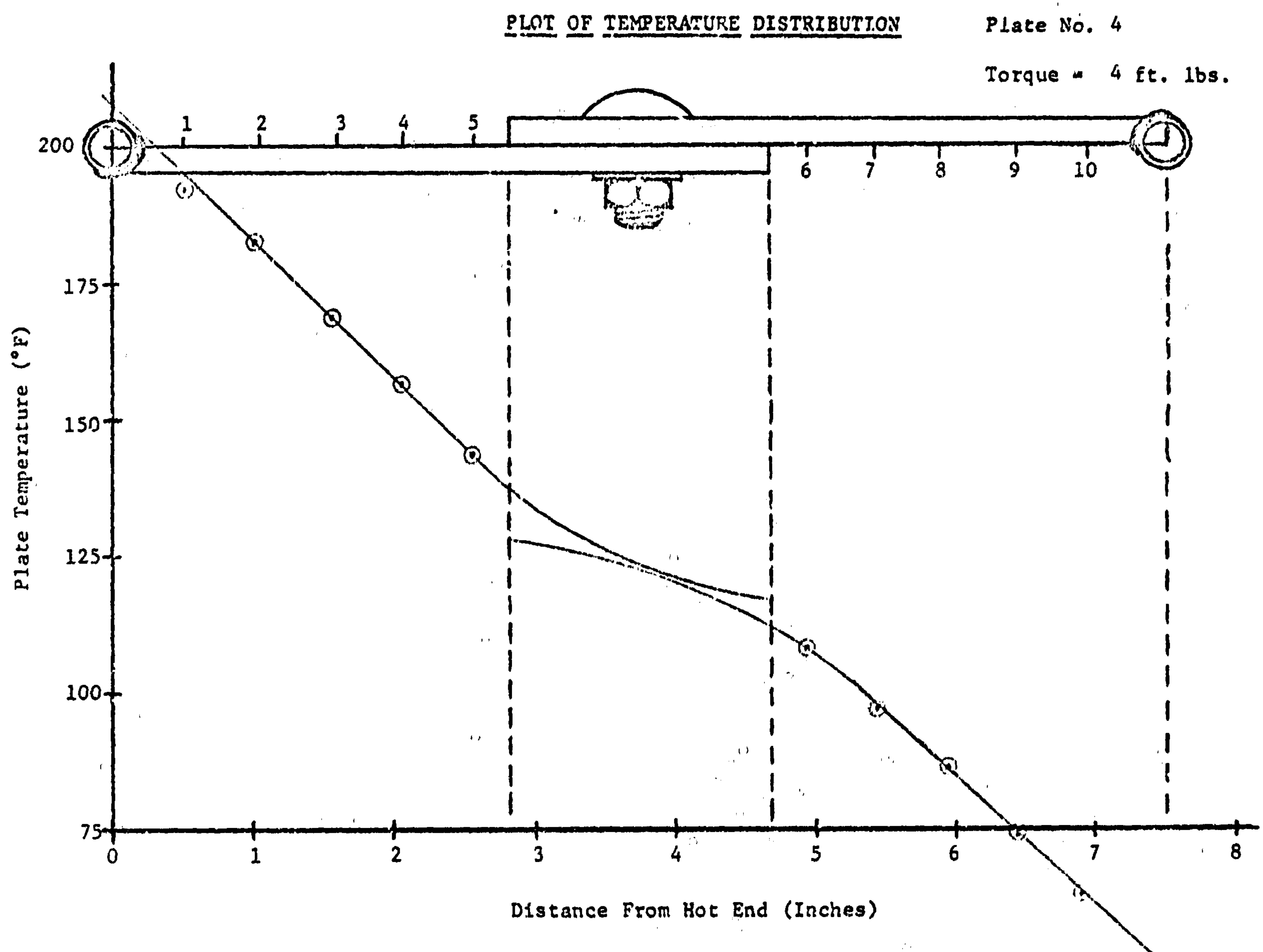

Figure IV-16. Temperature distribution plot for joint thermal conductivity determination.

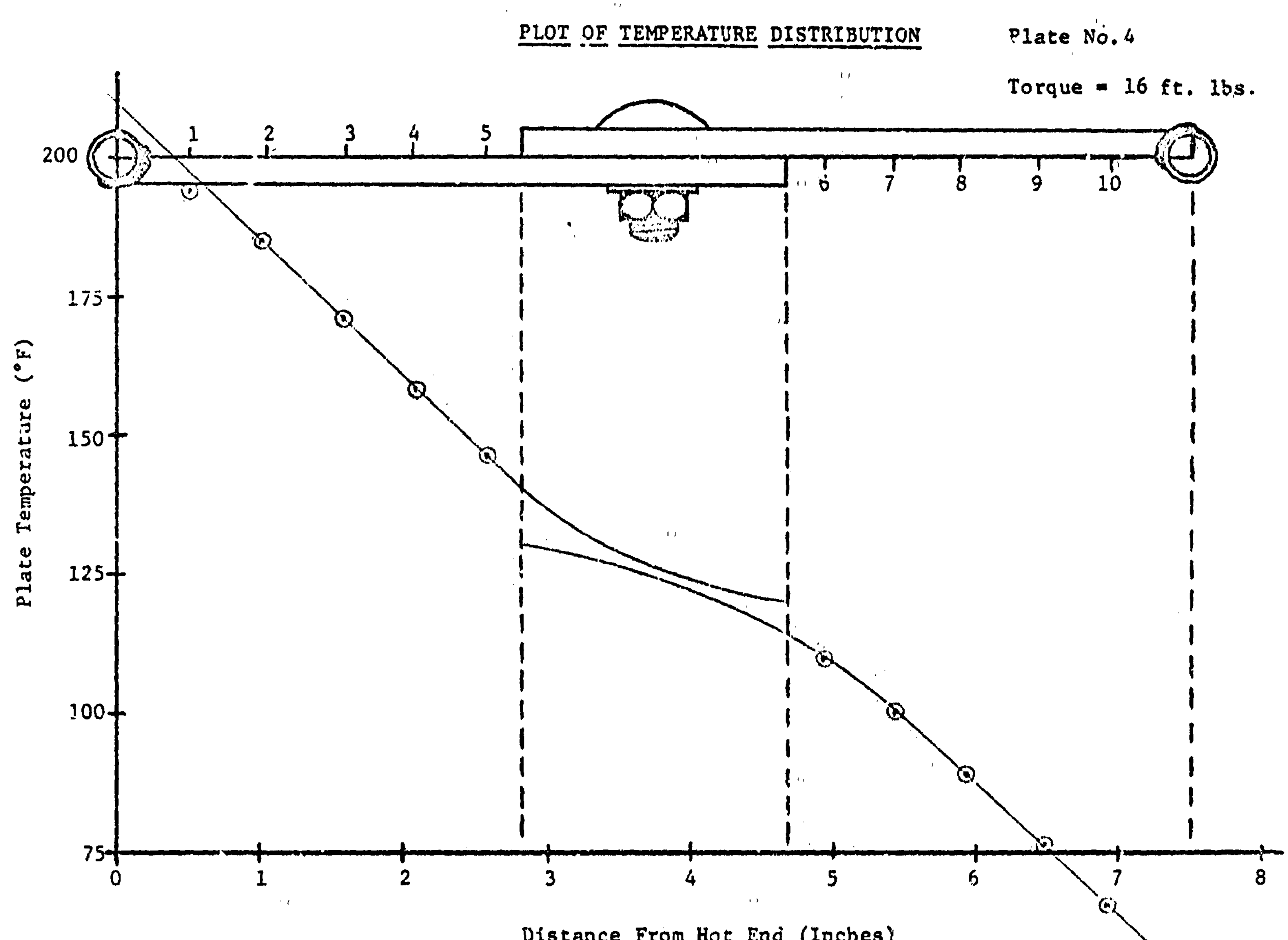

Figure IV-17. Temperature distribution plot for joint thermal conductivity determination.

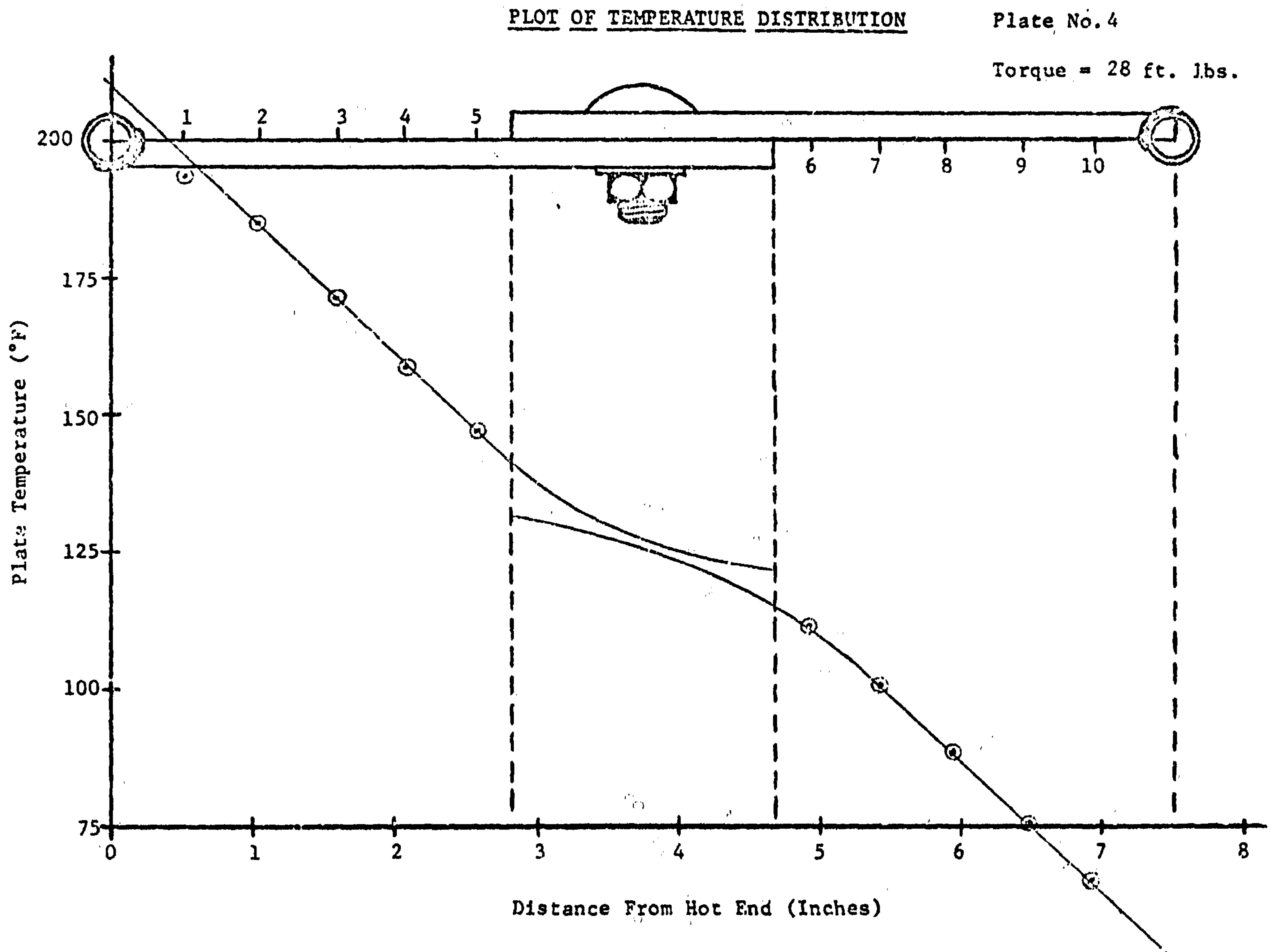

Figure IV-18. Temperature distribution plot for joint thermal conductivity determination.

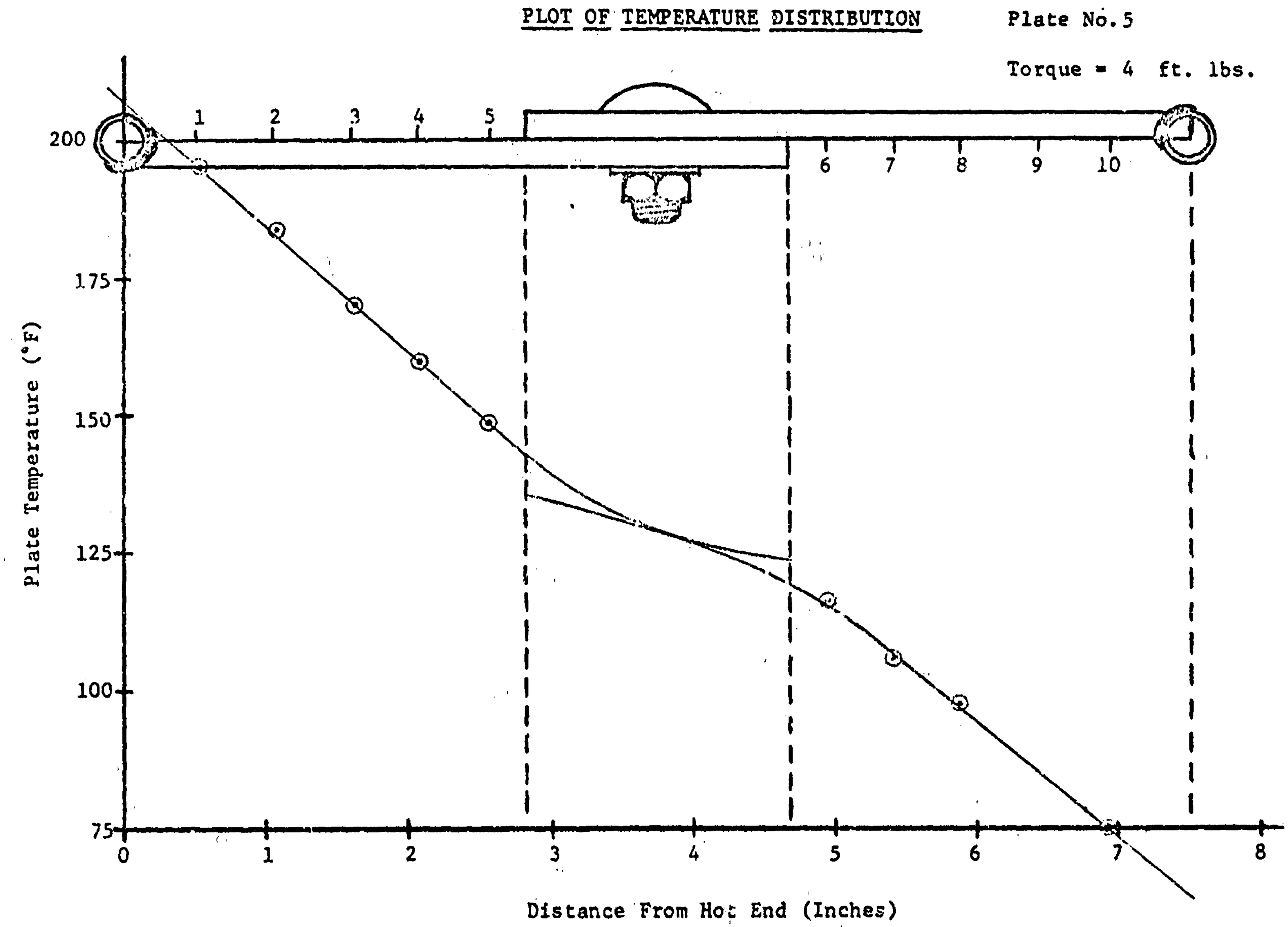

Figure IV-19. Temperature distribution plot for joint thermal conductivity determination.

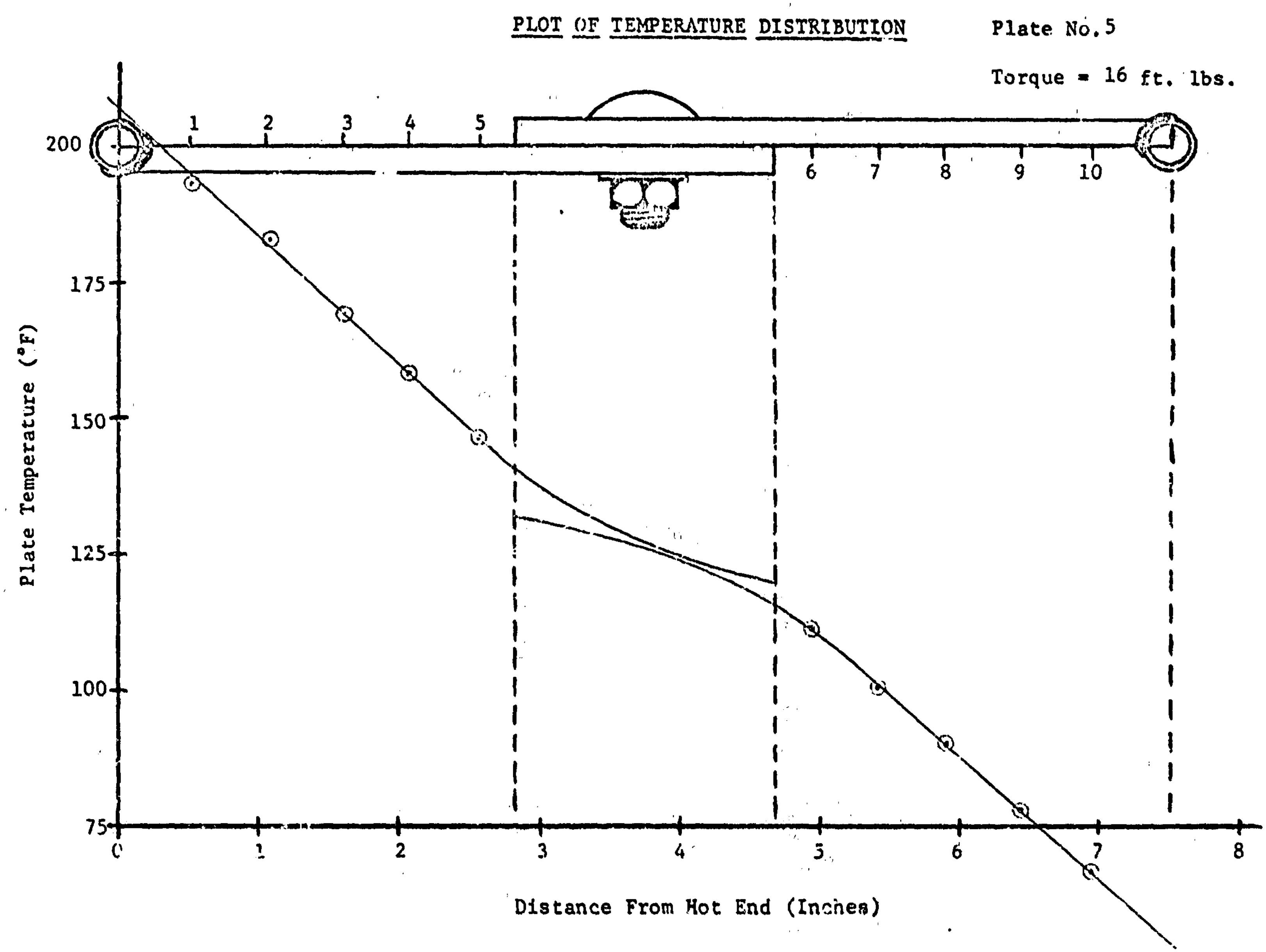

Figure IV-20. Temperature distribution plot for joint thermal conductivity determination.

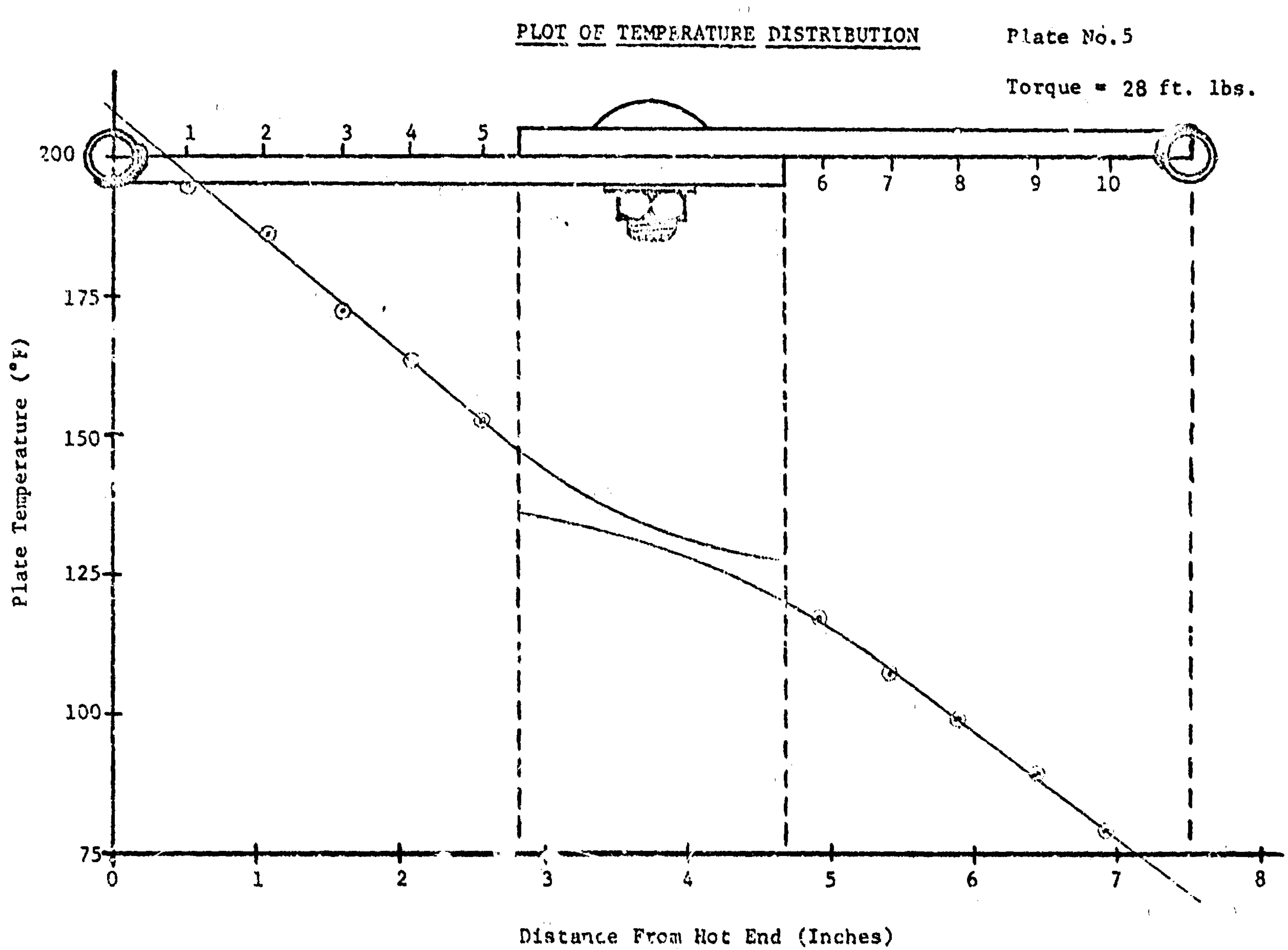

Figure IV-24 Temperature distribution plot for joint thermal conductivity determination.

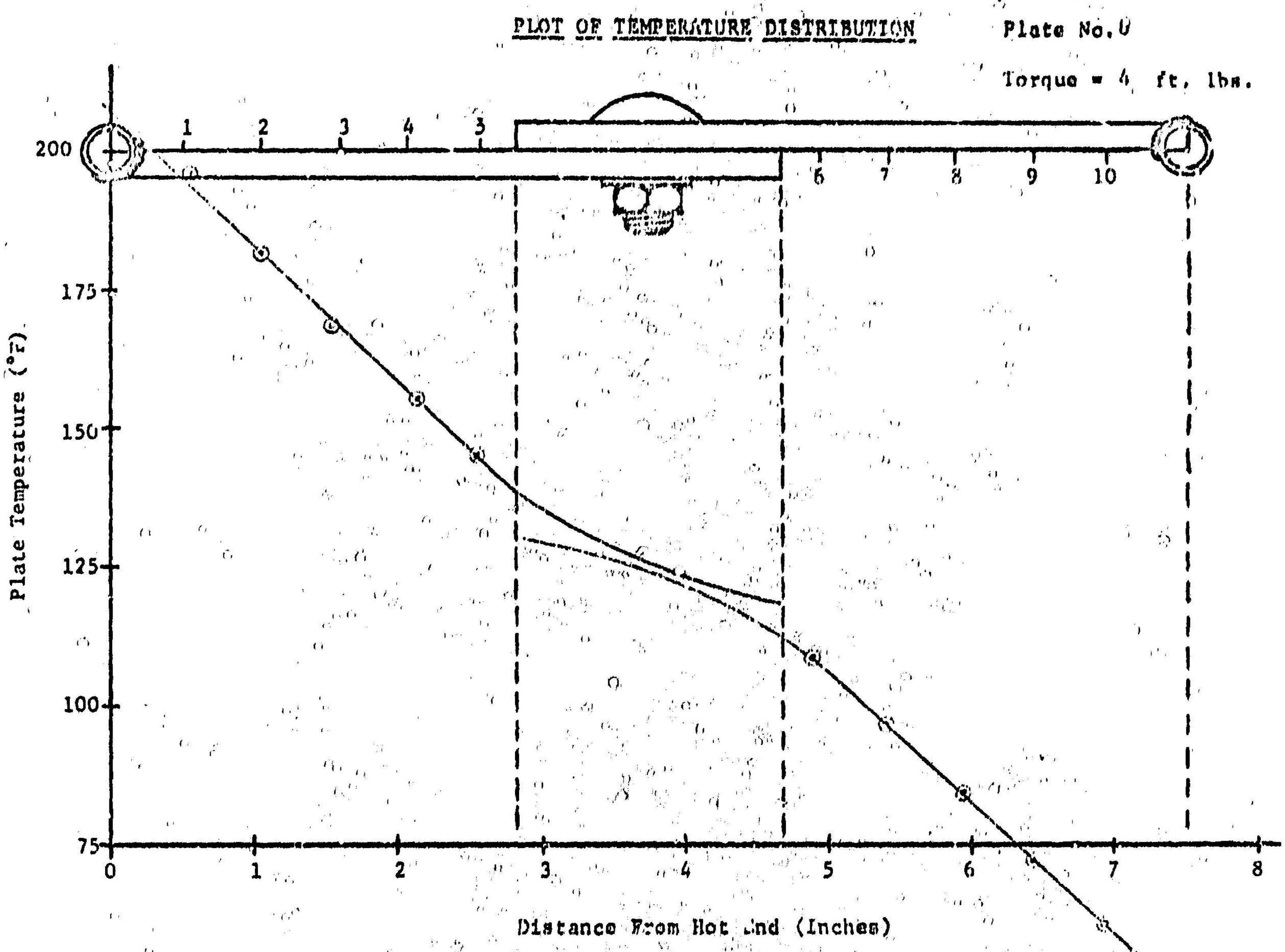

Figure IV-22. Temperature distribution plot for joint thermal conductivity determination.

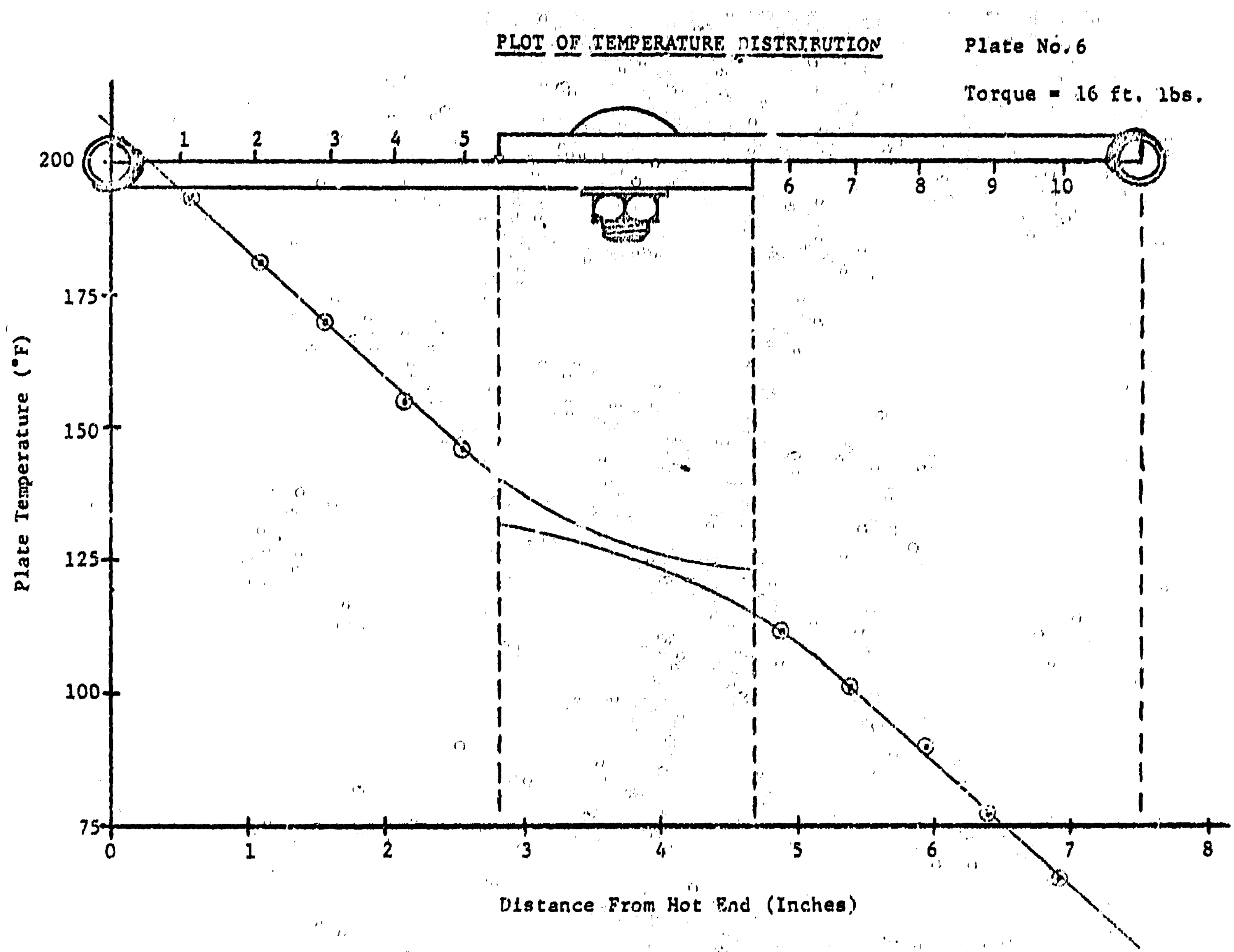

Figure IV-23. Temperature distribution plot for joint thermal conductivity determination.

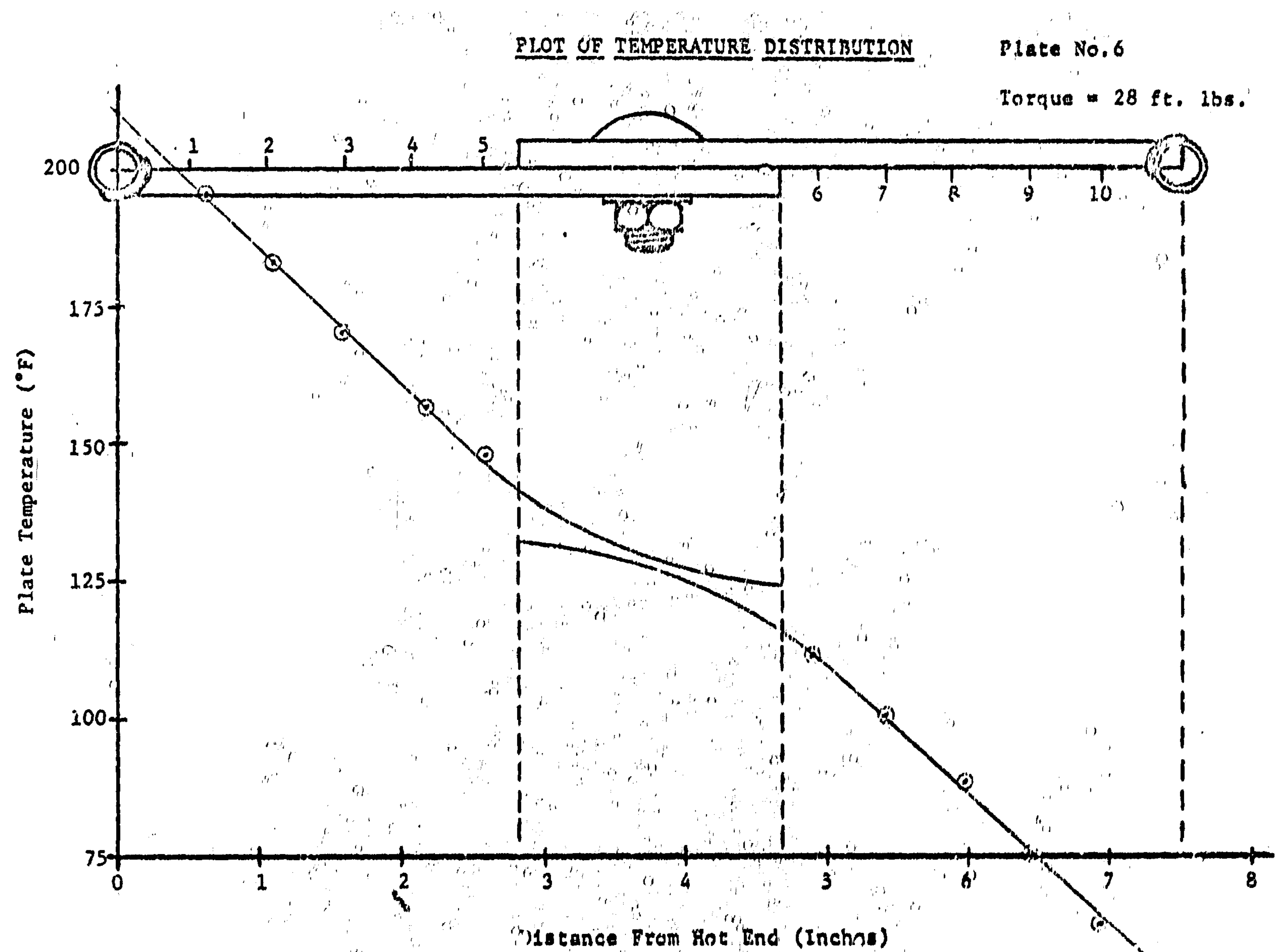

Figure IV-24. Temperature distribution plot for joint thermal conductivity determination.

$$x_2 = 1.875 \text{ in.}$$

$$k_2 = 1.178k_1 = 135.5 \frac{\text{BTU}}{\text{hr.ft.°F}}$$

Applying equation 4 to sections 2 and 3, we get the following:

$$k_2 = 1.178k_1 = 135.5 \frac{\text{BTU}}{\text{hr.ft.°F}}$$

Averaging the four values of k_2 gives the value needed in design computations.

$$k_2 = 1.180k_1 = 135.7 \frac{\text{BTU}}{\text{hr.ft.°F}}.$$

Similar calculations were carried out for each of the distribution plots and the results are tabulated in Table IV-12.

Also included in this table are the results of tests 3 and 4 in Reference 7 and test A-4/1 in Reference 5. The temperature distributions obtained in these studies were replotted in Figures IV-25, IV-26, and IV-27 and used with the EFM to determine the thermal conductivity of the respective specimens. The specimen in test 3 of Reference 7 was an aluminum lap joint very similar to the ones used in this study and was torqued to 8 ft.lbs. and tested in a vacuum. Test 4 of Reference 7 was the same specimen as test 3 of this study, but a torque of 15 ft.lbs. was used. The specimen used in test A-4/1 in Reference 5 was a copper lap joint fastened with flathead screws.

It is apparent from Table IV-12 that torque and surface finish have very little effect on the value of k_2 and the only important parameter shown in this data is plate material. A plot of surface finish

Plate No.	Torque (ft.lbs.)	JOINT CONDUCTIVITY RATIO $\frac{k_2}{k_1}$					k_2 (BTU/hr.ft.°F)
		Equation 1		Equation 2		Avrg.	
		Sec. 1 & 2	Sec. 2 & 3	Sec. 1 & 2	Sec. 2 & 3		
1	16	1.179	1.187	1.178	1.178	1.180	135.7
	22	1.171	1.142	1.185	1.119	1.154	132.8
	28	1.150	1.150	1.181	1.127	1.152	132.6
3	4	1.110	1.123	1.201	1.096	1.132	130.2
	16	1.171	1.178	1.205	1.183	1.184	136.1
	20	1.179	1.163	1.209	1.165	1.179	135.5
4	4	2.132	2.016	2.170	2.068	2.097	22.2
	16	2.105	2.016	2.170	2.030	2.080	22.0
	28	2.017	1.932	2.000	1.941	1.973	20.9
5	4	2.040	1.839	2.035	1.876	1.948	20.6
	16	1.953	1.856	1.968	1.897	1.926	20.4
	28	1.913	1.442	1.603	1.441	1.600	16.9
6	4	1.857	1.751	1.870	1.749	1.807	19.1
	16	1.973	1.934	1.987	1.928	1.955	20.7
	28	2.040	1.913	2.061	1.914	1.982	21.0
Test 3*	8	1.379	1.399	1.360	1.384	1.380	158.8
Test 4*	15	1.342	1.316	1.351	1.330	1.335	153.5
Test A-4/1**		0.575	0.553	0.568	0.546	0.560	123.0

* Data from Reference 7.
** Data from Reference 5.

Table IV-12. Tabulation of calculated results using the EFM.

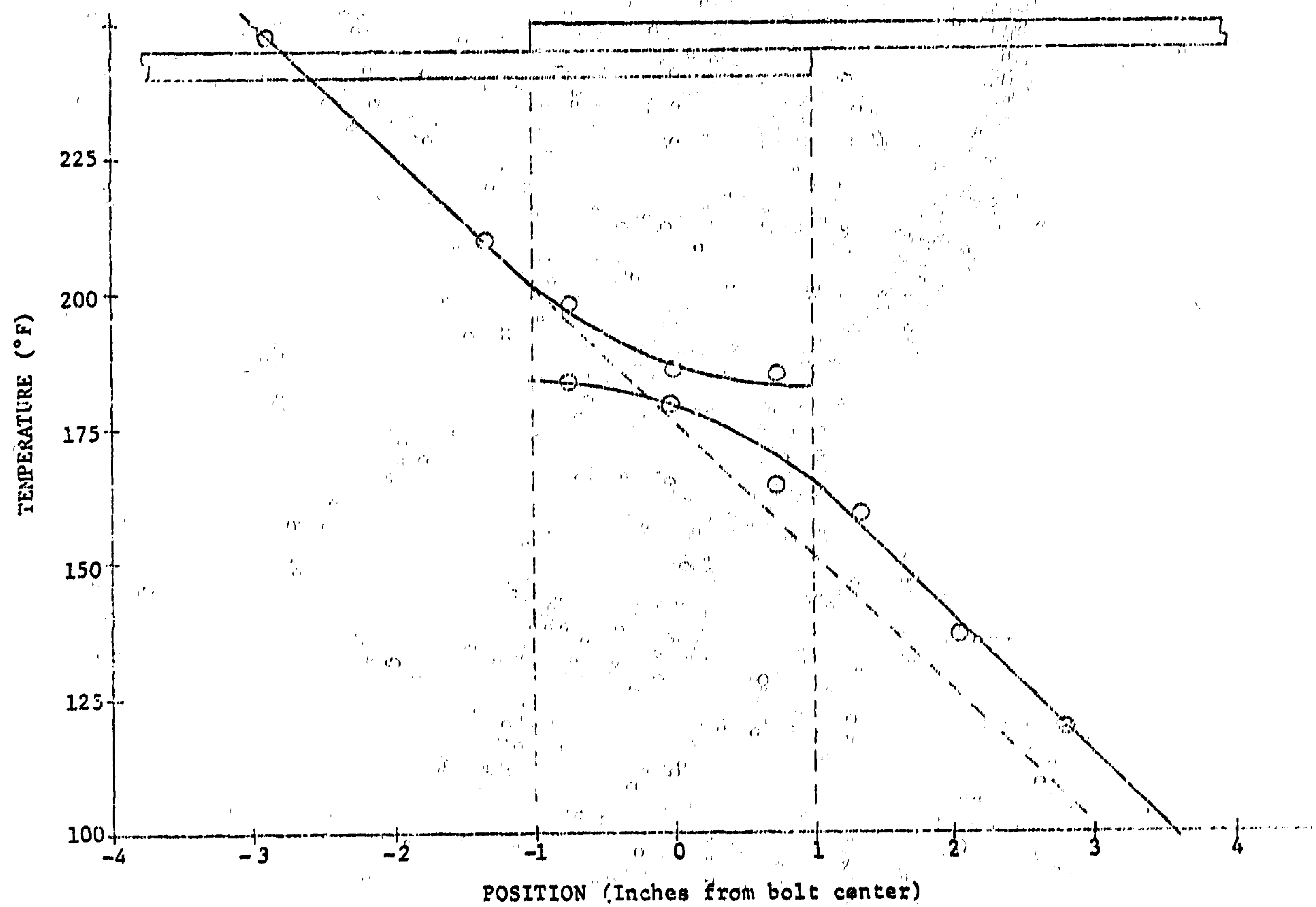

Figure IV-25. Plot of temperature distribution for Test No. 3 (0.25 in. Aluminum plates at 8 ft. lbs.) from Reference 7.

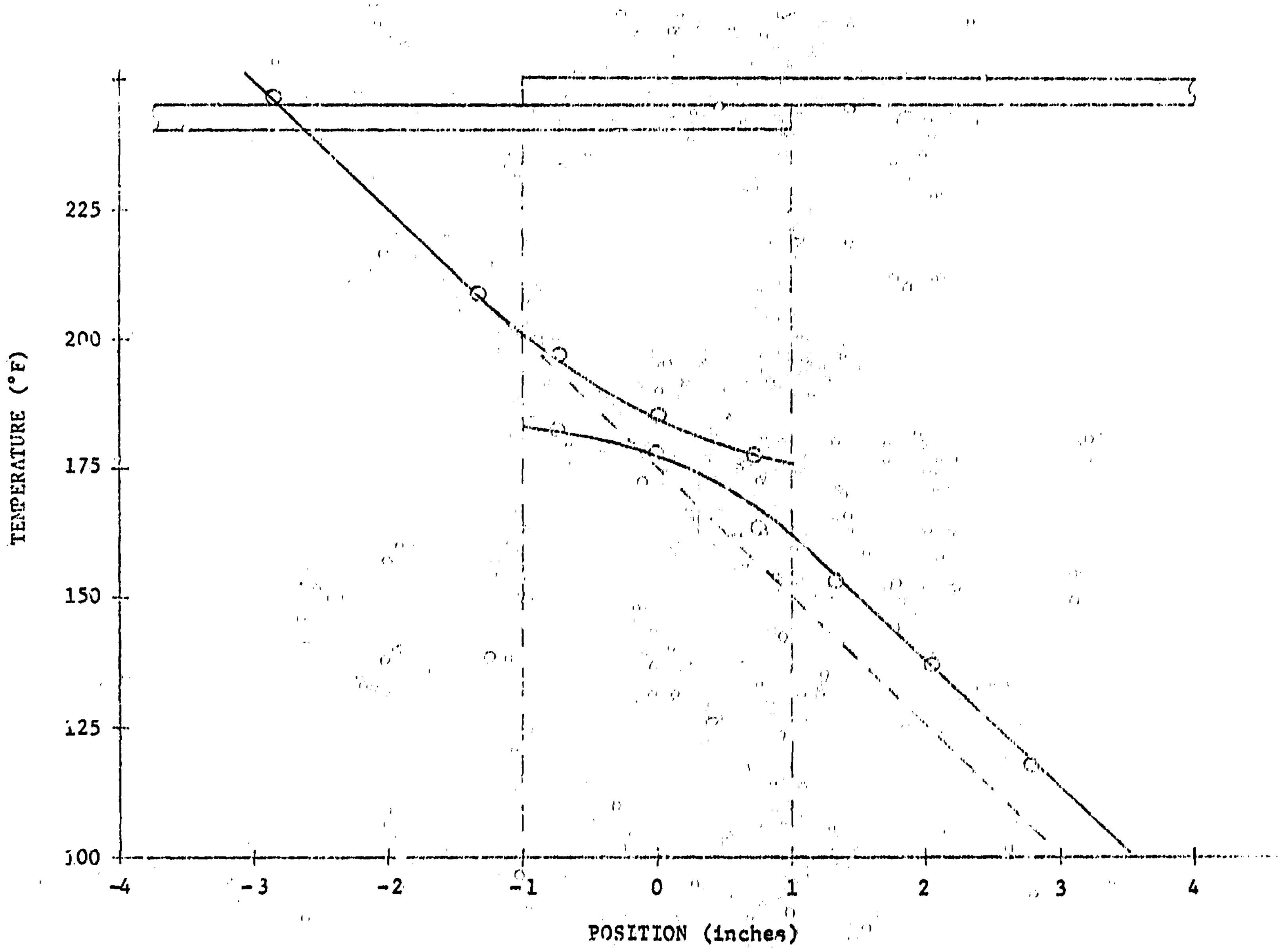

Figure IV-26. Plot of temperature distribution for Test No. 4 (0.25 in. Aluminum plates at 15 ft. lbs.) from Reference 7.

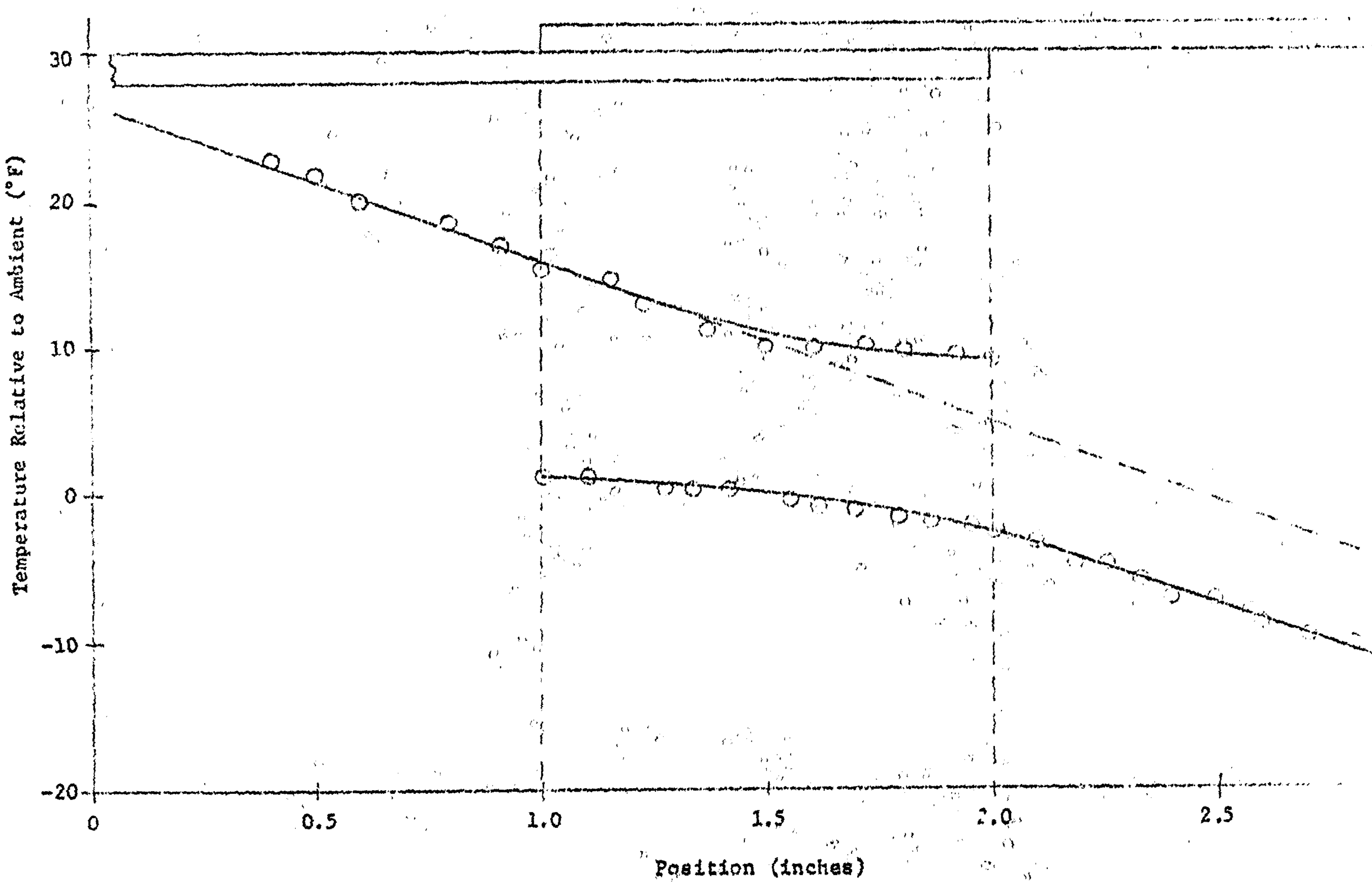

Figure IV-27. Temperature distribution for Test A-4/1 (0.064 in. copper plates; torque unknown) from Reference 5.

versus k_2 is given in Figure IV-33. The three values of k_2 obtained from the three torques on each plate were averaged and plotted as shown. These indicate the independence of surface finish on k_2. An average of all data with similar values of torque and plate material was made and the results plotted in Figure IV-32. The data from Reference 7 is also plotted here. This shows that k_2 is virtually independent of torque over the range of torques used and for these particular specimen. The final variable demonstrated by this data is plate material.

It is difficult to assess the influence of each material property, but since k_2 is a linear function of k_1, it is obvious that the greater the material thermal conductivity the greater the value of k_2 if all other variables could be held constant. However, there is a definite change in the joint conductivity ratio (k_2/k_1) for aluminum and stainless steel. The value for copper obtained from the data in Reference 5 also supports this trend, but can't be used conclusively since there is considerable difference in the geometry of this specimen as compared to our specimens. Figure IV-28 is a plot of the three material properties, which are considered to have an influence, versus the conductivity ratio. In Figure IV-29, these properties are plotted against k_2. The plots presented in Figures IV-28 and IV-29 indicate that the effect of thermal conductivity is opposite to the effect of hardness and modulus of elasticity. It must be pointed out that only the data obtained in this study can be used conclusively because the specimen used in References 5 and 7 were not constructed to the same geometrical parameters as the specimen used in this study.

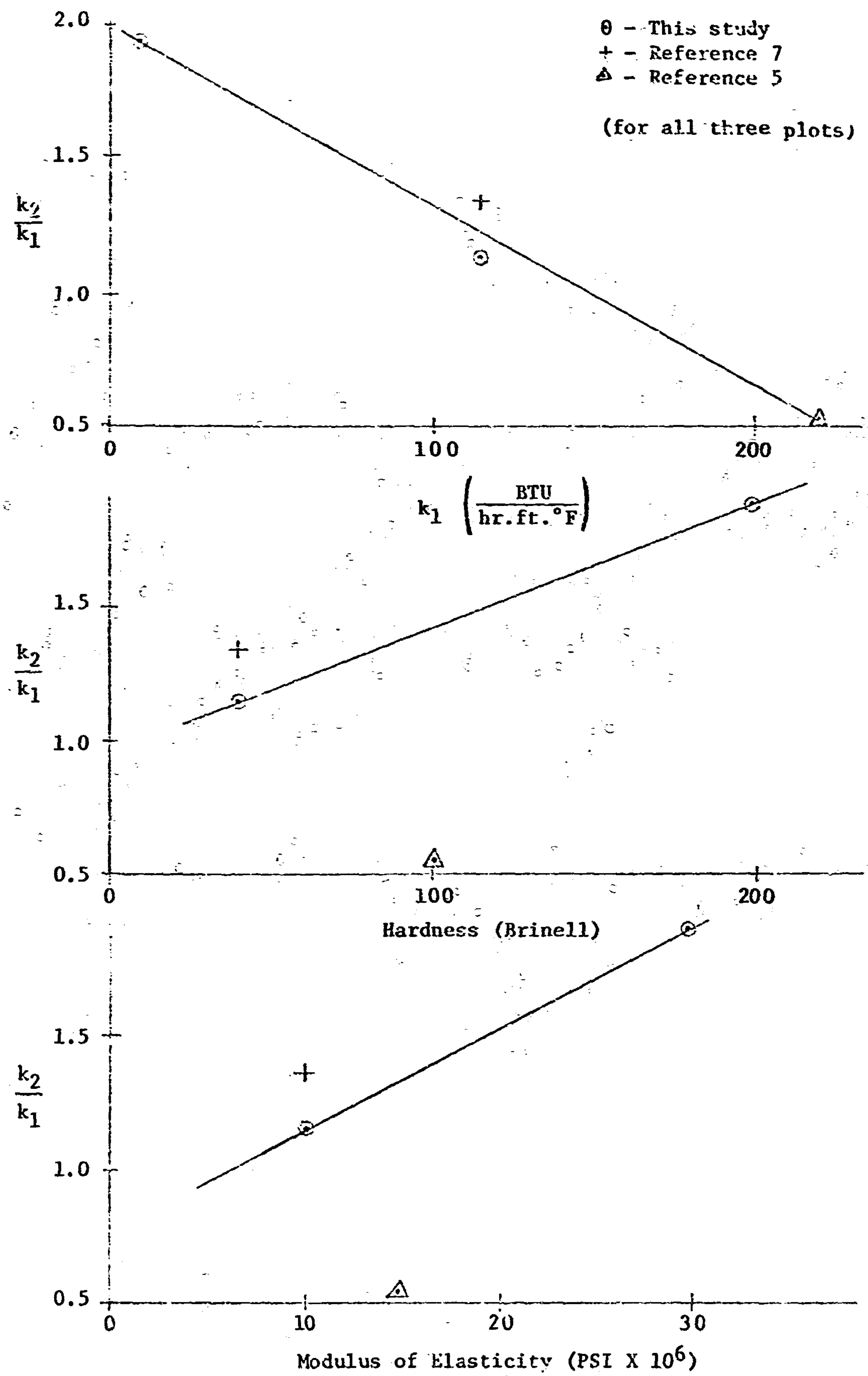

Figure IV-28. Plots of material properties of the plates versus conductivity ratio.

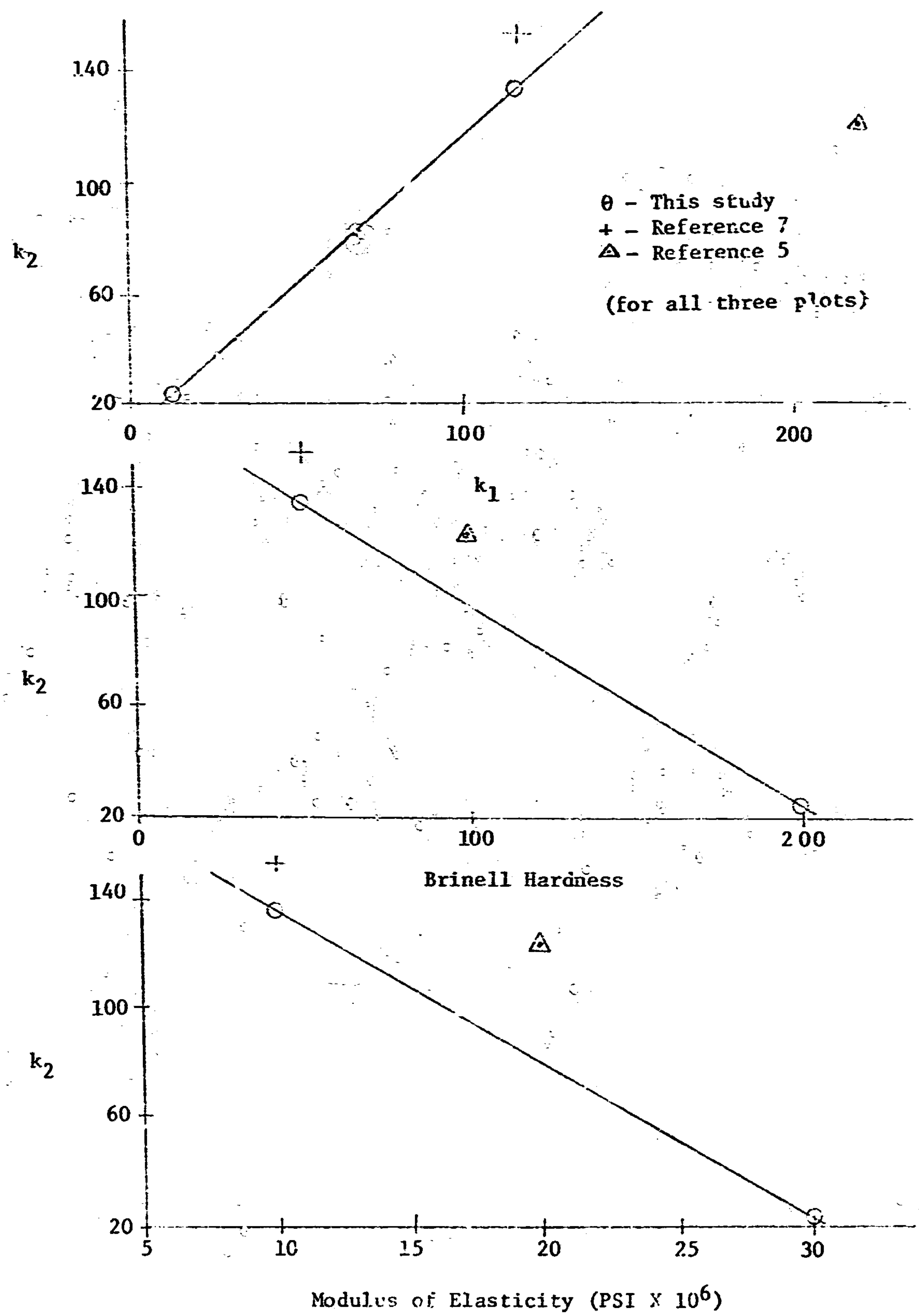

Figure IV-29. Plots of material properties of the plates versus k_2.

C. EVALUATION OF PARAMETERS WHICH INFLUENCE JOINT THERMAL CONDUCTIVITY

As stated previously, the variables which influence joint thermal conductivity are many. There is not sufficient data in the previous literature or from this study to conclusively define the influence of each of these variables, but there is sufficient data to predict the trends of some of these variables. Figures IV-30 and IV-31 present these trends in the form of plots. Each plot in order is discussed below.

Interface Pressure

Most of the references support the trend presented in plot 1. Thermal conductivity increases as pressure increases until approximately 1500 psi. The effect of pressure then diminishes and the conductivity is constant. The average interface pressure used on the specimens in this study is approximately 1000 psi for 4 ft.lbs. of torque and 6500 psi for 28 ft.lbs. The data taken over this range supports the independence of thermal conductivity on pressure at higher pressures. Figure IV-32 indicates the averaged results obtained. Each point is the average of all conductivities calculated from the data taken at a particular torque for the indicated plate material.

Surface Roughness

Of the several previous studies which predicted the influence of surface finish on joint conductivity, all agreed that conductivity decreases with increasing roughness as shown in plot 2. However, there is poor agreement with respect to the magnitude of the influence. The only conclusions which can be made in light of the available data is that conductivity decreases with increasing roughness and that the

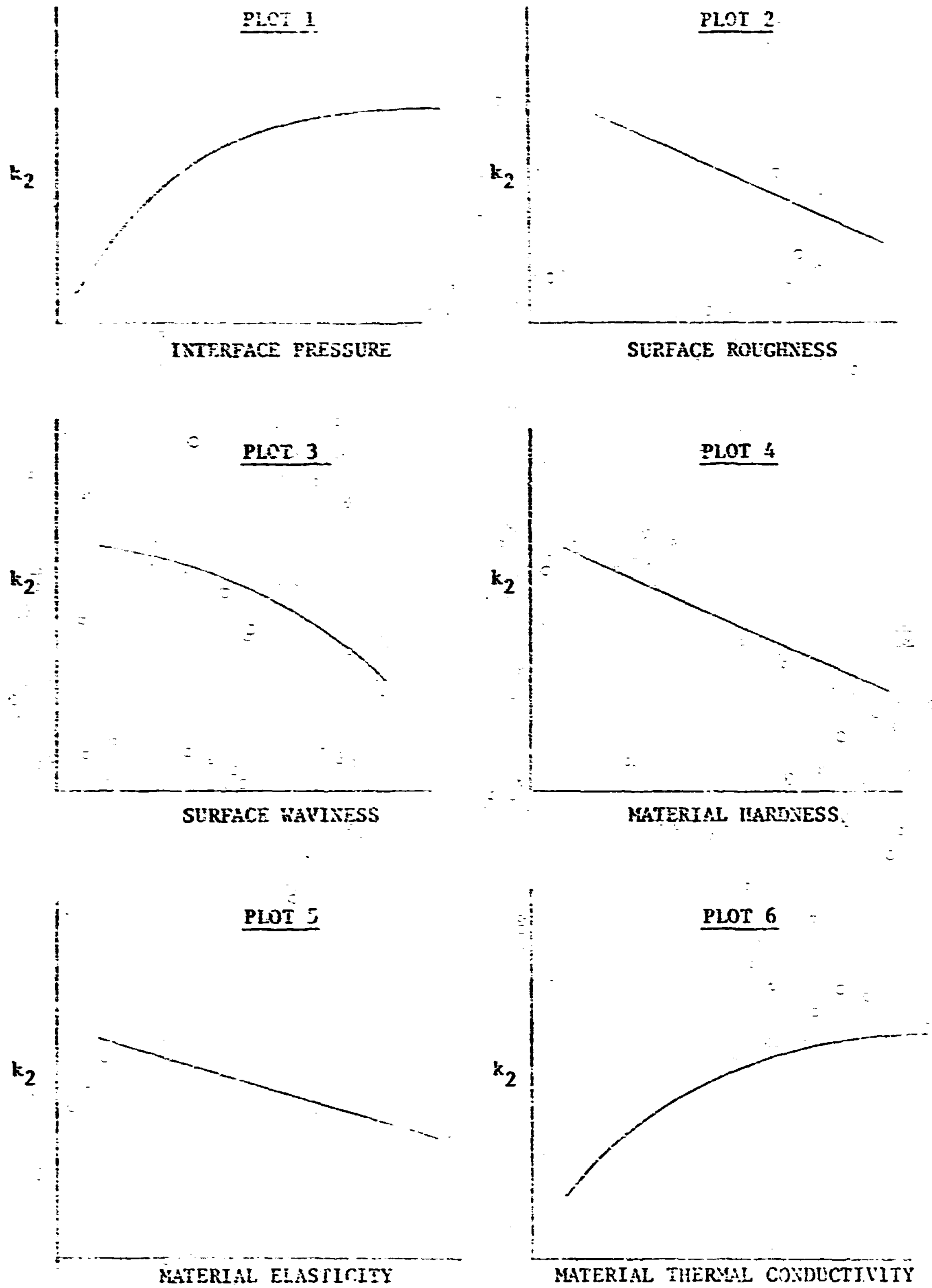

Figure IV-30. Generalization plots of the trends of pertinent parameters.

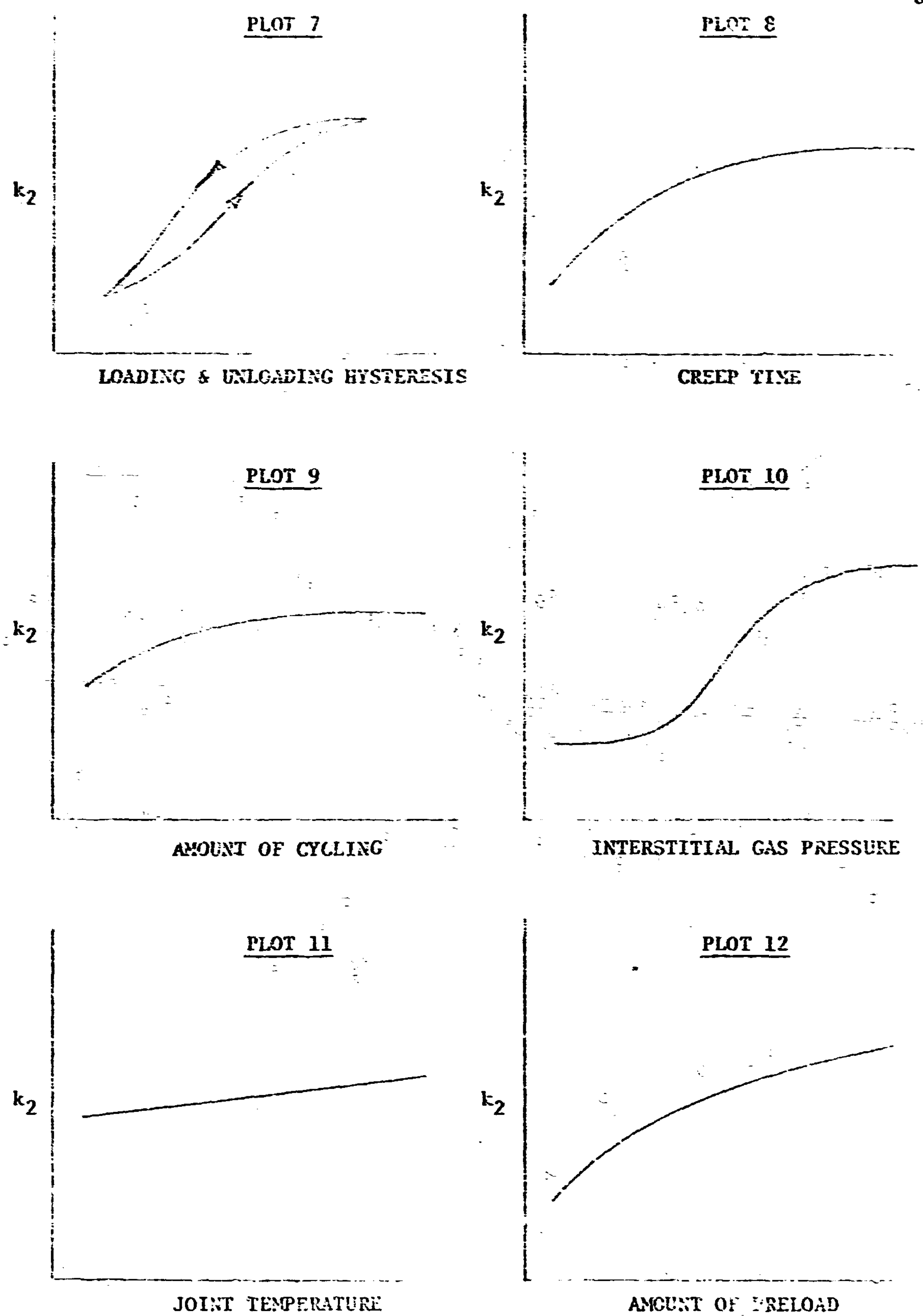

Figure IV-31. Generalization plots of the trends of pertinent parameters (continued.)

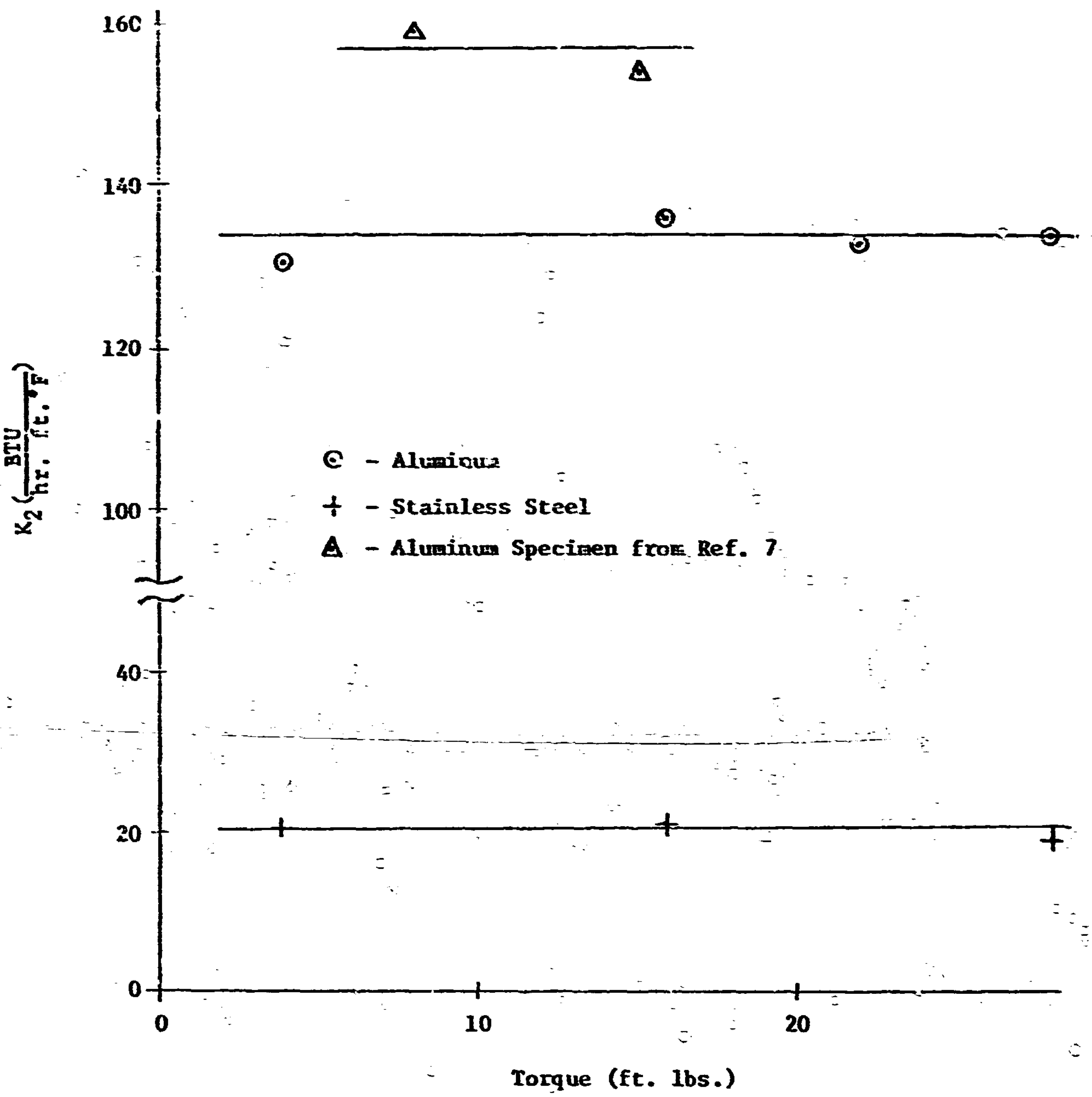

Figure IV-32. Plot of Torque versus K_2.

decrease is greater the lower the interface pressure. The data taken in this study indicates only a small decrease in conductivity with increasing roughness over a range of 16 RMS to 125 RMS. This data is shown in Figure IV-33.

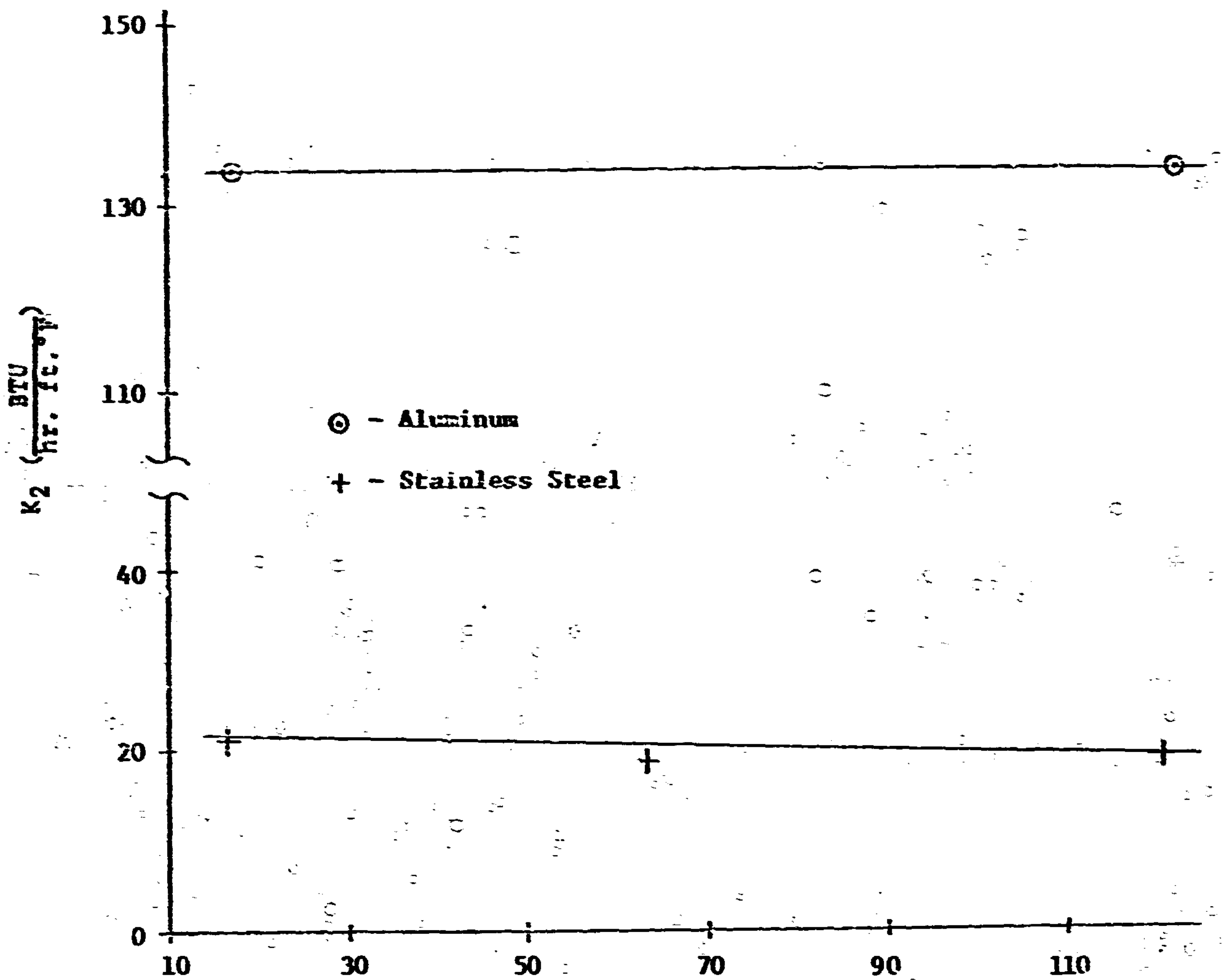

Figure IV-33. Plot of Surface Finish versus K_2.

Surface Waviness

The only significant data concerning surface waviness was found in Reference 18 which states that an increase in waviness produces an increase in resistance which "is small for small waviness and large at large waviness. A small amount of surface roughness has a large effect on waviness at light pressures." Plot 3 is based solely on this information. There was no attempt in this study to define the effect of waviness.

Material Hardness

It is difficult to determine the effect of the various plate metallurgical parameters on joint conductivity because of the problem of getting specimen materials which are similar enough that only one variable can be studied at a time. However, References 17 and 18 agree that conductivity decreases as hardness increases as shown in plot 4, and the investigators on this study tend to agree with their opinions.

Material Elasticity

Very little information is available concerning the effect of elasticity. Plot 5 is based on a plot given in Reference 18.

Material Thermal Conductivity

The value of k_2 increases as the conductivity of the plate metal increases; however, the ratio of $\frac{k_2}{k_1}$ decreases as k_2 increases. Data was taken from References 5 and 7 and combined with the results from this study to form the plot presented in Figure IV-34. This plot should not be considered as conclusive data because of the differences in joint configuration for the test specimens in each reference.

Hysteresis

Plot 7 shows the hysteresis effect noted by References 4, 14, and 17. No effort was made in this study to determine whether or not hysteresis exist but it is reasonable to assume that there is an effect.

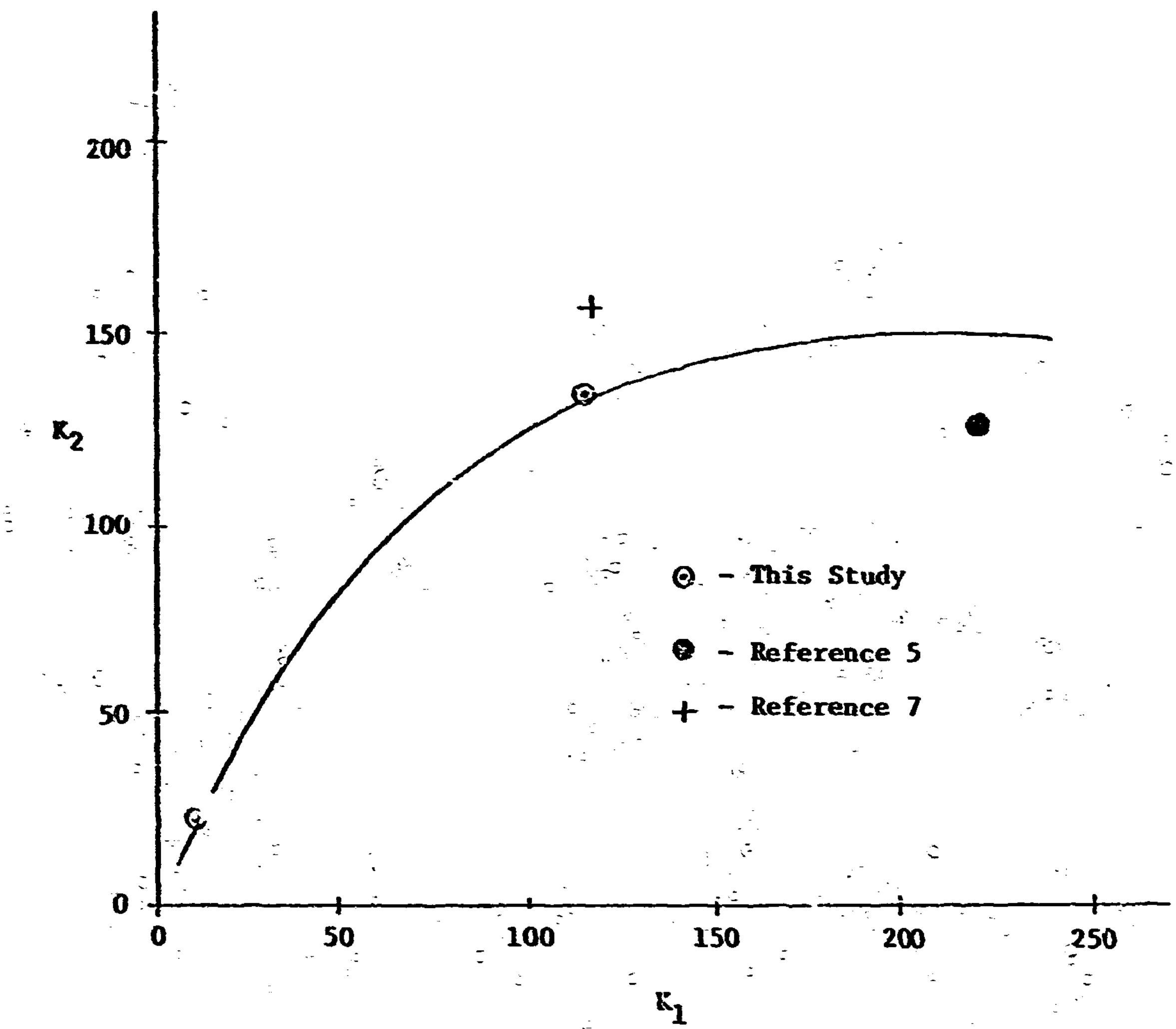

Figure IV-34. Plot of K_1 versus K_2 in. $\frac{BTU}{hr.\ ft.^{\circ}F}$.

<u>Creep</u>

The value of k_2 increases as time increases. The increase is large at first and eventually k_2 approaches a constant. This investigator believes that the area of microscopic contact increases with increasing time and thus increases k_2. Reference 18 states, "the resistance decreases continuously and finally assumes a constant level." Reference 4 also agrees with this conclusion.

Amount of Cycling

Plot 9 shows the effect on k_2 of the number of times a joint has been cycled. Cycling is simply the loading and unloading of the joint to obtain consistant results. Reference 14 states that this requires 2 or 3 cycles at high loads. The effect of cycling is an increase in k_2 as the number of cycles increases. Eventually, k_2 becomes constant and further cycling has no effect.

Interstitial Gas Pressure

The value of k_2 is considerably increased as the ambient fluid pressure is increased from a hard vacuum to atmospheric pressure. Plot 10 indicates this effect and is supported by References 15 and 18. Data taken in this study also supports this plot. Figure IV-35 is a plot of the temperature distribution obtained with test specimen 3 at 16 ft.lbs. of torque in a vacuum. Figure IV-36 is the temperature distribution for the same specimen at the same torque but at ambient pressure. The increase in k_2 is from 136.1 $\frac{\text{BTU}}{\text{hr.ft.°F}}$ for vacuum to 165.0 $\frac{\text{BTU}}{\text{hr.ft.°F}}$ for ambient, which represents a 21% increase.

Joint Temperature

Plot 11 represents the effect of joint temperature on k_2. Most of the references support this trend. The value of k_2 increases gradually and linearly as the temperature of the joint increases. Reference 18 suggests that this trend holds until the temperature exceeds 1000°F. Above this temperature, it is suggested that the increase is much more rapid.

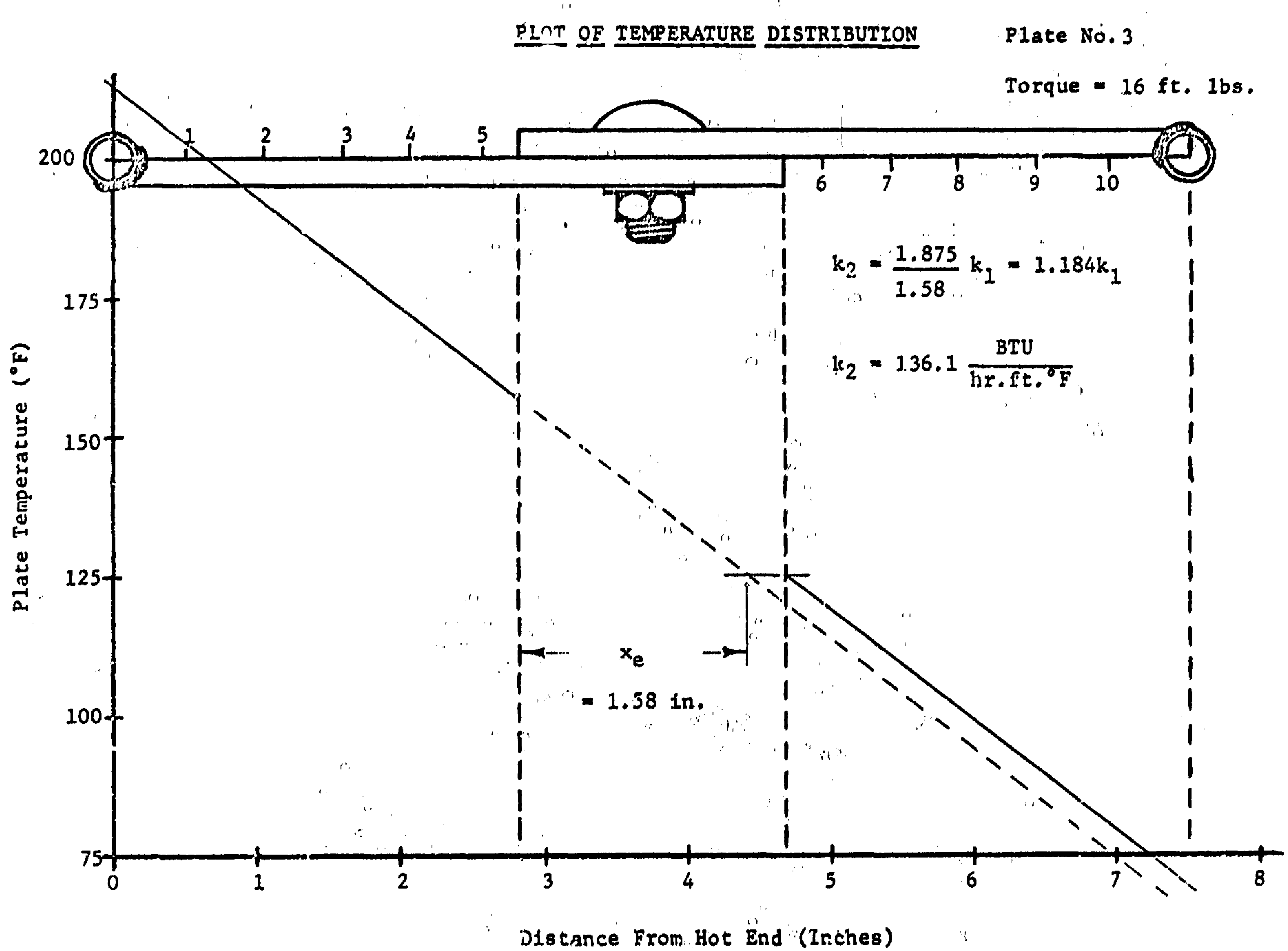

Figure IV-35. Temperature distribution plot for joint thermal conductivity determination for plate 3 at 16 ft.lbs. in a vacuum environment.

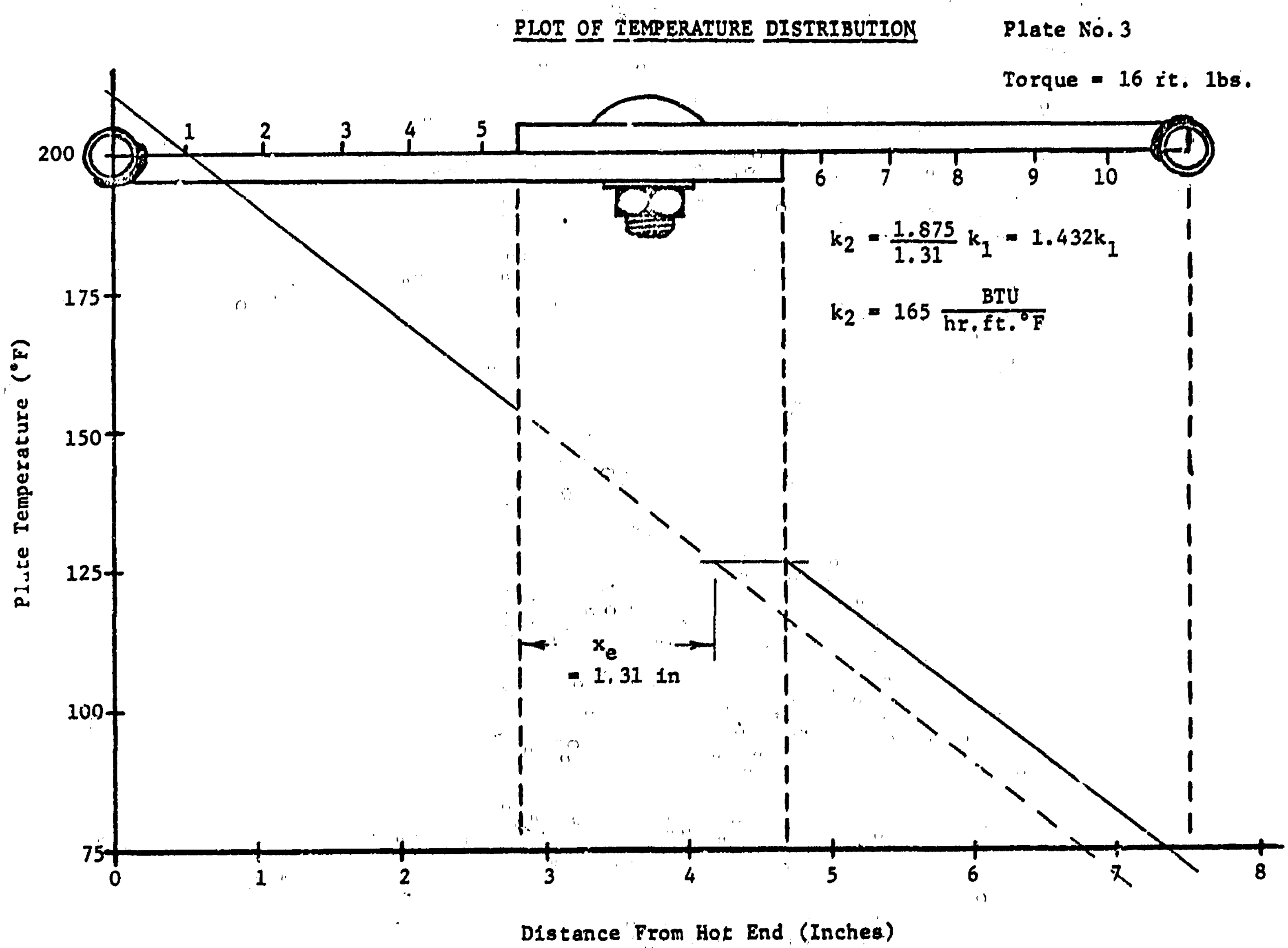

Figure IV-36. Temperature distribution plot for joint thermal conductivity determination for plate 3 at 16 ft.lbs. in an ambient environment.

Amount of Preload

Reference 16 states that the value of k_2 can be increased by increasing the amount of the preload applied to the joint. By overloading the mating surfaces of the plates, the small peaks can be plastically deformed and will permit an increase in microscopic contact area. This increase in k_2 is large initially, and becomes slight at high loading conditions.

Some of the above trends are not conclusively supported by data. In fact, there is a severe lack of good data involving most of the parameters. Caution should be observed in using these trends or any other joint conductivity data. The assumptions and experimental techniques of the respective investigator(s) should be closely scrutinized before the data or conclusions are used.

V. CONCLUSIONS AND RECOMMENDATIONS

It has been shown in this study that there are three important types of plate deflections which must be considered in any study of the reaction of bolted or riveted joints to static loading conditions. Any analytical method of predicting joint thermal conductivity must include a method of predicting the response of the plates to a particular set of these loading conditions. It must also include a method of predicting interface thermal conductances for numerous parameters. The investigators on this project are of the opinion that such an analytical method cannot be formulated without many assumptions and approximations which will eventually render the method inaccurate. The resulting equations that will have to be solved will be large in size and number, and the solutions to the equations will be extremely complicated. For this reason, the investigators have suggested a more practical solution, such as the experimental method presented in this study.

The EFM requires that temperature gradients be obtained on both sides of the joint for which the thermal conductivity must be determined. This can be obtained from the actual joint or from a model. The conductivity of the joint, k_2, can easily and quickly be calculated from these gradients. This value of k_2 represents the thermal conductivity of an equivalent section of metal with the same length as the overlapped section and cross-sectional area as the parent metal. The simple heat conduction equation, $q = kA \frac{\Delta T}{\Delta x}$, can be used to define the heat flow through the joint as well as the parent metal. The values of k_2, A, and Δx (Δx = length of plate overlap, l) will be constant for the particular joint in question. If the amount of heat, q, to be dissipated through the joint is known, then ΔT can easily be calculated and vice versa.

In some cases, it may be more convenient to express the heat flow capability of a joint in terms of overall conductances or resistances such as $U = \frac{kA}{l}$ or $R = \frac{1}{U}$. For this study, the use of a joint conductivity was satisfactory.

The greatest drawback to an experimental method of determining joint conductivity is that in many instances temperature gradients cannot be determined for the actual joint being used and a model must be constructed. If an extremely large number of joints are involved, then many models would need to be constructed and tested. However, if the joints can be standardized such that all joints will be similar in shape and differ only by a geometrical scale factor, then only one model must be constructed and tested. Through the use of thermal scale modeling techniques (under investigation by Dr. Maples in Mechanical Engineering at LSU), the conductivity of all the joints in the standardized group can be determined. The success of any other method of determining joint conductivity may depend on joint standardization also. There is an infinitely large variety of bolted and riveted joints. A single analytical solution cannot include every type of joint. Only by standardizing or grouping similar joints can a solution be formulated.

If an analytical solution is to be sought, then the approach used in Reference 7 represents a logical approach. In that reference, an analytical solution to define plate responses to loading conditions was formulated and programmed on a computer. The information obtained from this program was coupled with an analytical solution to the heat flow through the joint. This approach, in theory, should predict the thermal conductivity of a joint.

However, only a limited number of variables which influence joint conductivity have been included in the analysis in Reference 7. If this type of approach is to be accurate, then all of the pertinent variables must be considered.

In conclusion, the EFM is a method of determining joint thermal conductivity and can be used on any type of joint. It can be used on joints with any type of bolting or riveting pattern, with any type of interfacial filler material, or any other parameter or combination of parameters. The EFM essentially treats the joint as a black box and is not concerned with what is in the black box.

BIBLIOGRAPHY

1. Aron and Columbo. "Controlling Factors of Thermal Conductance Across Bolted Joints in a Vacuum Environment", ASME Paper No. 63-WA-196 (November 1963).

2. Bradley, Terry L. "Stress Analysis for Thermal Contact Resistance Across Bolted Joints", M.S. Thesis at M.I.T. (August 1968).

3. Brunot and Buckland. "Thermal Contact Resistance of Laminated and Machined Joints", ASME Transactions (April 1968).

4. Clausing and Chao. "Thermal Contact Resistance in a Vacuum Environment", ASME Paper No. 64-HT-16 (April 1964).

5. Coulbert and Lin. "Thermal Resistance of Aircraft Structural Joints", WADC Technical Note 53-50 (June 1953).

6. Elliott, D. H. "Thermal Conductance Across Aluminum Bolted Joints", ASME 65-HT-53 (May 1965).

7. Fontenot, John E. "Thermal Conductance of Bolted Joints", Ph.D. Dissertation at Louisiana State University (February 1968).

8. Fenech, Henry, and Rohsenow. <u>Developments in Heat Transfer</u>, pp 354-370 (1964).

9. Kaspareck and Dailey. "Measurements of Thermal Contact Conductance Between Dissimilar Metals in a Vacuum", ASME 64-HT-38 (1964).

10. Koewenhoven and Potter. "Thermal Resistance of Metal Contacts", Welding Research Supplement (October 1948).

11. Koh and John. "The Effect of Interfacial Metallic Foils on Thermal Contact Resistance", ASME 65-HT-44 (May 13, 1965).

12. Mikic, Yavanovich, and Rohsenow. "The Effect of Surface Roughness and Waviness Upon the Overall Thermal Contact Resistance", M.I.T. Report No. 76361-43 (October 1966).

13. Minges, M. L. "Heat Transfer Across Non-Metallic Interface at High Temperature", AFSCRP 80-1, Research and Technology Briefs (January 1969).

14. Rohsenow and French. "Prediction of Thermal Conductance of Metallic Surface in Contact", ASME 62-HT-32 (August 1962).

15. Stubstad, W. R. "Measurements of Thermal Contact Conductance in a Vacuum", ASME 63-WA-150 (September 1964).

16. Stubstad, W. R. "Thermal Contact Resistance Between Thin Plates in a Vacuum", ASME 65-HT-16 (April 1965).

17. Weills and Ryder. "Thermal Resistance of Joints Formed Between Stationary Metal Surfaces", ASME Transactions (April 1949).

18. Yovanovich and Rohsenow. "Influence of Surface Roughness and Waviness Upon Thermal Contact Resistance", M.I.T. Report No. 76361-48 (June 1967).